Copyright Undertaking

This thesis is protected by copyright, with all rights reserved.

By reading and using the thesis, the reader understands and agrees to the following terms:

1. The reader will abide by the rules and legal ordinances governing copyright regarding the use of the thesis.

2. The reader will use the thesis for the purpose of research or private study only and not for distribution or further reproduction or any other purpose.

3. The reader agrees to indemnify and hold the University harmless from and against any loss, damage, cost, liability or expenses arising from copyright infringement or unauthorized usage.

CHARACTERIZATION OF IN VIVO ACTIVITY OF FLAVONOID DIMER IN MODULATING P-GLYCOPROTEIN

KAN WING YIU

Ph.D

The Hong Kong Polytechnic University

2015

The Hong Kong Polytechnic University

Department of Applied Biology & Chemical Technology

CHARACTERIZATION OF IN VIVO ACTIVITY OF FLAVONOID DIMER IN MODULATING

P-GLYCOPROTEIN

KAN WING YIU

A thesis submitted in partial fulfillment of the requirements for the degree of

Doctor of Philosophy

October 2014

CERTIFICATE OF ORIGINALITY

I hereby declare that this thesis is my own work and that, to the best of my knowledge and belief, it reproduces no material previously published or written, nor material that has been accepted for the award of any other degree or diploma, except where due acknowledgement has been made in the text.

KAN Wing Yiu

ABSTRACT

Drug efflux by permeability-glycoprotein (P-gp) transporter in cancer cells is one of the well studied mechanisms for multidrug resistance (MDR). Modulating P-gp by inhibitors is a legitimate method to reverse MDR. Flavonoid dimers belong to a family of modulators that exhibit modulating effect on P-gp mediated MDR *in vitro*. Flavonoid dimer **18** is a novel synthetic flavonoid dimer with *in vitro* P-gp modulating activity of EC_{50} = 148nM. Here drug metabolism and pharmacokinetics study of flavonoid dimers **18** has been conducted using rodent models.

Plasma concentration profile of **18** was obtained by UPLC-MSMS. Limit of detection for **18** was 3.9 ng/mL. Intraperitoneal (IP) administration of **18** was chosen for *in vivo* efficacy study as it gave a systemic circulation level above EC_{50} for a longer duration compared to intravenous (IV) administration. Metabolites of **18** were identified by mass spectrometry analysis. Their identities were confirmed with authentic compounds. All three metabolites have better hydrophilic properties. Metabolite **M1** (named as **14a**) demonstrated P-gp modulating activity *in vitro* (EC_{50} = 305nM). **M2** (named as **FM04**) also possessed a better P-gp modulating activity *in vitro* when compared to parent **18**. **M3** (named **FM327**) did not show any P-gp modulating activity. EC_{50} of **FM04** in reversing paclitaxel (PTX) mediated MDR was 70 ± 26nM whereas EC_{50} of **18** was 148 ±

18 nM. Plasma concentration profile for **FM04** was obtained by a validated UPLC-MSMS detection method for pharmacokinetics analysis. The detection limit for **FM04** was 8.88ng/mL. **FM04** was bio-available via oral (5.26%) and IP (24.34%) administration.

Effect of P-gp modulators (**18** or **FM04**) on improving PTX oral bioavailability was investigated. Oral bioavailability of PTX was increased by 7 fold, from 6.7% to 47.12%, when **FM04** was co-administered. Oral bioavailability of PTX was increased by 4.13 fold, from 2.66% to 11.01%, when **18** was co-administered. Co-administration of PTX (oral, 80mg/kg) with **18** (oral, 30mg/kg) or **FM04** (oral, 45mg/kg) resulted in a significant suppression in a LCC6 breast carcinoma xenograft model. Tumor doubling time was increased from 12 ± 0.6 days (no treatment group) to 35.3 ± 6.4 days (oral PTX 80mg/kg with **18** 30mg/kg) or 35.3 ± 1.8 days (oral PTX 80mg/kg with **FM04** 45mg/kg).

To conclude, novel flavonoid compound **18** represent a new class of P-gp modulator. We have studied the pharmacokinetics and investigated the metabolism of **18**. Metabolites of **18** were identified. One metabolite **FM04** showed higher P-gp modulating activity. We then also demonstrated that co-administration of PTX with **18** or its metabolite **FM04** can enhance oral bioavailability of PTX to a level sufficient for suppressing breast

carcinoma xenograft growth *in vivo*. This opens up the possibility of administer PTX via

oral route.

LIST OF PUBLICATIONS AND CONFERENCE PRESENTATION BY THE AUTHOR

List of Publications

1. **Kan, J. W**.; Chan, K.F.; Yan, C.S; Wong, I.L.K.; Chan, T.H.; Chow, L. M. Pharmacokinetics and interaction study of flavonoid dimer, a P-glycoprotein reversing agent, with paclitaxel in rodent. Drug Metab Rev (2009), 41(Suppl.)

2. Chan, K.F.; Wong, I.L.K.; Burkett, B.A.; Zhao, Y.; Yan, C.S; **Kan, J. W**.; Tsang, K.H.; Lam, C.Y.; Chow, T.W.S.; Chan, T.H.; Chow, L. M. Flavonoid dimer as modulator of drug resistance in cancer. <u>Progress in Nutrition</u> **12**: 1-7. (2010)

3. Chan, K. F.; Wong, I. L.; **Kan, J. W.**; Yan, C. S.; Chow, L. M.; Chan, T. H. Amine linked flavonoid dimers as modulators for p-glycoprotein-based multidrug resistance: structure-activity relationship and mechanism of modulation. <u>J Med Chem</u> **55**(5): 1999-2014. (2012)

Conference Presentations

1. **Kan, J. W**.; Chan, K.F.; Yan, C.S; Wong, I.L.K.; Chan, T.H.; Chow, L. M. "Pharmacokinetics and interaction study of flavonoid dimer, a P-glycoprotein reversing agent, with paclitaxel in rodent". 16th North American Regional ISSX Meeting, Baltimore, Maryland, USA, October 18-22, P.28 (2009)

2. **Kan, J. W**.; Chan, K.F.; Wong, I.L.K.; Yan, C.S; Chong, T.C; Law, M.C; Zhao, Y; Chan, T.H.; Chow, L. M. "Novel Flavonoid Dimers for Reversing Cancer Drug Resistance In vivo". Inaugural Croucher Summer Course in Cancer Biology 2013, Hong Kong, Hong Kong, August 14-18, (2013)

3. **Kan, J. W**.; Chan, K.F.; Wong, I.L.K.; Yan, C.S; Chong, T.C; Law, M.C; Zhao, Y; Chan, T.H.; Chow, L. M. " Novel P-gp modulators, Flavonoid Dimers, Reverse P-gp mediated MDR in

vivo". Role of MDR proteins in pharmacokinetics and toxicology, Masurian Lake District, Poland, September 3-7, (2013)

4.   **Kan, J. W**.; Chan, K.F.; Wong, I.L.K.; Yan, C.S; Chong, T.C; Chan, T.H.; Chow, L. M.
     "Flavonoid dimer and its active metabolite reverses P-gp mediated MDR in vitro and in vivo". 5th FEBS Special Meeting ATP-Binding Cassette (ABC) Proteins: From Multidrug Resistance to Genetic Diseases, Innsbruck, Austria, March 8-14, (2014)

ACKNOWLEDGEMENTS

First and foremost, I will like to thank my supervisor Prof. Chow Larry Ming-Cheung for giving me this opportunity to take part in this project. It is a valuable life experience to work with him in the past years. His philosophies on education is inspiring. I was provided with an atmosphere with freedom to generate new ideas, acquiring new knowledge and most importantly coping with the project schedules. His guidance, valuable discussions and encouragements was deeply appreciated.

In this wonderful project of integrating biological studies with chemical studies tremendous thanks must be given to our chemist collaborators Prof. Chan Tak-Hang and Dr. Chan Kin-Fai. Prof. Chan Tak-Hang has provided me with valuable comments and his research experiences throughout my PhD study. Huge thank goes to Dr. Chan Kin-Fai for his enomous effort on synthesis and chemistry input. Dr. Chan is truly a team player, who is willing to spend extra hours of work to meet up with the large quantity of compounds for animal study in the tight schedule. His comments on chromatographies are very valuable. It is my pleasure to have worked with Dr. Chan.

Last but not least, I would like to express my sincere thank to my parents, my family and my friends for their love and support throughout the years. The love and support that fueled me in the past and shaped me into who I am today.

Jason W.Y. KAN

September, 2014

TABLE OF CONTENT

LIST OF FIGURES

LIST OF TABLES

LIST OF ABBREVIATIONS

ATP	Adenosine Triphosphate
$AUC_{(0 \text{ to infinity})}$	Cumulative Area Under The Curve From Time 0 to Infinity Using Trapezoid Rule
CYP450	Cytochrome P450 enzyme
EC_{50}	Half maximal effective concentration
HLM	Human liver microsomes
HPLC	High Pressure Liquid Chromatography
IC_{50}	Half maximal inhibitory concentration
IH	Intracellular Helices
LOQ	Limit of Quantification
MDR	Multidrug Resistance
MDR1	Multidrug Resistance Protein
MRM	Multiple reaction monitoring
MRT	Mean residence time

NADPH   β-Nicotinamide adenine dinucleotide phosphate sodium salt hydrate

PTX   Paclitaxel

P-gp   Permeability-Glycoprotein

QqQ   Triple quadrupole

RE   Relative error

RLM   Rat liver microsomes

RSD   Relative standard deviation

SAR   Structure-Activity Relationship

SD   Standard deviation

UPLC   Ultra Pressure Liquid Chromatography

1. INTRODUCTION

1.1 P-GLYCOPROTEIN MEDIATED MULTI DRUG RESISTANCE (MDR)

Unresponsiveness of cancer cells to chemotherapies has been a huge obstacle in extending life span of patients. Combining chemotherapeutic agents with non-overlapping mechanisms of action gave partial success (Mansouri et al. 1994). Three major mechanisms of multidrug resistance (MDR) include; firstly, decreased uptake of water-soluble drugs such as cisplatin and folate antagonists; secondly, increased DNA repair and altered metabolism of drugs; thirdly, increased energy-dependent efflux of hydrophobic drugs that enter the cells by diffusion (Grossi and Biscardi 2004; Szakacs et al. 2006). Energy-dependent efflux of hydrophobic cytotoxic drugs is commonly encountered in the laboratory setting where cell lines are selected to become drug resistant. Amplification of a family of energy-dependent transporter known as ATP-binding cassette (ABC) transporters (Szakacs et al. 2006) is frequently observed. The superfamily of ABC transporter consists of 7 families from ABCA to ABCG. These overexpressed transporters are most commonly observed *in vitro*. Three major ABC transporters responsible for MDR include P-glycoprotein (P-gp), breast cancer resistance protein (BCRP), and multidrug resistance related protein 1 (MRP1) (Holland

et al. 2003; Breedveld et al. 2006; Dawson and Locher 2006; Szakacs et al. 2006; Chan et al. 2010; Robey et al. 2010; Shukla et al. 2011).

The most widely studied drug efflux transporter protein is the Permeability-Glycoprotein (P-gp), encoded by *ABCB1* (Ambudkar et al. 2003; Szakacs et al. 2006; Robey et al. 2010). *In vitro* data has demonstrated that inhibition of P-gp leads to an increase in intracellular drug level. Thus modulating P-gp may be effective in improving clinical outcomes in drug-resistant cases. In addition, clinical studies suggested that P-gp overexpression may be associated with poor clinical outcome. Patients with poor prognosis were generally positive for P-gp expression (Dalton 1993; Mansouri et al. 1994; Saeki et al. 2005; Szakacs et al. 2006; Robey et al. 2010). Cell lines derived from these P-gp overexpressing samples were also drug resistant *in vitro.* (Holland et al. 2003; Chan et al. 2006). These clinical observations suggest that P-gp is related to poor prognosis and that P-gp is a potential target for overcoming MDR.

1.2 STRUCTURE FUNCTION OF P-GP

MDR is correlated with P-gp expression level. P-gp, like other members of the superfamily ABC transporters, is an ATP-dependent membrane spanning multidrug transporter. It is widely found in different species ranging from microbes to human beings. It is a transmembrane protein of 170kDa with 1280 amino acids, consisting of 12 transmembrane segments forming 4 core domains. These 4 domains include 2 nucleotide-binding domains (NBDs), which are highly hydrophilic and responsible for ATP hydrolysis and 2 transmembrane domains (TMDs) which are highly hydrophobic and responsible for substrates binding (Holland et al. 2003; Chan et al. 2006). Eukaryotic ABC transporters play a role in exporting a wide variety of substrates. The physiological function of P-gp is suggested to be involved in defense mechanism. P-gp in human was found on luminal surfaces of epithelial cells of kidney proximal tubules, blood-brain barrier, intestines, testes, adrenal gland, and biliary hepatocytes. Such localization fulfills its protective role through excreting endogenous or exogenous toxins that are mostly hydrophobic or amphipathic in nature (Gottesman et al. 1996; Gottesman and Ling 2005; Shukla et al. 2011).

Crystal structure of P-gp could help to reveal its mechanism of action. However, crystal structure of human P-gp is still in progress. Crystal structures of several homologs have been determined, including Sav1866, an ABC transporter from *S. aureus* (Dawson and Locher 2006), P-gp homolog of mouse (Aller et al. 2009), *C. elegans* (Jin et al. 2012), and *Cyanidioschyzon merolae* (Kodan et al. 2014). These structures have provided us with better understanding of the functionality and gating mechanism of P-gp (Kodan et al. 2014). The crystal structure of Sav1866 was a homodimer consisting of 2 subunits. The full transporter is 120Å long, 65 Å wide and 55 Å deep. The observed 12 transmembrane helices were consistent with human P-gp crosslinking studies (Dawson and Locher 2006). The Sav1866 structure was obtained in the presence of ADP. From the crystal structure it can be seen that the bundle of transmembrane helices diverges and points toward the exterior, demonstrating an outward facing conformation. The cavity of the transporter is accessible from extracellular side in this conformation (Dawson and Locher 2006). It is known that P-gp is an energy driven transporter. In the absence of ATP, substrate transport ceases. Each subunits has their amino-terminal TMD twisted and embraced with the carboxy-terminal NBD (Figure 1-1), suggesting that there is a link between TMD and NBD. The interface of the NBD and TMD (intracellular loops ICL1 and ICL2) is evolutionally conserved among different ABC

transporters (Dawson and Locher 2006). The intracellular loops ICL1 and ICL2 may

contribute to the transmission of signal from ATP binding and hydrolysis to the TMD,

through non-covalent interactions and conformational changes in TMD. This will

eventually opens up the transporter for substrate binding/drug efflux (Dawson and

Locher 2006).
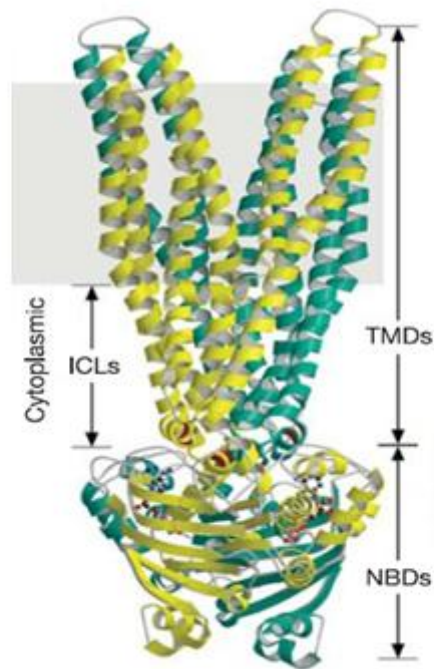
Figure 1-1 Structure of Sav1866

Sav1866 was crystallized in the presence of ADP and that the transporter was purified and
crystallized in the ATP-bound state with an outward facing structure. TMD, transmembrane
domain; NBD, nucleotide binding domain; ICLs, intracellular loops (Dawson and Locher 2006).

Structural information of Sav1866 can be interpreted together with mouse P-gp structure (Aller et al. 2009). Mouse P-gp is considered as the inwardly facing structure whereas Sav1866 is considered outward facing (Figure 1-2). In the absence of ADP or ATP, the mouse P-gp structure obtained is in an inward-facing conformation. The internal cavity volume was estimated. The apo protein structure of P-gp has a large 6000$Å^3$ internal cavity within the lipid bilayer for substrate binding. It was suggested that P-gp substrates can partition into the lipid bilayer and reach the P-gp internal cavity. With the aid of ATP hydrolysis, substrates are expelled outside the cell (Aller et al. 2009). Co-crystal structure of mouse P-gp with inhibitors like verapamil also revealed the importance of membrane-spanning residues previously shown to be important in biochemical crosslink studies (Loo and Clarke 1997; Loo et al. 2006). F724 (human F728) of TM7 and V978 (human V982) of TM12 are found to be important for drug binding (Loo and Clarke 1997; Loo et al. 2006; Aller et al. 2009).
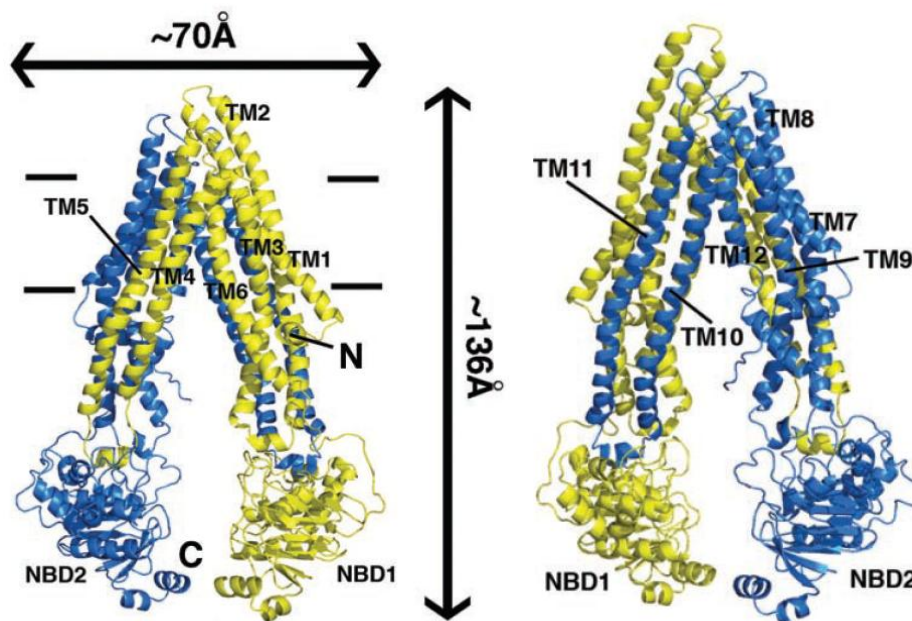
Figure 1-2 Structure of mouse P-gp

The structure of nucleotide-free inward-facing conformation mouse P-gp at a 3.8Å resolution that was suggested to be involved in binding substrates (Aller et al. 2009). A large internal cavity of 6000Å^3 was observed (Aller et al. 2009).

The crystal structure of Sav1866 (Dawson and Locher 2006) and mouse P-gp transporter (Aller et al. 2009) provided important structural information in understanding the conformational change of P-gp in substrate transport. A large internal cavity was present for substrates binding. These results were consistent with the structural information from *C. elegans* P-gp crystal structure obtained in the absence of nucleotides and substrates (Jin et al. 2012).

The *C. elegans* P-gp crystal structure strengthened the model of Sav1866 and mouse P-gp, in particular the ATP dependence and interaction between TMD and NBD by means of salt bridge. In the study of *C. elegans* crystal structure three highly conserved residues, Arg946 (intracellular helices, IH4), Asp188 (IH1) and Tyr 468 (NBD1) form a network of salt bridge that served as important connection between NBD and TMD (Figure 1-3). Similar atomic interactions were also observed in the other NBD-TMD interface. The roles of these salt bridges have been suggested to be similar to that of maltose transporters and destruction of these salt bridges was predicted to lead to defective transporters (Jin et al. 2012).
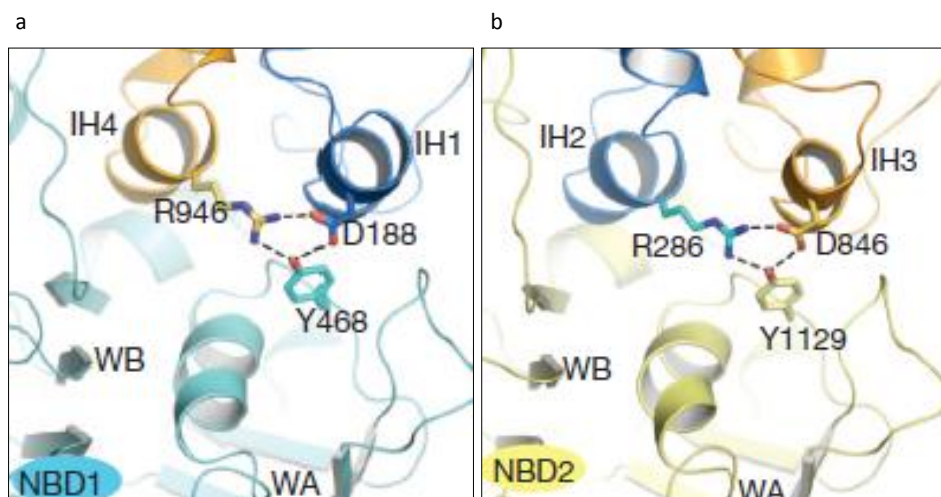
Figure 1-3 Salt bridge interaction in NBD-TMD interface of *C. elegans*

Three highly conserved residues, Arg946 (IH4), Asp188 (IH1) and Tyr 468 (NBD1) on NBD1 (a) and three highly conserved residues Arg286 (IH2), Asp 846 (IH3) and Tyr 1129 (NBD2) (b) (Jin et al. 2012)

Results from *C. elegans* study strengthen the vacuum cleaner model. A significant increase in ATPase sensitivity was observed for *C. elegans* P-gp expressed on yeast membrane when compared to purified P-gp reconstituted in detergents. The authors suggested that this was in agreement with the hydrophobic vacuum cleaner model. The hydrophobic vacuum cleaner model describes the extraction of P-gp substrate from the lipid bilayer during the diffusion of the substrate across the lipid bilayer and reaches the internal cavity of P-gp (Raviv et al. 1990; Loo and Clarke 2005; Gottesman and Ling 2006). Although the increase in ATPase sensitivity may not be critical evidence in explaining the hydrophobic vacuum cleaner action, other lines of evidence has illustrated that hydrophobic vacuum cleaner action is a possible route for P-gp substrate uptake (Raviv et al. 1990; Loo and Clarke 2005; Gottesman and Ling 2006).

1.3 P-GLYCOPROTEIN MODULATORS

It is widely believed that modulation of P-gp can restore the chemosensitivity of MDR cancer cells. A short summary of three generations of P-gp modulators are shown in (Figure 1-4). Among the first generation P-gp modulators, verapamil, a calcium channel blocker, was one of the earliest compounds used for restoring P-gp mediated MDR (Cairo et al. 1989). Verapamil, however, was ineffective and toxic at doses required to suppress P-gp (Winniford and Hillis 1985; Cairo et al. 1989; Grossi and Biscardi 2004; Szakacs et al. 2006). In general, the binding affinities of the first generation P-gp modulators were too low for P-gp modulation in clinical settings (Grossi and Biscardi 2004; Szakacs et al. 2006).

Despite the limited success from first generation P-gp modulators, a randomized phase III clinical trial demonstrated that cyclosporine was beneficial to AML patients with poor prognosis, suggesting that P-gp modulation was still a feasible approach in reversing MDR and may be advantageous to leukemia patients (Grossi and Biscardi 2004; Szakacs et al. 2006). One of the most promising compounds among the second generation P-gp modulators was a non-immunosuppressive cyclosporine D analogue, valspodar (PSC-833) (Atadja et al. 1998; Grossi and Biscardi 2004; Szakacs et al. 2006). PSC-833 was capable of modulating P-gp mediated MDR in a dose dependent manner in

a xenograft model (Boesch et al. 1991). Pharmacokinetics studies found that PSC-833 might have a drug-drug interaction effect during the development process (Boesch et al. 1991; Advani et al. 2001; Bates et al. 2001). In contrast to the efficiency found *in vitro*, phase III clinical trial suggested that PSC-833 was not beneficial to patients (Friedenberg et al. 2006; Szakacs et al. 2006).

First generation	Amiodarone	
	Cyclosporine	
	Quinidine	
	Quinine	
	Verapamil	
	Nifedipine	
	Dexniguldipine	
Second generation	PSC-833	
	VX-710 (Biricodar)	
	GF120918 (Elacridar)	
Third generation	LY475776	
	LY335979 (Zosuquidar)	
	XR-9576 (Tariquidar)	
	V-104	
	R101933 (Laniquidar)	
Other	Disulfiram	
	FTC (Fumitremorgin C)	
	MK571	
	Tricyclic isoxazoles	
	Pluronic L61	
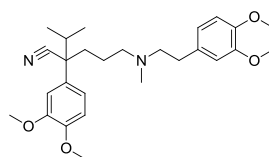
Structure of Verapamil
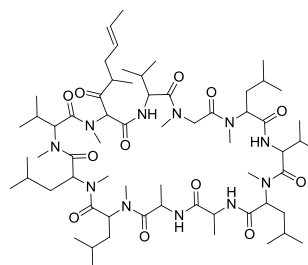
Structure of Valspodar (PSC-833)

Figure 1-4 Three generations of P-gp modulators

Three generations of P-gp modulators and the structures of verapamil and valspodar are shown (Szakacs et al. 2006)

The third generation P-gp modulators are designed with high affinity towards P-gp and low pharmacokinetic interactions when co-administered drugs such as PTX or doxorubicin. Third generation P-gp modulators include zosuquidar (LY335979), Laniquidar (R101933), elacridar (GF-120918), Tariquidar (XR9576) and OC144-093 (ONT-093) (Thomas and Coley 2003; Gergely Szakacs et al. 2006; Szakacs et al. 2006; Kelly et al. 2011). Among the aforementioned candidates, OC144-093 was once found to have no effect on drug clearance when co-administrated with PTX (E.Dates and Fojo 2004; Chi et al. 2005; Gergely Szakacs et al. 2006; Szakacs et al. 2006; Baumert and Hilgeroth 2009). Recent data, however, revealed mild pharmacokinetics interaction with PTX at high doses in one of the patients in phase I study (Chi et al. 2005).

1.4   FLAVONOIDS AS P-GLYCOPROTEIN MODULATORS

Another group of potent P-gp inhibitors are natural flavonoids. Flavonoids are polyphenolic compounds found in a wide variety of plants, including nuts, stems, vegetables, flowers and tea. There has been considerable interest in the benefits of flavonoid consumption (Schroeter and Spencer 2003). Diets rich in flavonoids can provide health effects such as antioxidant, anti-inflammatory, antiviral, anticancer, and cardioprotective effects (Olivier Dangels and Dufour 2006; Chan et al. 2009). The health

effects of flavonoids might be related to their reducing properties. Among the various flavonoids, apigenin, a monomeric member of the flavones, has received considerable attention as it has been considered as a potential anticancer drug candidate (Panaro et al. 1999; Spencer et al. 2003).

Recent work from our lab has demonstrated that apigenin dimers have promising P-gp modulating activity (Figure 1-5). Apigenin is a flavone abundantly found in green leafy species. When linked by polyethylene glycol (PEG) at various lengths, apigenin dimers exhibited potent modulating activity (Chan et al. 2006). Apigenin dimers with an optimal length of 4 units of PEG units were effective in reversing P-gp-mediated PTX resistance in human breast cancer cells, MDA435/LCC6 MDR and adriamycin resistance in murine leukemia cells P388/ADR (Chan et al. 2006). Intracellular accumulation of doxorubicin (DOX) was increased in the presence of apigenin homodimers (Chan et al. 2006).
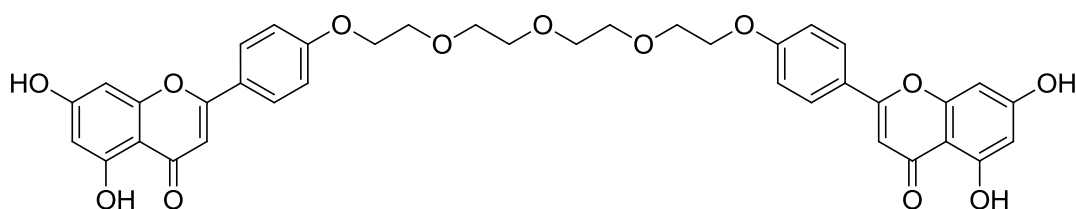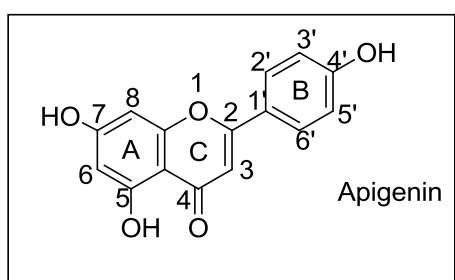
Figure 1-5. Structure of apigenin dimer **9d**

The structure of apigenin dimer **9d** is shown. A linker with 4 EG units is used to link apigenin moieties into a homodimer. Structure of apigenin is shown in the inset

Lead optimization has been performed on apigenin dimers (Chan et al. 2009). Improvements on the potency of flavonoid dimers were observed by substitution in the A-ring (Chan et al. 2009). Several homodimers such as compound **61** (Figure 1-6) have an improved P-gp reversal activity than the parent compound **9d**. In general, the second generation flavonoid homodimers with nonpolar substituent at positions, 5, 6 and 7 demonstrated a higher P-gp modulating activity. The flavonoid heterodimer, with two different substituent on each side of the dimers, demonstrated an intermediate modulating activity compared to their homodimer counterparts, suggesting that the

binding sites of flavonoid dimers on P-gp are similar and are lipophilic (Chan et al. 2009).
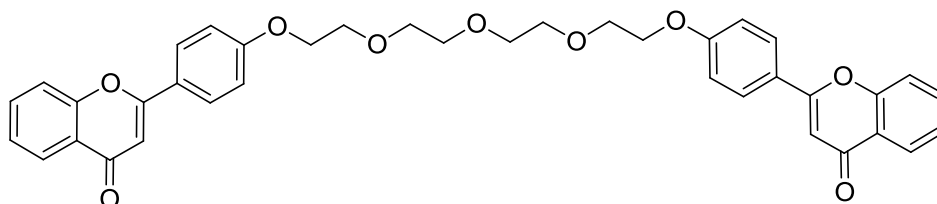
Figure 1-6 Structure of second generation flavonoid dimer compound, **61**.

Structure of flavonoid dimer **61**, is shown. The hydroxyl groups of position 5 and 7 on ring A of apigenin dimer have been replaced by hydrogen. The removal of hydroxyl groups increased the hydrophobicity and enhanced the potency in modulating P-gp *in vitro* (Chan et al. 2009).

Despite the increase in P-gp modulating activity, the increased hydrophobicity of the second generation flavonoid dimers was a great obstacle from the drug development point of view. The compounds were insoluble in water and *in vivo* studies were impractical. Our group therefore developed the third generation flavonoid dimers. The structure activity relationship (SAR) information from second generation flavonoid dimers revealed that lipophilic properties on the flavones rings are crucial to P-gp modulation and cannot be modified. This leaves the linker as a possible site for modification. With this rationale, a series of third generation flavonoid dimers was

synthesized with amine group introduced to the linker region (Chan et al. 2012). A

series of flavonoid dimers with amino group containing PEG linker was synthesized.

Hydrochloride salts of these compounds have tremendous improvement in solubility. In

addition to the solubility improvement, a marked increase in potency was observed for

one of these compounds, **18** (Figure 1-7). EC_{50} of **18** was 148 nM in reversing PTX

resistance in LCC6 MDR cells, making it a potential candidate for further development

(Chan et al. 2012). A summary of the three generations of flavonoid dimers are shown

in TABLE 1.

Figure 1-7. Structure of third generation flavonoid dimer **18**

18 is one of the third generation flavonoid dimers. The hydroxyl groups on apigenin moiety
have been replaced by hydrogen, the PEG linker has been modified by introducing an N-benzyl
group into the linker. The addition of N-benzyl group allowed **18** to be prepared in a
hydrochloride salt form, which leads to improvements in aqueous solubility.

Table 1 Relative P-gp modulating activity and their cLogP of three generations of flavonoid dimers

Generation	Compound	EC$_{50}$ on PTX (nM)	ClogP	Reference
1	9d	900	5.08	(Chan et al. 2009)
2	61	360	6.28	(Chan et al. 2009)
3	18 (free base)	148	7.07^	(Chan et al. 2012)

The **18** hydrochloride salt demonstrated enhanced aqueous solubility (Chan et al. 2009; Chan et al. 2012). ^ClogP for **18** (free base) was obtained from CS ChemDraw Pro. ClogP for **18** (HCl.salt) is not available.

1.4.1 IN VITRO CHARACTERIZATION OF **18**

18 exhibits preferential inhibition on P-gp over MRP1 and BCRP (Chan et al. 2012). The modulating activity of **18** in reversing P-gp mediated MDR was 28 folds and 15.5 folds higher than MRP1 and BCRP, respectively (Chan et al. 2012). At 200µM of **18** ATPase activity of P-gp was stimulated by 2.7 fold over the basal level. The Lineweaver-burk plot suggested that **18** was a competitive inhibitor of doxorubicin with a K_i of 0.28 µM (Chan et al. 2012). **18** itself was possibly a P-gp substrate (Chan et al. 2012). **18** probably competed with DOX to bind to the substrate binding site of P-gp. Other than DOX, **18** was also very potent in reversing P-gp mediated MDR to PTX, vinblastine, vincristine, daunorubicin and mitoxantrone in LCC6 MDR cell line (Table 2). EC_{50} of **18** in reversing resistance towards these anticancer drugs were in nanomolar range.

Table 2 P-gp reversal activity of **18** towards various anti-cancer drugs

Anti-cancer agents	EC$_{50}$ of 18 (nM)
PTX	148 ± 18
Vinblastine	173 ± 27
Vincristine	179 ± 32
Doxorubicin	131 ± 13
Daunorubicin	95 ± 25
Mitoxantrone	90 ± 20

EC$_{50}$ of **18** on reversing P-gp mediated drug resistance towards various anti-cancer drugs are shown. Results were obtained from LCC6 MDR cell lines *in vitro* (Chan et al. 2012)
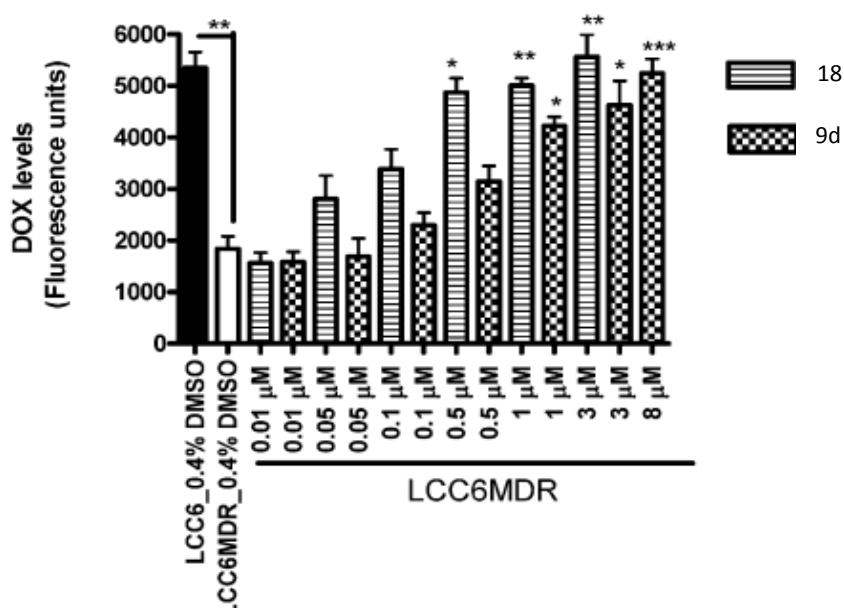
Figure 1-8 Intracellular DOX accumulation of **18** and **9d** in LCC6 MDR cell line.

Intracellular DOX accumulation of LCC6 MDR cells can be increased by **18** and **9d**. **18** is a more potent P-gp modulator than **9d**. At 0.5 μM concentration, **18** is capable of restoring DOX level back to wild type level (Chan et al. 2012).

The effect of overexpressing P-gp in lower intracellular level of anti-cancer drugs is evident. We demonstrated that intracellular level of doxorubicin was lowered in P-gp overexpressed LCC6 MDR cancer cell line when compared to wild type LCC6 cancer cell line. The data suggested that the reduced intracellular level of doxorubicin attributed to the active efflux of overexpressed P-gp. We investigated whether **18** was capable of modulating P-gp and thus changes the intracellular concentration of doxorubicin. Data suggested that intracellular doxorubicin accumulation in P-gp overexpressed cell line can be increased by co-treatment with **18** in a dose dependent manner (Figure 1-8). Accumulation level of doxorubicin can be restored to a level comparable to that of wild type cell line when 0.5 μM of **18** was added (Figure 1-8). This suggested that **18** is effective in modulating P-gp to increase intracellular level of doxorubicin.

1.5   OBJECTIVES OF THE CURRENT PROJECT

- The first objective of this project is to study the pharmacokinetic properties of **18** *in vivo*. Together with our preliminary data, information from pharmacokinetics study will be used to determine dose regimen needed to reverse P-gp mediated drug resistance in *in vivo* xenograft studies.

- The second objective of the project is to investigate the metabolism of **18** and identify the metabolites of **18** by means of *in vitro* metabolism study using human and rat liver microsomes. P-gp modulating activities of the metabolites were determined *in vitro*.

- The third objective of the project is to characterize the pharmacokinetics properties of **FM04**, one of the active metabolites of **18**, and to investigate the *in vivo* efficacy of **FM04** in enhancing oral bioavailability of PTX by modulating P-gp in the GI tract. *In vivo* efficacy of **18** in enhancing oral bioavailability of PTX is studied as well. The long term goal is to investigate the possibility of delivering PTX orally with the help of **FM04** or **18**.

2 PHARMACOKINETICS STUDY ON FLAVONOID DIMER **18** AND DOSE REGIMEN DESIGN FOR *IN VIVO* EFFICACY STUDY

2.1 INTRODUCTION

We have previously reported that flavonoid dimers are active in reversing P-glycoprotein (P-gp) mediated drug resistance *in vitro* (Chan et al. 2006; Chan et al. 2009). Previous SAR study revealed that hydrophobic substitution generally increased P-gp modulating activity of flavonoid dimers (Chan et al. 2009). The resultant increase of hydrophobicity, however, created an obstacle for further development as a drug candidate. Lead optimization led to the discovery of flavonoid dimer, **18**, which possessed favorable *in vitro* P-gp modulating activity and improved aqueous solubility when prepared in hydrochloride salt form (Chan et al. 2012). Here, pharmacokinetics characterization of **18** was conducted on a validated, reliable and sensitive UPLC-MS/MS method.

The fate of a drug candidate inside the body is governed by 4 stages, absorption, distribution, metabolism and elimination (ADME). The study of these stages by means of a plasma concentration profile against time on a mathematical basis is called pharmacokinetics. Administration of drug candidates via intravenous route bypasses

absorption and undergoes DME stages only. In contrast, drug candidate administered via oral or other parenteral routes such as intramuscular, intraperitoneal or subcutaneous undergoes absorption before reaching the systemic blood circulation for distribution, metabolism and elimination. A well-planned pharmacokinetics study can establish *in vitro-in vivo* correlation and thus allow proper design of dose regimen. Application of pharmacokinetics is particularly useful for early preclinical drug discovery, when not much *in vivo* information is known for a drug candidate. Both compartmental modeling and noncompartmental analysis are used for pharmacokinetics study (Gillespie 1991). Compartmental modeling has a longer history but less convenient as it suffers from the need to identify model parameters for model confirmation (Gillespie 1991). On the other hand, noncompartmental analysis is more convenient as it implies a mathematical description on the plasma concentration profile against time for pharmacokinetics study (Gillespie 1991).

Accurate determination of plasma concentration is needed for pharmacokinetics study. The use of ultra performance liquid chromatography tandem mass spectrometry (UPLC-MS/MS) and internal standard for detection is commonly used in industry for good specificity, accuracy and sensitivity (Borges et al. 2011; Pabbisetty et al. 2012; Sun et al. 2012). Given the hydrophobicity nature of flavonoid dimers, normal phase separation

provided advantage on detection and analysis by HPLC-DAD in our preliminary PK study. Flavonoid dimer **18** was first time ever detectable in animal plasma samples in the preliminary PK study. This leads up to the development of high accuracy mass spectrometry analysis for quantification of **18**. Mass spectrometry analysis is more compatible with reverse phase separation. Therefore reverse phase separation was employed for mass spectrometry analysis and quantification of **18**. Separation and detection is done on an Acquity Waters UPLC interfaced with triple quadrupole mass analyzer (Micromass model Quattro Ultima) equipped with an electrospray ionization source in positive mode.

Ultra performance liquid chromatography (UPLC) is an advancement of high performance liquid chromatography (HPLC). The columns of UPLC is more practical than HPLC in terms of having high quality small porous packing material and capable of operating under very high pressure (Gumustas et al. 2013). The particle size of UPLC columns is less than 2µM while the particle size of HPLC columns is generally 3-5µM. According to the van Deemter equation, with regard to the relationship between flow rate and column efficiency, reducing the particle size to less than 2µM leads to significant gain in efficiency and analysis time (Gumustas et al. 2013). The shorter analysis time is beneficial for mass spectrometry analysis by increasing peak

concentration and at the same time reducing chromatographic dispersion(Gumustas et al. 2013).

Mass spectrometer equipped with electrospray ionization (ESI) was employed in this study. A strong electrical field (3000V) is applied to the sample eluted off UPLC, resulting in formation of charged droplets. Desolvation temperature of ESI is set to 350°C, which allows solvent to evaporate from the surface of the charged droplets. The size of the droplet decreases until the repulsion between the charges on the surface exceeds the surface tension; ions are ejected into the gas phase and reach the mass analyzer.

Triple quadrupole mass analyzer is used for quantification in the current study. Ion of interest is selected by radio frequency (RF) and constant DC voltages using 2 sets of four precisely-positioned parallel rods. The set up of triple quadrupole includes 2 quadrupole analyzers connected with a collision chamber (Figure 2-1) and (Figure 2-2). The field on the quadrupole determines which particular ion with selected mass over charge ratio (m/z) to reach the detector. The combination of 2 quadrupoles has great advantage on quantification by multiple reaction monitoring (MRM). Under MRM condition, both quadrupoles 1 and 2 are static. Only selected parent ions and daughter

ions are allowed to pass through quadrupole 1 and quadrupole 2, respectively. Under

this configuration the specificity and signal to noise ratio can be greatly improved.
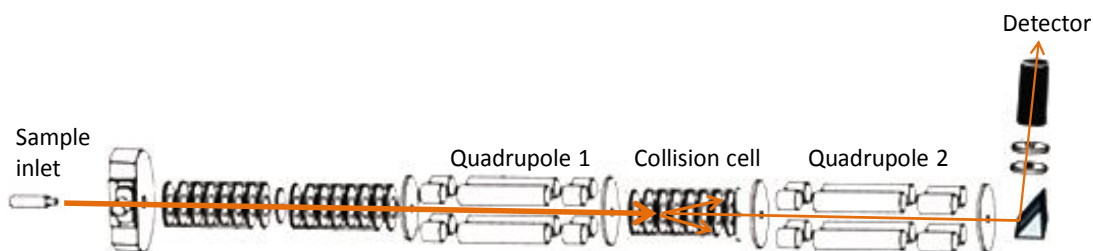
Figure 2-1 Scheme diagram of triple quadrupole mass analyzer for multiple reaction monitoring (MRM)

Sample from UPLC enters mass spectrometer through sample inlet and ionizes by electrospray ionization. The ion of interest is selected base on the mass over charge ratio (m/z) in quadrupole 1. Only selected ions of particular m/z reaches collision cell for collision induced decomposition (CID) by argon gas. Following CID, daughter ions are formed and will be selected during the second quadrupole. Signals reaching the detector will be digitalized and amplified.
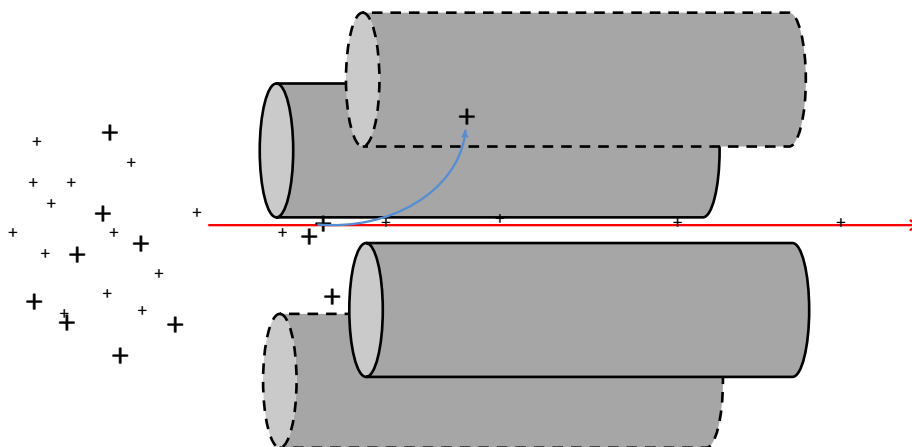
Figure 2-2 Scheme diagram of ion selection by quadrupole mass analyzer

Quadrupole mass analyzer consists of four precisely parallel rods operating in 2 pairs with 2 different setting. One pair of the rods is connected at same DC and superimposed RF voltages (the pair shown in dashed line). While the other pair of rods (the pair shown in solid line) operates in opposite DC voltage and a RF field with phase shifted by 180°. The electric field controls ions with particular mass over charge ratio (m/z) to pass through.

To improve the specificity and accuracy for quantification for UPLC-MS/MS study, internal standard method has been employed. Known amount of deuterium labeled **18** (named as **D7 NBn**) will be added to plasma samples for quantification of **18**. Plasma concentration of **18** will be quantified with reference to the peak area ratio of **18** to **D7-NBn**. By using **D7 NBn** (a deuterium labeled isotope of **18**) as an internal standard separation, co-elution of **18** and **D7-NBn** can be achieved to further minimizing the experimental variables and leads to a more accurate and precise analysis by avoiding the background noise and endogenous interferences.

2.2 MATERIALS AND METHODS

2.2.1 MATERIALS AND REAGENTS

All reagents or solvents used were either analytical or high-performance liquid chromatography (HPLC) grade and were purchased from Tedia. Acquity UPLC BEH C8 (2.1 x 50mm, 1.7μM) purchased from Waters was used for separation. Flavonoid dimers, **18** and **D7 NBn,** used in this project are synthesized in our lab. Purity of all compounds used in this project is >98%. Compounds **18** were weighed and prepared to a concentration of 0.5 mg/ml in methanol and Milli-Q water (50:50, v/v) with 0.5% TFA for standard curve construction and quality control samples. **D7 NBn** was prepared at a concentration of 10 μg/mL in methanol and Milli-Q water (50:50, v/v) with 0.5% TFA as internal standard. **18** was prepared in 14% Cremophor, 14% ethanol and 72% saline at a concentration of 4 mg/ml for all animal studies.

2.2.2 ANALYTICAL METHOD FOR THE DETECTION OF **18** BY UPLC-MS/MS

The UPLC-MS/MS system consists of an Acquity Waters UPLC interfaced with triple quadrupole mass spectrometer (Micromass model Quattro Ultima) equipped with an

electrospray ionization source in positive mode. Multiple reaction monitoring (MRM) was set to monitor the transitions for **D7 NBn** [M +H]$^+$ and **18** [M +H]$^+$ at 731>449m/z and 724>114m/z, respectively. The collision energy, cone voltage, source temperature, desolvation temperature and capillary voltage are 30, 30, 150°C, 350°C and 3Kv, respectively. The cone gas and desolvation gas was 150L/Hr and 600L/Hr, respectively.

The chromatography separation was done on an Acquity UPLC BEH C8 column (2.1 x 50mm, 1.7μM). The mobile phase consists of methanol + 0.1% formic acid (solvent B) and Milli-Q water + 0.1% formic acid (solvent A). The flow rate was 0.4 ml/min. The initial condition was 90% solvent A and 10% solvent B. After 1 minute elution by initial condition, a linear gradient was performed with solvent B increasing from 10% to 100% for 10 minutes. Following so, solvent B was gradually decreased from 100% to 10% in 3 minutes; the mobile phase was restored to initial condition at 13th minutes for re-equilibration. **18** and **D7 NBn** were eluted at 2.97 minutes. Including re-equilibrium, the total analysis time was 20 minutes per injection.

2.2.3 STANDARD CURVES FOR LC-MS/MS

Compound **18** in methanol and Milli-Q water (50:50, v/v) with 0.5%TFA at 0.5mg/ml was used for standard curve construction. A series of **18** working stocks from 10 µg/mL to 0.0195 µg/mL was prepared by serial dilutions in methanol and Milli-Q water (50:50) with 0.5% TFA stock solution. Ten microliter of the working stocks are spiked to 90 µL of blank plasma to form standard solutions of 1 µg/mL to 0.00195 µg/mL for standard curve construction. Five microliter **D7 NBn** internal standard stock solution at 10 µg/mL was added to all spiked plasma. All spiked plasma was processed as indicated previously.

2.2.4 VALIDATION

The current UPLC-MS/MS methods have been validated in terms of accuracy, precision, stability, specificity and selectivity. Pooled blank plasma from 6 animals was used analyzed to determine the specificity and selectivity. Stability of the extracted samples in the -20°C storage condition and the internal standard storage at -20°C were determined. The accuracy and precision of the current method was illustrated by intra-day and inter-day analysis of quality control samples. Aliquots of plasma spiked with **18**

of 500, 62.5, 3.9ng/ml were used as quality control samples (QC). The QC samples were prepared similarly as the standard curve solutions. QC samples were processed and analyzed on 5 different days and 5 consecutive injections on the same day to determine the inter-day and intra-day variations, respectively.

2.2.5   SURGICAL PROCEDURE

Right jugular vein cannulation was done on male Sprague-Dawley rats (220g-300g). The rats were housed individually per cage in 23 ±2 °C with relative humidity of 50-60% and 12 hour lighting. Prior to conducting the cannulation surgery, the rat is anesthetized by inhalation of ethyl ether in air tight jar. The cannulation surgery is conducted as previously reported, with slight modification (Bardelmeijer et al. 2003). In brief, a piece of polyethylene tubing (0.46mm ID, 0.91mm OD) was inserted into the right jugular vein a day before blood sampling. The depth of polyethylene tube inserted into the jugular vein might vary between animals. The tube is inserted carefully with sufficient depth to ensure smooth blood sampling. After optimum insertion, the tube is secured to the vein by threads. Following so, with aid of a 15G needle, the polyethylene tubing was directed towards the dorsal side of the neck subcutaneously to reach a small

incision made at the back of the head. The 15G needle is only used to direct the polyethylene tubing through the skin. After this process, the needle is removed.

To prevent the animal from damaging the cannulation setting, the polyethylene tubing was tunneled through a metal spring. Finally, all incisions and openings on the animal for this surgery were closed by stitches.

The cannula was flushed with 0.20 ml heparinized saline (250 units/mL) daily until the day of experiment. Free access to water was provided to the rat overnight and in the absence of severe discomfort, drug would be administrated for corresponding studies.

2.2.6   PHARMACOKINETICS STUDY OF **18**

Pharmacokinetics study of **18** was done on SD rats (n=3-5). Animals were administered with **18** either by tail vein injection or intra-peritoneal injection, blood samples (approx. 200uL) were taken via jugular vein at 10, 30, 60, 120, 240 and 420 minutes post administration (for dosage of 2.5mg/kg, experiment was terminated at 240minutes). Blood samples were centrifuged at 16,100g for 10 minutes to obtain plasma. One

hundred µL aliquots of blood samples were spiked with 5 µL of internal standard (**D7-NBn,** 10 µg /ml). Samples were stored at -20°C until further analysis.

2.2.7 PLASMA SAMPLE PRETREATMENT FOR UPLC-MS/MS ANALYSIS

Plasma samples were brought to room temperature. Five microliter of 15 M sodium hydroxide solution was added to the sample and mixed thoroughly. Sample cleanup was done by liquid-liquid extraction using 1 mL of ethyl ether. Organic solvent from liquid-liquid extraction was transferred to a new tube and dried under mild heating at 60°C. Extraction by ethyl ether was done trice. Prior to UPLC/MSMS analysis, samples were reconstituted in 100 µL methanol with 1% TFA and filtered through a 0.22 µm syringe filter.

2.2.8 PHARMACOKINETICS ANALYSIS

Plasma concentration-time profiles were analyzed by non-compartmental analysis. The area under the plasma concentration-time curve by trapezoid rules (AUC) (from 0 to

infinity), the elimination half life ($t_{1/2 \ \beta}$), absorption or distribution half life ($t_{1/2 \ \alpha}$), apparent volume of distribution (V_d), systemic clearance (CL), mean residence time (MRT), maximum observed concentration (C_{max}) and time to maximum concentration (T_{max}) were calculated by PK Solutions 2.0 (Summit Research Service, Ashland, U.S.A). Bioavailability (F) was calculated by the dose normalized ratio of AUCs from IP and IV administration.

2.3   RESULTS AND DISCUSSION

Plasma concentration profile and noncompartmental pharmacokinetics analysis was conducted for **18** using rodent models**.** Plasma concentration of **18** was determined using a validated UPLC-MS/MS setting with multiple reaction monitoring (MRM). Using pure compounds MRM for **18** and **D7 NBn** was selected based on stable daughter ion spectra of **18** and **D7 NBn.** Fragments 114m/z and 449m/z yields the most stable fragments for **18** and **D7 NBn**, respectively (Figure 2-3).

Once the determination method for pure compounds were established, we added rat plasma to **18** or **D7 NBn** to determine if rat plasma could interfere with signal on UPLC-MS/MS. Separation was done by C8 UPLC column, the retention time for **18** and **D7 NBn** was 2.97 and 2.95 minutes, respectively (Figure 2-4). No endogenous interferences was

detected when **18** was spiked to rat plasma (Figure 2-4). The peak shape and symmetry of **18** and **D7 NBn** was good. No carry over was observed under the current setting. The standard curve constructed by **18** (m/z 724>114) and **D7 NBn** (m/z 731>449) fitted well in a quadratic equation with a R^2 of 0.9991 (Figure 2-5). The dynamic range for this standard curve in our study was 1μg/mL to 0.0039μg/mL. The lowest concentration detected under the current setting is 0.0039μg/mL.

To investigate if sample stability can be maintained, the **D7 NBn** stock solution and quality control (QC) samples were analyzed for intra-day (5 consecutive injections on same day) and inter-day variations (injections on 5 consecutive days), respectively. The internal standard **D7 NBn** stock solution was stable for 5 days at 4ºC with a RSD of less than 15%. A consistent 55% recovery was noted for the QC samples. The intra-day and inter-day results suggested that the current method was capable of quantifying plasma samples within the acceptable limits of ±15% in high (500 ng/ml) and medium (62.5 ng/ml) concentrations. Acceptable limit for LOQ range (3.9ng/ml) was ±20% (Table 3).

(A)
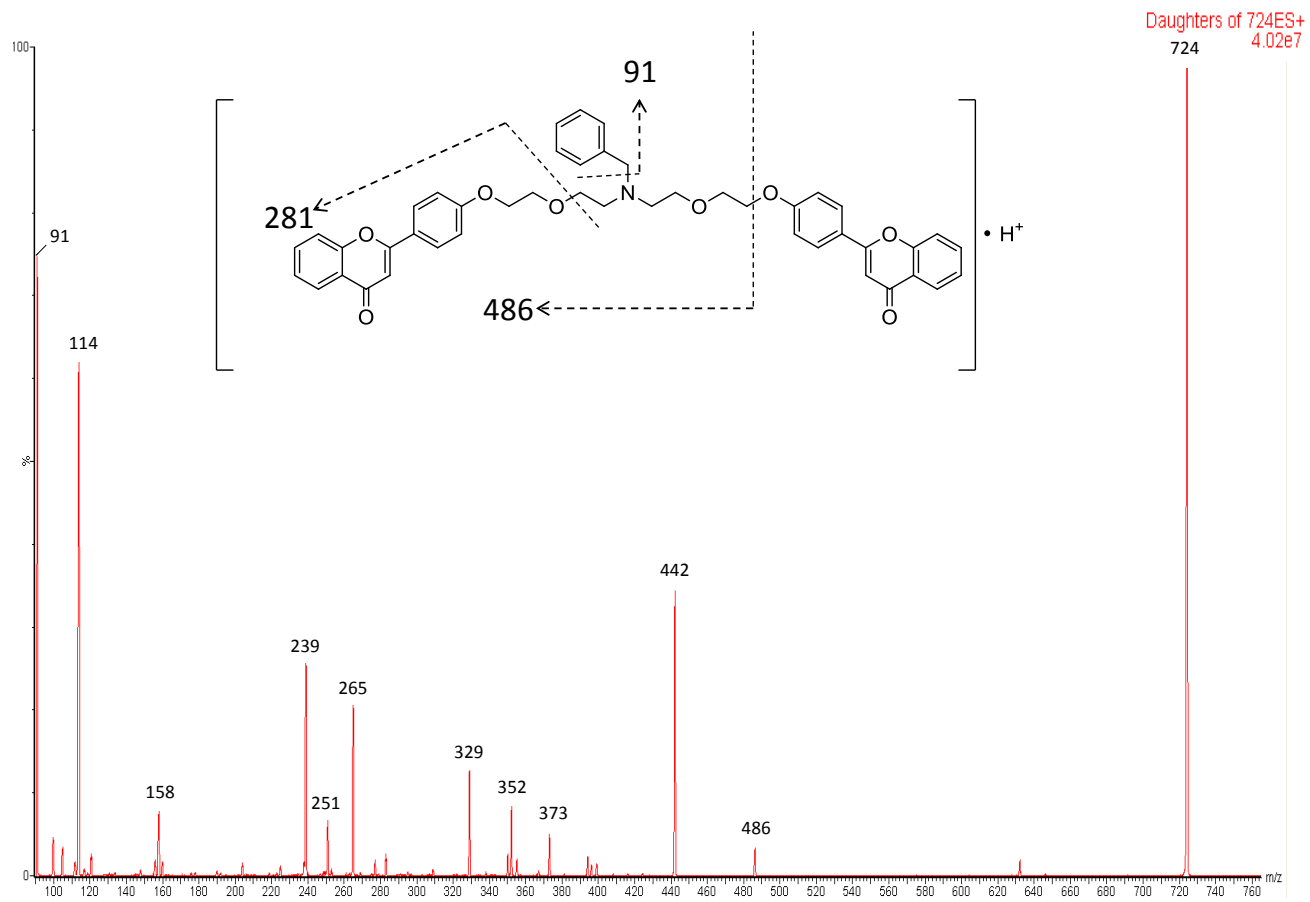
(B)
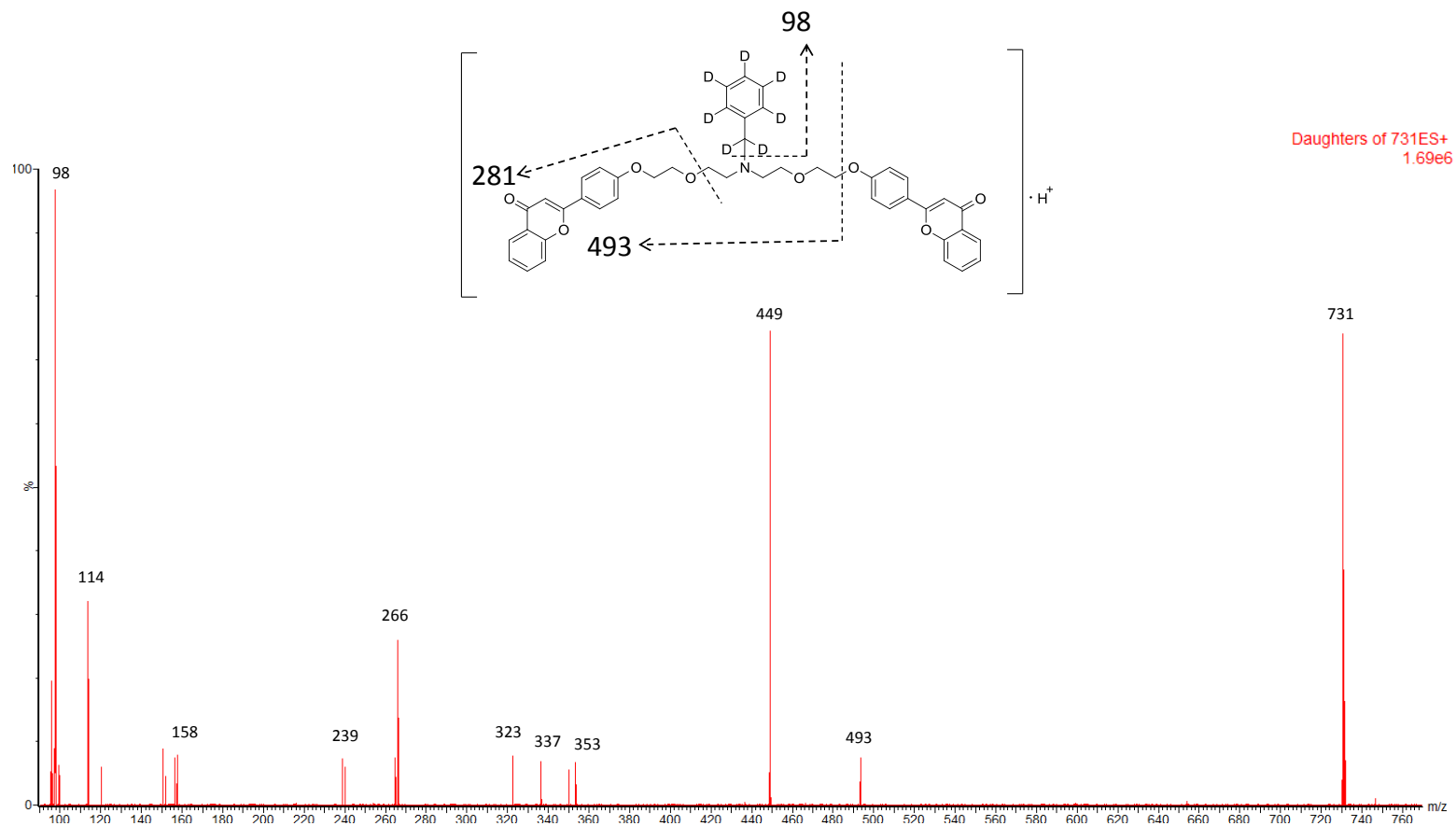
Figure 2-3 Product ion spectra of **18** and **D7 NBn.**

Standard solutions of **18** and **D7 NBn** were subjected to MS/MS analysis. (A) Mass spectrum of **18** (MSMS724 m/z) and (B) mass spectrum of **D7 NBn** (MSMS731 m/z). Same collision energy was employed for both analyses. Predicted fragmentation sites are shown with dashed lines with the m/z of resultant daughter ions shown. The most stable fragments for **18** and **D7 NBn** are m/z = 114 and 449, respectively.

(A)

(B)

38
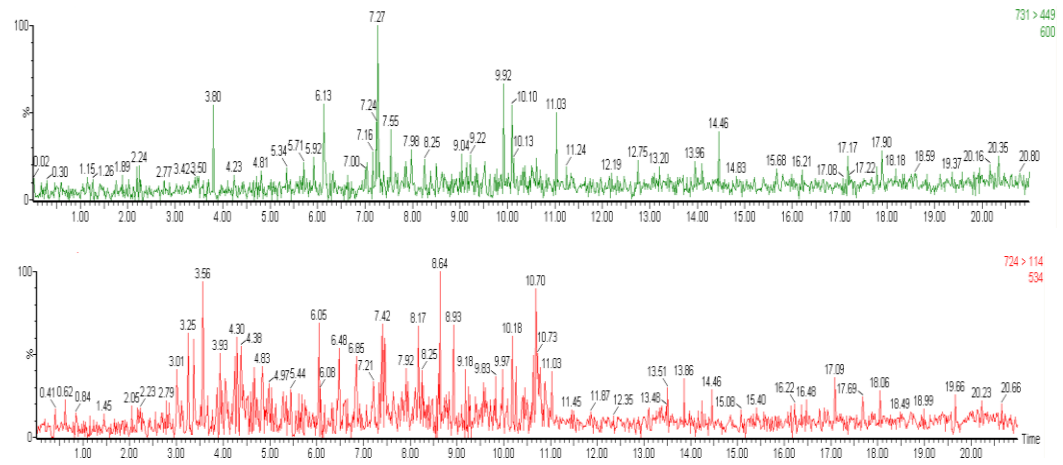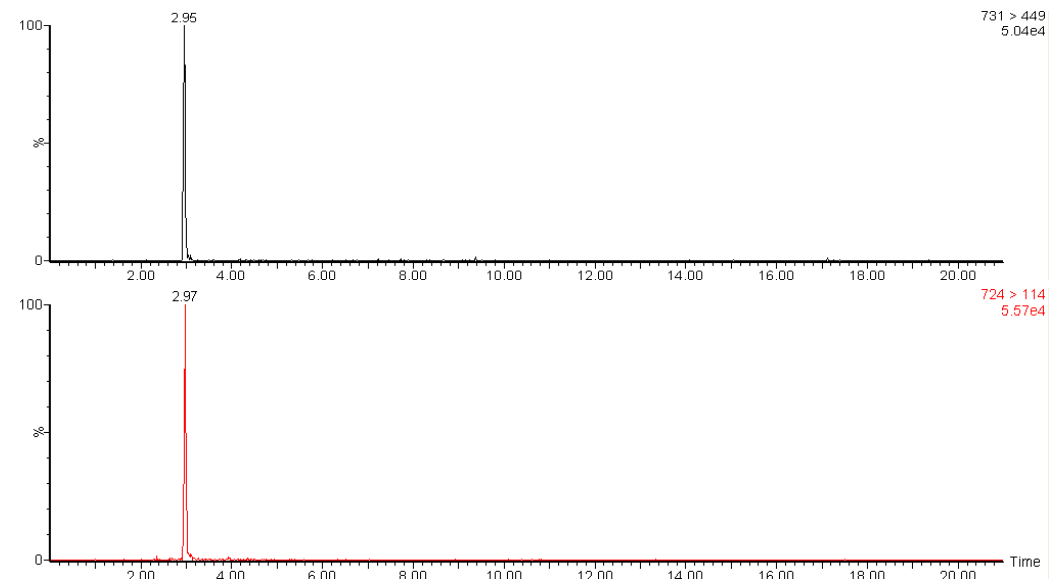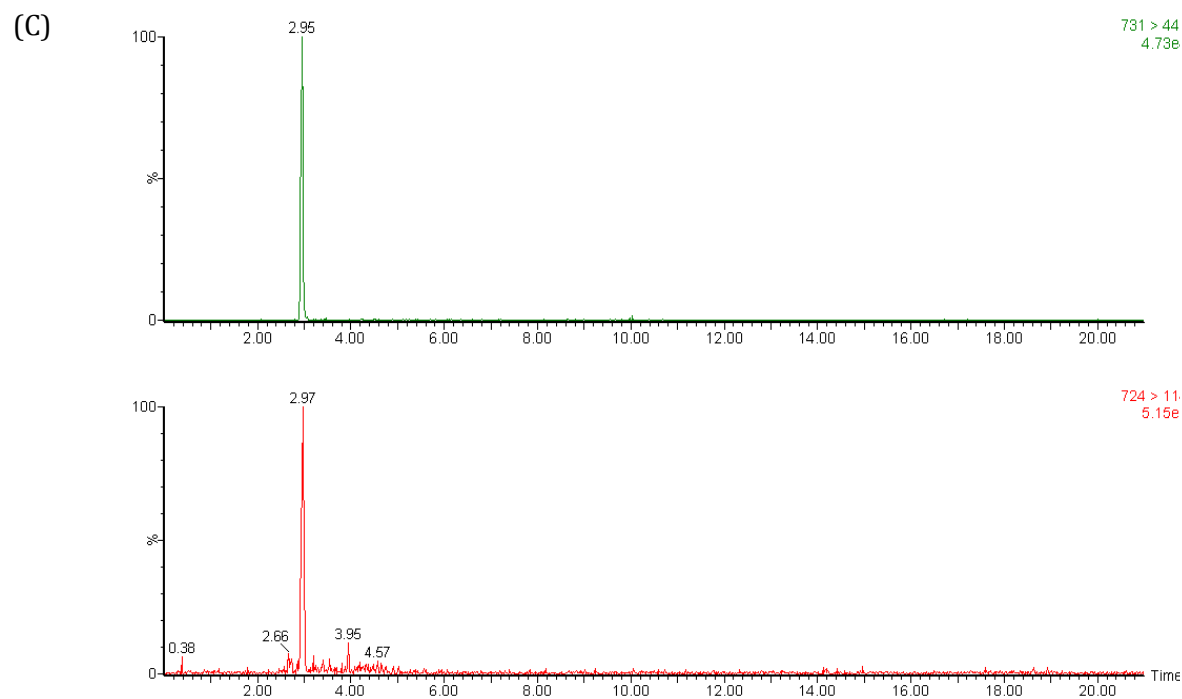
Figure 2-4 Chromatogram of plasma spiked with **18** and **D7 NBn** on UPLC-MS/MS

UPLC-MS/MS was performed on **18** and **D7 NBn**. (A), Chromatogram of blank rat plasma. (B), Chromatogram of blank rat plasma spiked with **18** (0.5 μg/mL) and **D7 NBn** (0.5 μg/mL). (C) Chromatogram of blood plasma sample at 30 minutes from SD rat dosed with 5 mg/kg **18** through IP administration.
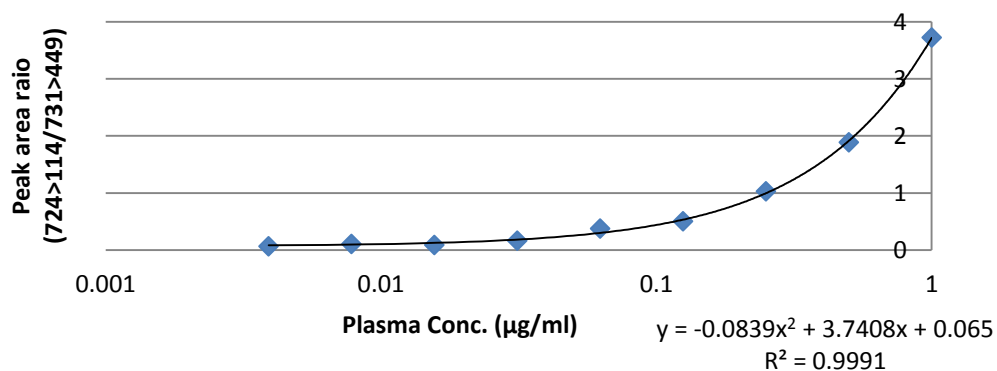
Figure 2-5 Standard curve of **18** on UPLC-MS/MS

Plasma concentration of **18** is quantified by monitoring the peak area ratio of **18** (724>114) against **D7 NBn** (731 >449) in spiked plasma.

Table 3 Intra-day and inter-day precision and accuracy for detection of **18** by UPLC-MS/MS.

Spiked conc. (µg/mL) [a]	Intra-day				Inter-day			
	Detected conc. (µg/mL) [b]	SD [c]	RSD [c/b]	RE [(b-a)/a]	Detected conc. (µg/mL) [d]	SD [e]	RSD [e/d]	RE [(d-a)/a]
0.5000	0.5047	0.0288	5.7%	0.9%	0.5561	0.0256	4.6%	11.2%
0.0625	0.0645	0.0052	8.0%	3.3%	0.0646	0.0088	13.6%	3.4%
0.0039	0.0044	0.0005	11.4%	12.4%	0.0032	0.0004	12.5%	-16.9%

The detection method was verified by quantifying QC samples on intra-day and inter-day basis. Intra-day analysis (n=5) was done by 5 consecutive analysis of the same sample with known concentration on the same day. FDA guidance for bioanalytical method validation (2001) suggested a deviation of less than 15% for high (0.5µg/mL) and mid concentration range (0.0625 µg/mL) and a deviation of less than 20% for lower limit of quantification (0.0039µg/mL) samples. Inter-day analysis (n=5) was done by analyzing spiked solution for 5 consecutive days. SD = standard deviation; RSD = relative standard deviation; RE = relative error.

After we have established the UPLC-MS/MS method and that it is suitable for quantitation of **18**, we performed pharmacokinetics studies of **18** in SD rats. Plasma concentration profiles of **18** were analyzed by non-compartmental analysis. Intravenous administration of **18** at 2.5 mg/kg demonstrated zero order kinetics while IV administration of **18** at 5 mg/kg demonstrated first order kinetics (Figure 2-6). The normalized AUC (AUC/dose) suggests a non-linear plasma pharmacokinetics of **18** following IV administration. Detailed PK parameters are summarized in Table 4. The Vd was significantly lower at 5 mg/kg (IV) when compared to 2.5 mg/kg (IV), suggesting a reduced tissue distribution and a higher initial plasma concentration. No distribution phase was observed at 2.5 mg/kg. Overall, increased dose of **18** (5 mg/kg) resulted in non-linear pharmacokinetics of **18**, reduced tissue distribution, lowered clearance and non-linear drug exposure. The non-linearity of **18** may have been attributed by CremophorEL. Cremophor EL was previously reported as the cause of pharmacokinetics non-linearity of PTX by increasing the affinity of PTX to plasma components (Sparreboom et al. 1996; van Tellingen et al. 1999) .

We have also administered **18** via intra-peritoneal route. Intra-peritoneal bioavailability at 5 mg/kg was 45%. IP administration of **18** demonstrated a longer $T_{½\,\alpha}$ and $T_{1/2\,\beta,,}$ when compared to IV administration of **18** (Table 4),

reflecting **18** was continuously being absorbed from peritoneal cavity. In the application to reverse MDR *in vivo*, this is advantageous in maintaining the plasma concentration of **18** for P-gp modulation.

The *in vitro* EC_{50} of **18** on modulating P-gp mediated MDR with PTX was 148 ± 18 nM and the IC_{50} cytotoxicity of **18** on L929 mouse fibroblast was 85 ± 5 μM (Chan et al. 2012). Plasma concentration of **18** equivalent to 148 nM and 85 μM is approximately 100 ng/ml and 61.46 μg/ml, respectively (Mw of **18** is 723 g/mol). Taking into account of our preliminary pharmacokinetics on **18** (data not shown), we hypothesize that increasing the dose of **18** to 45 mg/kg via IP administration can achieve higher C_{max} and maintain plasma concentration of **18** for longer duration. We think that maintaining plasma concentration of **18** above EC_{50} is advantageous for *in vivo* P-gp modulation and therefore, for further xenograft efficacy study, **18** should be administered via IP at 45 mg/kg or above to ensure sufficient P-gp modulation.
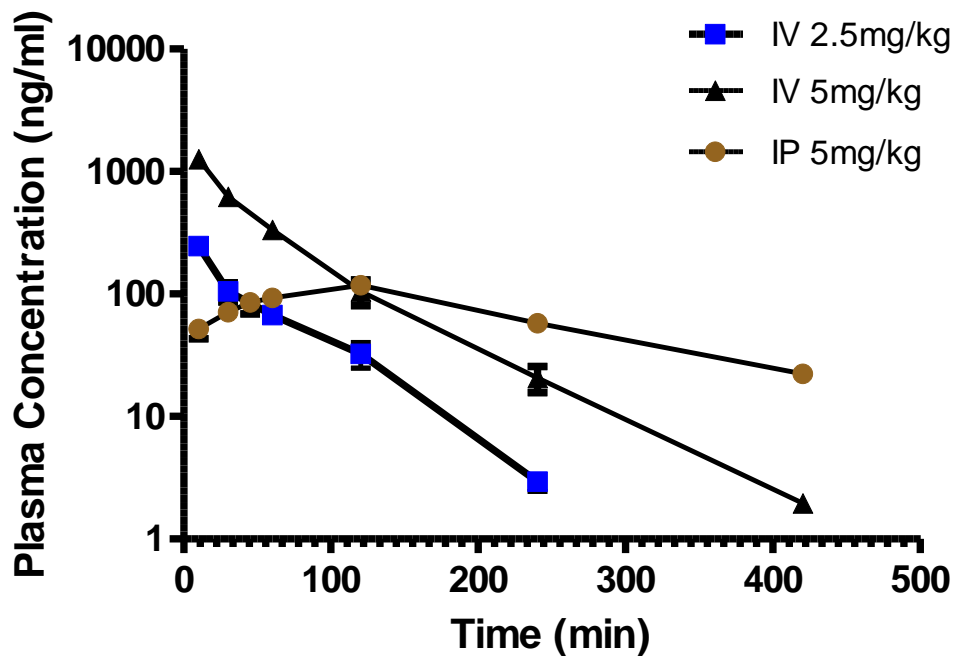
Figure 2-6 Plasma concentration-time profiles of **18** administered to SD rats.

Plasma concentration of **18** was quantified with peak area ratio of **18** against **D7-NBn** by UPLC-MSMS. Noncompartmental pharmacokinetics analysis of **18** was conducted on SD rats. Each time point represents mean ± SEM. Plasma concentration profile of **18** via IV (2.5 mg/kg, n=3), IV (5 mg/kg, n=4), and IP (5 mg/kg, n=5) were used to assess the pharmacokinetics linearity of **18** via tail vein administration and bioavailability of **18** via IP administration.

Table 4 Pharmacokinetics parameters of **18** in rats, analysis by UPLC-MS/MS.

18	IV (n=3)	IV (n=4)	IP (n=5)
Dose (mg/kg)	2.5	5	5
AUC $_{(0\text{ - infinity})}$ (ng-min/ml)	14470 ± 3593	71264 ± 18388	32248 ± 4848
AUC/DOSE	5788	14253	6450
AUC $_{(0\text{-}t)}$ (ng-min/ml)	14397 ± 3681	70349 ± 18145	28278 ± 3297
Vd (ml/kg)	10670 ± 3355	5550 ± 1018	-
CL (ml/min/kg)	180 ± 42	74 ± 18	-
MRT (min)	56 ± 4	49 ± 9	210 ± 32
T $_{½\,α}$ (min)	-	15 ± 6	38 ± 11
T $_{1/2\,β}$ (min)	39 ± 5	54 ± 10	123 ± 27
C $_{max}$ (ng/ml)	-	-	132 ± 21
T $_{max}$ (min)	-	-	93 ± 37
Bioavailability (%)	-	-	45[1]

Plasma-concentration profile was obtained from 2 routes of administration (IV and IP) (Figure 2-6). Non-compartmental pharmacokinetics analysis of **18** in SD rats was performed by PK solutions 2.0 (Summit Research Service, Ashland, U.S.A). PK parameters Vd and CL following IP administration is affected by the percentage of absorption and is suggested to be considered as a valid parameter given absorption is complete. Since percentage of absorption through IP administration has not been validated, Vd and CL are not listed in the PK parameters following IP administration.

[1] IP bioavailability is obtained by comparing AUC $_{(infinity,\,IV)}$ of **18** at 5mg/kg with AUC $_{(infinity,\,IP)}$ of **18** at 5mg/kg

2.4 CONCLUSION

To conclude, an UPLC-MS/MS method for detecting flavonoid dimers, **18**, has been optimized and validated. The use of **D7 NBn** as internal standard allowed accurate measurement of **18** with good selectivity, accuracy and precision. Non-compartmental pharmacokinetics analysis on **18** has been conducted in rats. IP administration of **18** was advantageous in maintaining plasma concentration for P-gp modulation as well as for its convenience of administration in future *in vivo* studies. Further studies will be conducted with **18** to extrapolate the potential of developing **18** as a P-gp modulator for clinical use.

3 IN VITRO METABOLISM AND METABOLITE IDENTIFICATION OF FLAVONOID DIMER **18** IN HUMAN AND RAT

3.1 INTRODUCTION

Flavonoid dimers can reverse P-gp and MRP1 mediated drug resistance *in vitro* (Chan et al. 2006; Wong et al. 2007; Chan et al. 2009; Wong et al. 2009; Chan et al. 2010). Not only can flavonoid dimers reverse P-gp mediated drug resistance at nanomolar range (Chan et al. 2012) they also have promising anti-leishmanial activity (Wong et al. 2007; Wong et al. 2012). Pharmacokinetics of flavonoid dimer **18** has been conducted in SD rats (Chapter 2). Metabolism and metabolite identification is another important part of drug discovery and development. Metabolite identification is necessary for clinical study (Baranczewski et al. 2006). Early incorporation of metabolite identification is advantageous on discovery of active metabolites or identification of "metabolic soft spots" of compounds with low metabolic stability (Baranczewski et al. 2006). Generation of metabolites by *in vitro* liver microsomes incubation followed by detection of metabolites by LC-QTOF tandem mass spectrometry has helped metabolite

identification studies. This approach has been used in this study to identify the metabolites of **18**.

Detoxification begins when xenobiotics reach the animal host. In general, drug metabolism (or biotransformation) for detoxification is briefly categorized into 2 phases, namely phase I and phase II metabolic reactions (Brandon et al. 2003; Asha and Vidyavathi 2010).

Phase I metabolic reaction induces small changes like oxidation, reduction and hydrolysis in order to reduce the hydrophobicity or drug, thereby facilitating better elimination from the body (Brandon et al. 2003; Ramanathan et al. 2005).

Phase II metabolic reactions generally involves modification of functional groups by glucuronidation, sulfation or conjugations (by glutathione or amino acid) (Ramanathan et al. 2005). Phase II reaction often leads to greater aqueous solubility of drugs, thereby facilitating subsequent excretion through urine or bile. Phase II metabolic reaction, however, by the name does not imply temporal relationship of the biotransformation. Phase II metabolic reactions can occur before phase I reactions.

Biotransformation takes place in many tissues, but liver is the most important organ for biotransformation to take place (Asha and Vidyavathi 2010). Liver

contains high abundance of oxidative enzymes cytochrome P450 (CYP450) that plays an important role in phase I oxidation (Brandon et al. 2003; Ghosal et al. 2005; Asha and Vidyavathi 2010). CYP450 is a large family of heme-containing enzymes that requires NADPH co-factors to undergo oxidation (Asha and Vidyavathi 2010). Certain *in vitro* human liver models such as isolated perfused liver, liver slices and primary hepatocytes themselves are well-established system for metabolism studies. They do not require exogenous NADPH cofactors for activity (Asha and Vidyavathi 2010). These systems, however, are limited by their complexity (Brandon et al. 2003). On the other hand, *in vitro* models such as cytosol, S9 fractions, supersomes, cell lines, transgenic cell lines and microsomes that requires exogenous NADPH cofactors for activity are more convenient to use and are more accessible (Brandon et al. 2003).

In vitro human liver microsomes (HLM) and SD rat liver microsomes (RLM) models were chosen for this study. Our objective is to understand the metabolic fate of **18** in rodents and to identify metabolites of **18**.

3.2 MATERIALS AND METHODS

3.2.1 MATERIALS AND REAGENTS

CYP M-class 50-donor pooled human liver microsomes, rat liver microsome and NADPH reagent were purchased from Research Institute for Liver Diseases (Shanghai). Zorbax Eclipse XDB-C8 (4.6 x 150mm, 5µM) was purchased from Tegent Technology. PTX was purchased from Wuhan Hezhong Biochemical Manufacture Co. Ltd. All flavonoid dimers including **18** and other synthetic compounds used in this project are synthesized in our lab. Purity of all flavonoid dimers used in this project is >98%. All other reagents or solvents used were either analytical or high-performance liquid chromatography (HPLC) grade and were purchased from Tedia. Water used in this study was prepared using Milli-Q water purification system.

3.2.2 ANALYTICAL METHOD FOR METABOLISM STUDY BY LC/QTOF-MS AND LC/QTOF TANDEM MS

The LC/QTOF-MS system consisted of a Perkin Elmer Series 200 HPLC interfaced with Applied Biosystems PE SCIEX/API QSTAR Pulsar Hybrid Quadrupole-TOF mass spectrometer equipped with an electrospray ionization source in positive mode. The mobile phase for chromatographic separation consisted of methanol + 0.1% formic acid (solvent B) and Milli-Q water + 0.1% formic acid (solvent A). The flow rate was 0.3ml/min. The initial condition was 90% solvent A and 10% solvent B. After 3 minutes, a linear gradient was applied with solvent B increasing from 10% to 100% in 65 minutes. Solvent B at 100% was then applied for 5 minutes to wash out remaining elutes. Afterwards, mobile phase was restored to initial condition for re-equilibration. A sample volume of 5 μL was injected for each analysis. MS detection for full scan LC/QTOF-MS and LC/QTOF-MSMS were done in the same instrument, the mass range of m/z 50-1900 was set for LC/QTOF-MS. The settings for LC/QTOF-MS were as follows, curtain gas, 30; gas 1, 30; gas 2, 80; desolvation temperature, 350°C; ionization voltage, 5.5Kv. The collision energy used for metabolites identification by LC/QTOF-MSMS, was, 18 - 55eV; nitrogen was used as collision gas. Data were processed by Analyst QS 1.1.

3.2.3 IN VITRO METABOLISM STUDIES

SD Rat liver microsomes, human liver microsomes and NADPH were thawed on ice before the experiment. **18** dissolved in methanol were added to 100 μL of liver microsomes (1 mg/mL) at a final concentration of 20 μM. Methanol content for each reaction was less than 0.25% to avoid metabolism interference (Chauret et al. 1998). Water was added to reach the incubation volume of 200μL. After pre-incubated at 37°C for 3 minutes, 4 μL of NADPH (final concentration of 2mM in the reaction) was added to initiate the reaction. The reaction mixture was kept at 37°C for 30 minutes. The reaction was terminated by adding ether after incubation. The reaction mixture was extracted with 1 mL ether extraction thrice. Supernatant was dried on a dry bath at 60°C. The extract was reconstituted in 100 μL of methanol and filtered through 0.22 μm syringe filter before LC/QTOF-MS analysis.

3.3 RESULTS AND DISCUSSION

We were interested in how **18** was metabolized by human liver microsomes

(HLM) and rat liver microsomes (RLM) *in vitro.* **18** was mixed with either HLM

or RLM and metabolites of **18** was extracted and analyzed by LC/QTOF-MS.

Three new peaks were found in human liver microsomes after incubation with

NADPH (Figure 3-1). We hypothesized that they were metabolites of **18** and they

were labeled as **M1, M2** and **M3**, respectively (Figure 3-1). Identical result was

obtained in RLM (Figure 3-2). The singly charged mass over charge ratio for **M1,**

M2 and **M3** were 634m/z, 416m/z and 327m/z, respectively. **M1, M2** and **M3**

were eluted before the parent compound **18** in reverse phase HPLC condition.

This suggested that they were more hydrophilic. It is possible that such

hydrophilic property will allow the metabolites to be excreted or metabolized by

phase II metabolism.
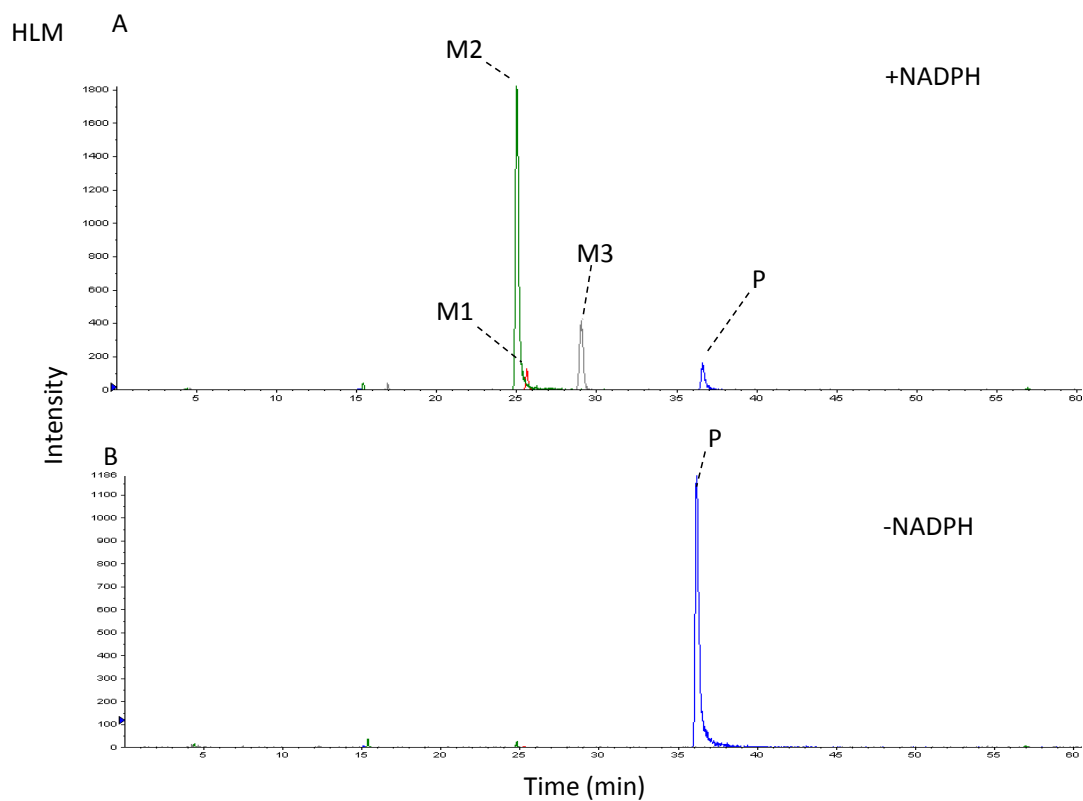
Figure 3-1 LC/QTOF-MS extracted ion chromatograms of **18** incubated with human liver microsomes (HLM)

HLM was incubated with **18** in the presence (A) or absence (B) of NADPH for 30 minutes at 37ₒC. Metabolite mixture was separated by LC/QTOF-MS. Three metabolites were found as HLM metabolites; P = **18** (m/z 724); **M1** = metabolite 1 (634m/z); **M2** = metabolite 2 (416m/z); **M3** = metabolite 3 (327m/z).
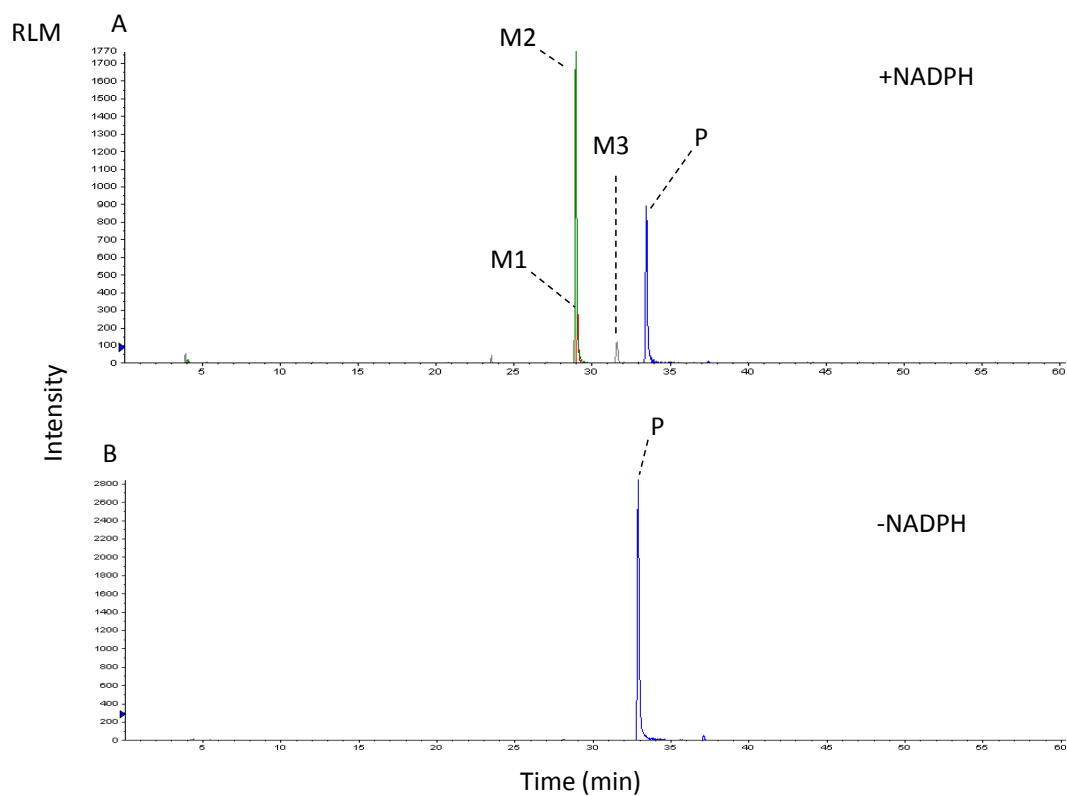
Figure 3-2 LC/QTOF-MS extracted ion chromatograms of **18** incubated with rat liver microsomes (RLM)

RLM was incubated with **18** in the presence (A) or absence (B) of NADPH for 30 minutes at 37°C. Metabolite mixture was separated by LC/QTOF-MS. Three metabolites were found as RLM metabolites; P = **18** (m/z 724); **M1** = metabolite 1 (634m/z); **M2** = metabolite 2 (416m/z); **M3** = metabolite 3 (327m/z).

Metabolite identification for **M1, M2** and **M3** was performed on the basis of LC/QTOF-MSMS product ion spectrum of **18** (Figure 3-3A). Product ion spectrum of **18** provided an overview of the MS/MS fragmentation pathway on **18** (Figure 3-3B). Product ion spectra of metabolites were compared with product ion spectrum of **18** for structure prediction. Metabolites structures were first predicted before comparing with authentic compounds.

Predicted structure of **M1** was identical to **14a** reported previously (Chan et al. 2012). We have therefore compared the MSMS fragmentation pattern of **M1** and that of **14a** and found that they were identical (Figure 3-4). The result suggested that **M1** was **14a**. **M1** has been reported to have similar modulating activity as **18** (Chan et al. 2012).

(A)
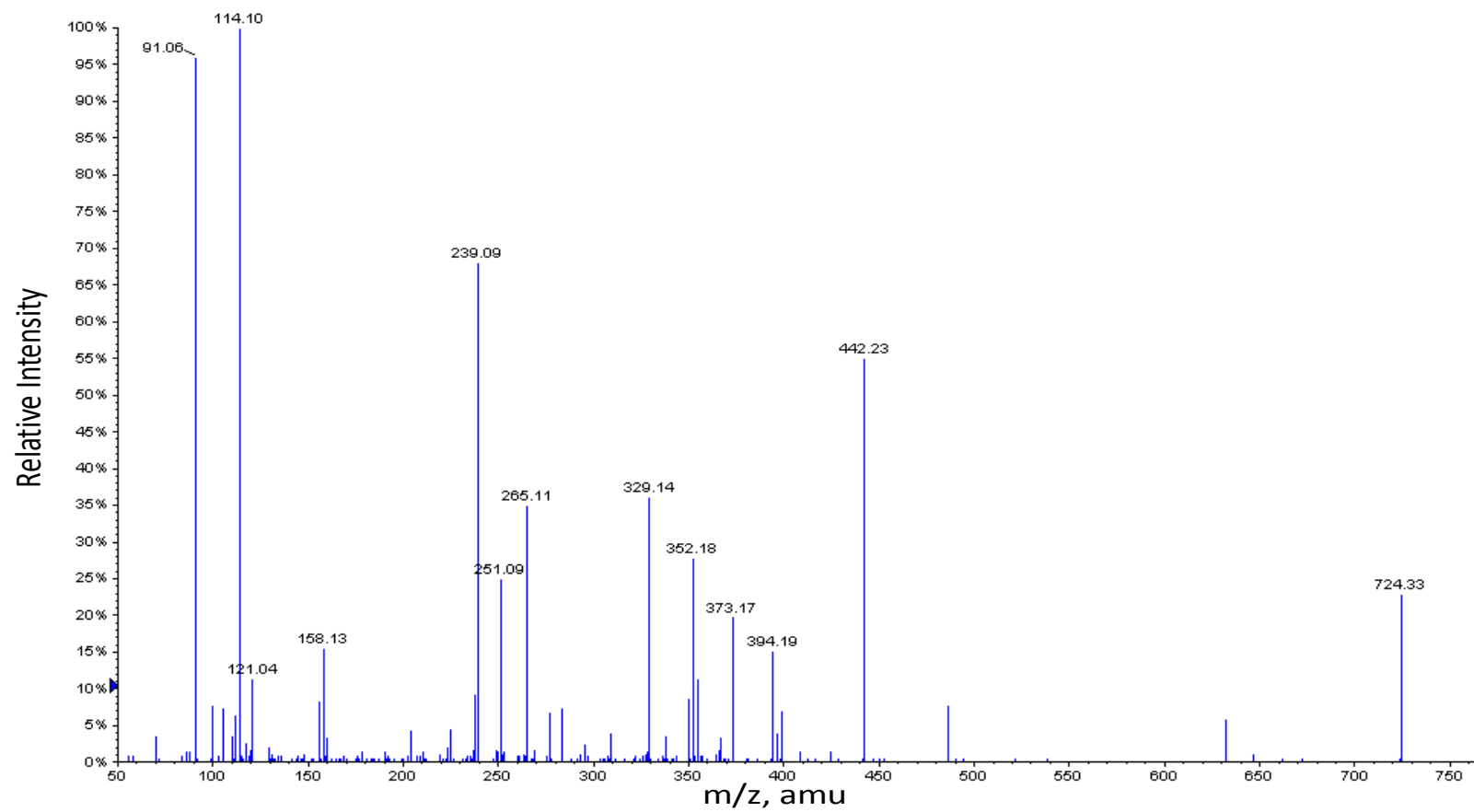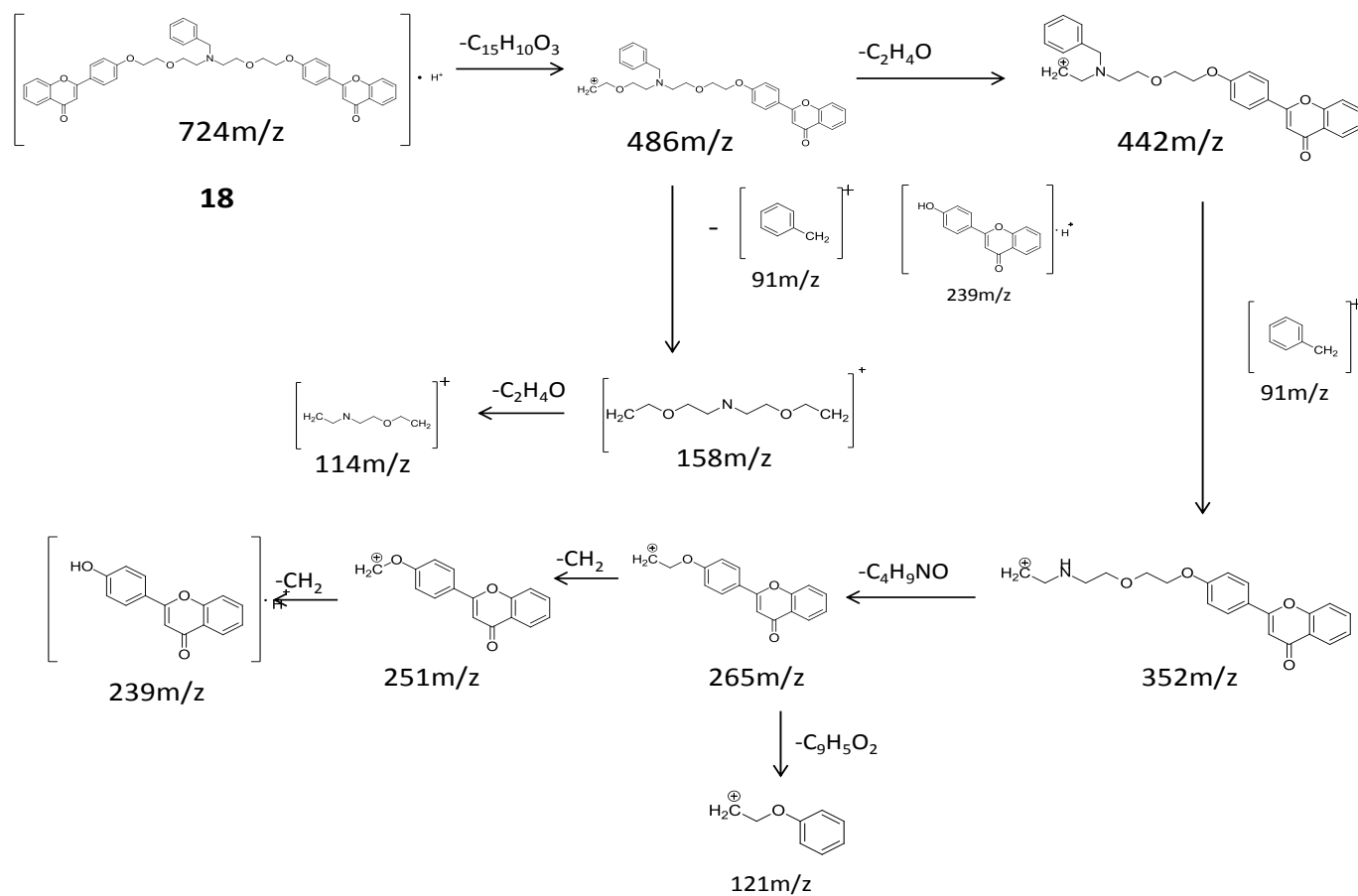
Figure 3-3 Product ion spectrum of **18** and the predicted fragmentation pathway of **18**.

(A) Product ion spectrum of **18**, (B) proposed fragmentation pathway and structures of fragmentation products, together with their predicted m/z.
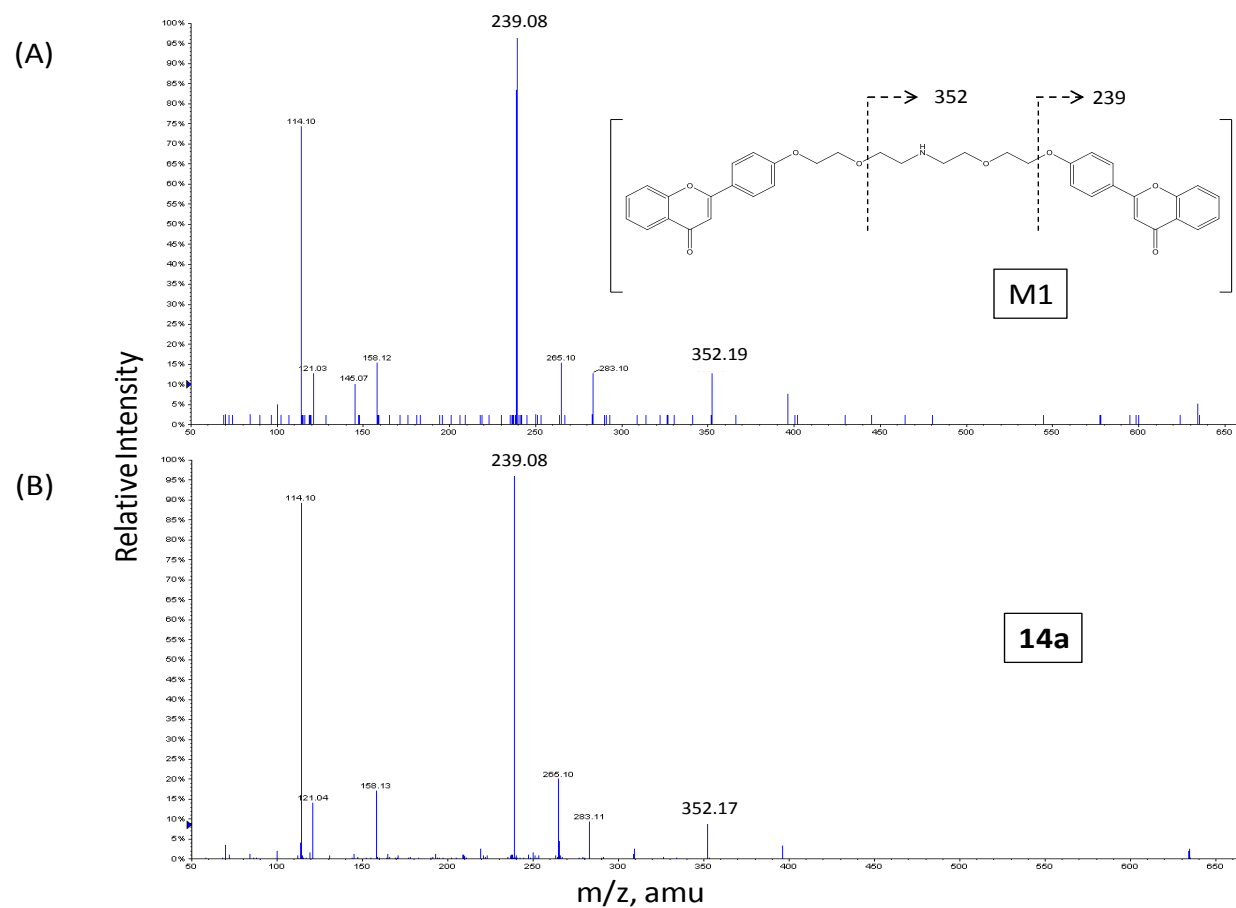
Figure 3-4 Product ion spectra comparison of *in vitro* metabolites **M1** and synthetic compound **14a**

M1 was subjected to LC/QTOF-MSMS analysis and its mass spectrum is shown in (A). Based on the mass spectrum of **M1**, structure of **M1** was predicted and compound **14a** (reported previously (Chan et al. 2012)) was synthesized to confirm the identity of **M1**. Mass spectrum of **14a** is shown in (B)

Product ion spectrum of **M2** revealed that fragments 91m/z and 239m/z were also present in the product ion spectrum, suggesting the presence of the flavone ring and methylbenzene. Based on the mass over charge ratio of 416m/z, we postulated that **M2** was produced from a bond cleavage of **18** and has a structure shown in (Figure 3-5B). Based on the predicted structure, the authentic compound **FM04** was synthesized. We found that the product ion spectrum of **FM04** (Figure 3-5B) was identical to **M2** (Figure 3-5A), suggesting that **M2** has the structure of **FM04**.

Based on the mass over charge ratio of 327, we have predicted the structure of **M3** and called it **FM327**. The synthesized **FM327** has identical product ion spectrum (Figure 3-6B) as **M3** (Figure 3-6A), suggesting that **M3** and **FM327** have identical structure. Putting together, we have hypothesized a metabolism pathway of how **18** can be metabolized by HLM and RLM to give metabolites **M1**, **M2** and **M3** (Figure 3-7).
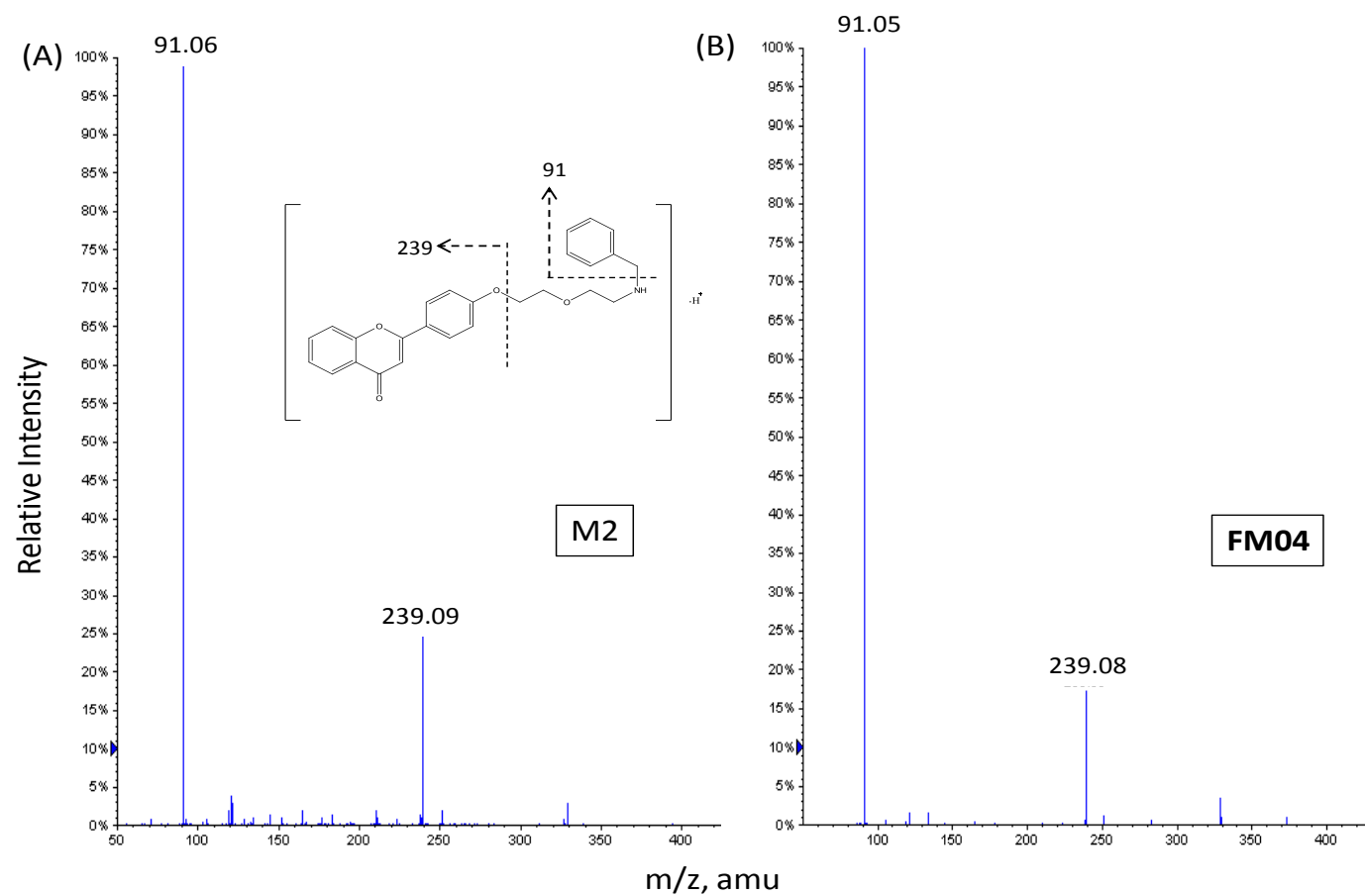
Figure 3-5 Product ion spectra comparison of *in vitro* metabolites **M2** and synthetic compound **FM04**

M2 was subjected to LC/QTOF-MSMS analysis and its mass spectrum is shown in (A). Based on the mass spectrum of **M2**, structure of **M2** was predicted and **FM04** was synthesized to confirm the identity of **M2**. Mass spectrum of **FM04** is shown in (B)
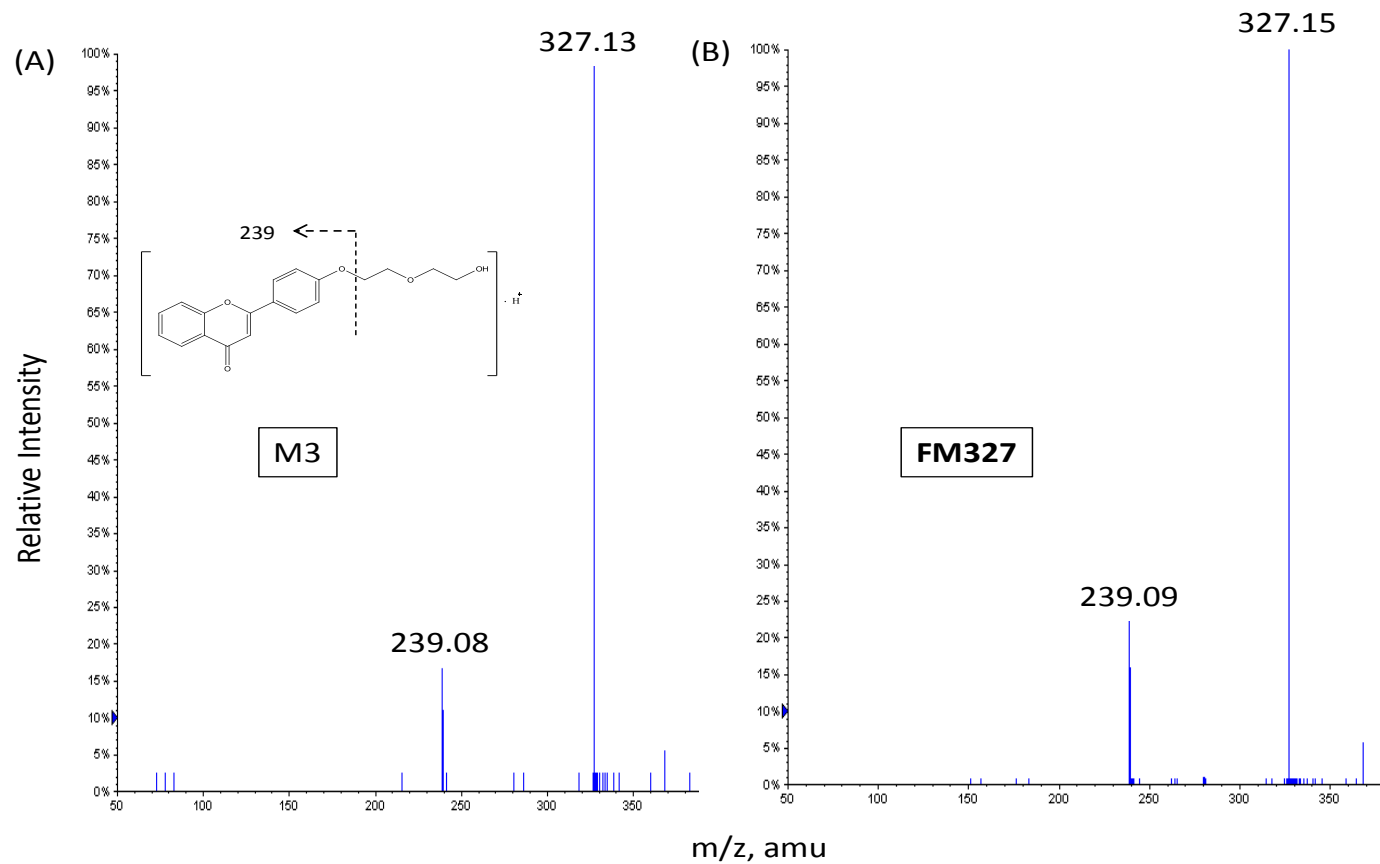
Figure 3-6 Product ion spectra comparison of *in vitro* metabolites **M3** and synthetic compound **FM327**

M3 was subjected to LC/QTOF-MSMS analysis and its mass spectrum is shown in (A). Based on the mass spectrum of **M3**, structure of **M3** was predicted and **FM327** was synthesized to confirm the identity of **M3**. Mass spectrum of **FM327** is shown in (B)
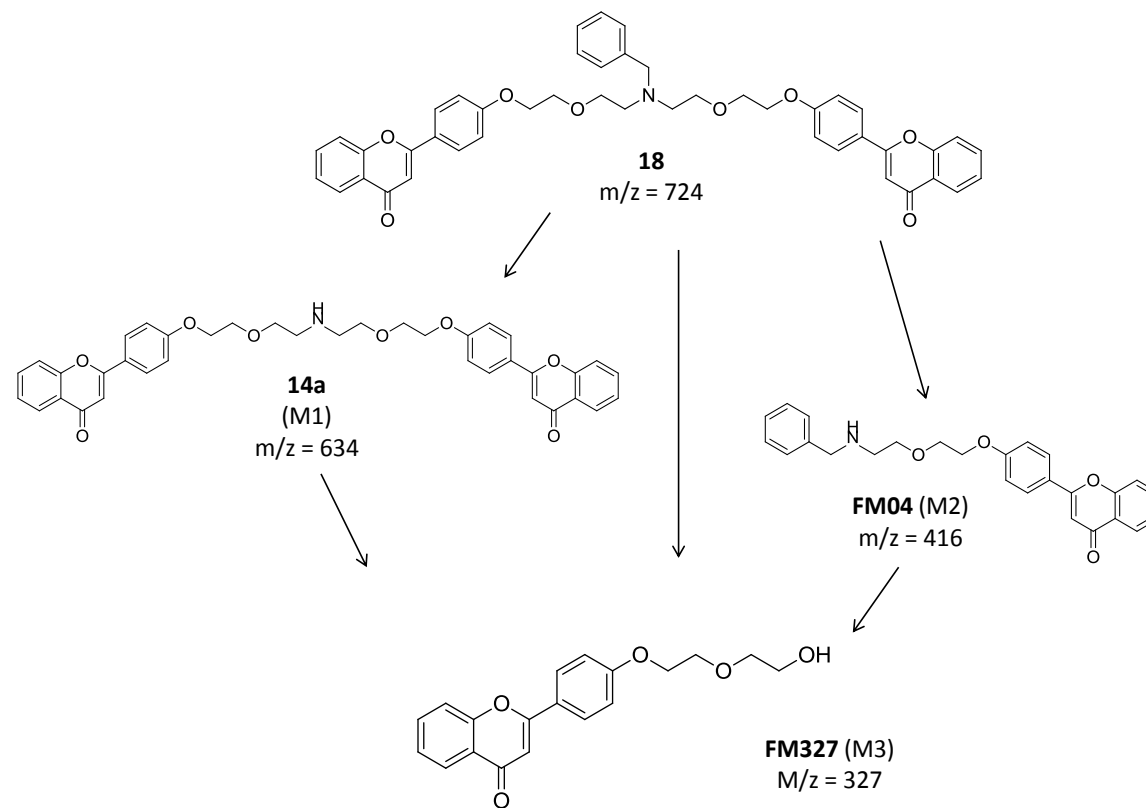
Figure 3-7 Proposed metabolism pathway of **18** in HLM and RLM

Metabolism study of **18** was conducted on HLM and RLM *in vitro*. Chemical structure of the 3 metabolites was predicted by LC/QTOF-MS/MS and confirmed by synthetic compounds. Proposed metabolism pathway of **18** in HLM and RLM is shown

We are also interested in the P-gp modulating activity of these metabolites. *In vitro* P-gp modulating activity of **18** and its metabolites **14a, FM04** and **FM327** against various anticancer drugs was determined (Table 5). P-gp modulating activity of **14a** has been reported previously with EC_{50} of 305 ± 35 nM, suggesting **14a** is less active than **18** (Chan et al. 2012). Surprisingly, metabolite **FM04** demonstrated a higher potency with EC_{50} generally below 100 nM (Table 5). **FM327** did not exert any P-gp modulating activity even when 1 μM was used (Table 5). Cytotoxicity of the 3 compounds on L929 fibroblast was investigated as a measure of toxicity to normal cells. Therapeutic index of **18** and **FM04** were 574.3 and >471, respectively (Table 5) suggesting that **18** and **FM04** were non-toxic.

Table 5 P-gp modulating activity of **18**, **14a**, **FM04** and **FM327**

	EC_{50} in reversing resistance of LCC6 MDR towards different drugs (nM)						Cytotoxicity (nM)	Therapeutic Index
Compound	PTX	vinblastine	vincristine	doxorubicin	daunorubicin	mitoxantrone	L929[1]	
18	148 ± 18	173 ± 27	179 ± 32	131 ± 13	95 ± 25	90 ± 20	85000 ± 5000	574.3
14a	305 ± 35	N.D	N.D	N.D	N.D	N.D	5900 ± 600	19.3
FM04	70 ± 26	61 ± 13	83 ± 11	153 ± 39	88 ± 52	64 ± 27	> 33000	[2]>471
FM327[3]	>1000	N.D	N.D	N.D	N.D	N.D	N.D	N.D

Synthetic compounds **18, 14a, FM04** and **FM327** were tested for their P-gp modulating activities on LCC6 MDR cells. Effective concentration (EC_{50}) was determined as the concentration needed to reduce the IC_{50} of various anticancer drugs in LCC6 MDR cells. Inhibition concentration (IC_{50}) of L929 mouse fibroblasts serves as toxicity indicator. Therapeutic Index is a ratio of the EC50 in LCC6 MDR/ IC50 in L929 mouse fibroblasts to illustrate the selectivity of the compounds on LCC6 MDR cells over mouse fibroblast. High therapeutic index suggests that the compounds are selective on LCC6 MDR cells. All EC_{50} values were presented as the mean ± standard error of mean. N=1-7 independent experiments. N.D: Not determined.

---

[1] Inhibition concentration (IC_{50}) of L929 mouse fibroblasts serves as toxicity indicator

[2] No toxicity on L929 at highest concentration tested (33μM)

[3] No modulating activity was found at 1 μM of **FM327**. At such concentration, IC_{50} of PTX in LCC6 MDR cell line remained unchanged.

Current metabolism study of **18** suggested that **18** might be able to sustain a high level of P-gp modulating activity *in vivo.* **18** can be metabolized into **14a**, **FM04** and **FM327** in human and rat. As a metabolite of **18**, **FM04** demonstrated an even more potent P-gp modulating activity than **18**. This result suggests that **18** can provide a dual mechanism of P-gp modulation *in vivo*.

3.4   CONCLUSION

Three *in vitro* HLM and RLM metabolites of **18** (**M1, M2** and **M3**) were identified and their structures have been confirmed by authentic compounds **14a, FM04** and **FM327,** respectively. A metabolism pathway of **18** has been proposed (Figure 3-7). **M1** exerts mild P-gp modulating activity. **M2** has an improved P-gp modulating activity than **18**. **M3** exerts no P-gp modulating activity. All three metabolites are more hydrophilic than parent compound **18**.

4 PHARMACOKINETICS STUDY OF P-GP MODULATOR FM04 BY UPLC-TRIPLE QUADRUPOLE TANDEM MASS SPECTROMETRY

4.1 INTRODUCTION

We have previously reported that flavonoid dimers were capable of reversing P-gp mediated drug resistance in cancer cells when used together with anticancer drugs (Chan et al. 2006; Chan et al. 2009; Chan et al. 2010). Activity of the first generation apigenin dimer was improved by removal of OH groups at 5 and 7 position of ring A (Chan et al. 2006; Chan et al. 2009). Aqueous solubility of the second generation flavonoid dimers, however, was low and was not suitable for *in vivo* efficacy study. We have recently made further modifications of flavonoid dimers to give **18**, an amine linked flavonoid dimer with increased aqueous solubility when used in HCl salt form (Chan et al. 2012). **18** has been used in pharmacokinetics study (chapter 2) and *in vivo* efficacy (in preparation for submission). Preliminary study proved that **18** was active *in vivo.* **18** can sensitize LCC6 MDR cells to PTX in a breast carcinoma xenograft model. Metabolism study of **18** (Chapter 3) revealed that one of the metabolites of **18, M2** (known as **FM04**) possessed better *in vitro* P-gp modulating activity and aqueous

solubility when compared to **18.** EC_{50} of **M2** in reversing PTX resistance in LCC6 MDR

cells was 70 ± 26nM whereas that of **18** was 148 ± 18 nM.

According to the Lipinski's rule of five, drug candidates with appropriate molecular

weight, ClogP, number of hydrogen bond donors and hydrogen bond acceptors are

likely to be orally bioavailable as well as druggable (Keller et al. 2006). In this regard,

FM04 is more druggable than **18;** with molecular weight of 415, ClogP of 4.61, H-bond

donor of 1 and H-bond acceptor of 5 (Table 6).

Given **FM04** is a metabolite of **18** and has a higher P-gp modulating activity and better

aqueous solubility; it can be further developed into an orally-administered P-gp

modulator.

Table 6 Comparison of **FM04** properties with **18** (free base) according to Lipinski's Rule of 5

	Lipinski's Rule of 5	FM04	18 (free base)
Molecular weight	$\leqq 500$	415	723
ClogP	$\leqq 5$	4.06	7.07
H-bond donors	$\leqq 5$	1	1
H-bond acceptors	$\leqq 10$	5	9

For quantification of **FM04** an analytical method of **FM04** was developed, optimized and validated using UPLC-triple quadrupole tandem mass spectrometry with appropriate internal standard. We have used a deuterium labeled **FM04** (**D7-FM04**) as internal standard. Throughput was one of our concerns; we used Balb/c mice for pharmacokinetics analysis of **FM04,** instead of SD rats. This provided us with PK data on rodents and increased the development throughput by avoiding surgical procedures on SD rats. One of the main objectives in establishing this platform is to investigate the PK properties of **FM04**, in particular the oral bioavailability of **FM04** in Balb/c mice for localized P-gp modulation in the GI tract.

4.2   MATERIALS AND METHODS

4.2.1   MATERIALS AND REAGENTS

Heparin Sodium Salt and diethyl ether were purchased from Sigma-Aldrich. All other reagents or solvents were either analytical or high-performance liquid chromatography (HPLC) grade and were purchased from Tedia. Acquity UPLC BEH C8 (2.1 x 50 mm, 1.7 µM) from Waters. All flavonoid monomers, (i.e. **FM04** and **D7-FM04)** are synthesized in our lab. Purity of all compounds used in this project was >98%. **FM04** was prepared in

5% ethanol and 95% saline at a stock concentration of 10mg/ml for all animal studies. Stock solutions of **FM04** and **D7-FM04** were weighed and prepared in methanol and Milli-Q water (50:50, v/v) to a stock concentration of 10 µg/ml. Serial dilution of **FM04** stock solution in 50% methanol was done to obtain standard curve and quality control samples.

4.2.2 STANDARD CURVES CONSTRUCTION FOR LC-MS/MS

FM04 dissolved in methanol and Milli-Q water (50:50, v/v) at 1mg/ml was used for standard curve construction. Blank plasma was spiked with **FM04** to give standard solutions with concentration ranging from 2.27 µg/mL to 8.878ng/mL for standard curve construction. Five micro liters of **D7-FM04** (10 µg/mL) internal standard was spiked to plasma and used for internal standard.

4.2.3 SAMPLE PRETREATMENT FOR **FM04** QUANTIFICATION

Plasma samples from **FM04** studies were brought to room temperature. Protein precipitation was done by adding 300 μL of methanol to 100 μL of plasma sample. After thorough mixing, samples were centrifuged at 16,000g for 3 minutes. Supernatant was filtered by 0.22 μm syringe filter prior to further analysis.

4.2.4 ANALYTICAL METHOD FOR THE DETECTION OF FM04 BY UPLC-MS/MS

The UPLC-MS/MS system consisted of an Acquity Waters UPLC interfaced with triple quadrupole mass spectrometer (Micromass model Quattro Ultima) equipped with an electrospray ionization source in positive mode. Multiple reaction monitoring (MRM) was set to monitor the transitions of **D7 FM04** $[M +H]^+$ (423>239 m/z) and **FM04** $[M +H]^+$ (416>239 m/z). Five μL of the processed plasma sample was injected for each analysis. The collision energy, cone voltage, source temperature, desolvation temperature and capillary voltage were 30, 30, 150°C, 350°C and 3KV, respectively. The flow rate of cone gas and desolvation gas was 150 L/Hr and 600 L/Hr, respectively.

Separation was done on Acquity UPLC BEH C8 column (2.1 x 50 mm, 1.7 μM). UPLC Liquid chromatography setting consisted of a binary solvent gradient elution profile, methanol + 0.1% formic acid (solvent B) and Milli-Q water + 0.1% formic acid (solvent A). The flow rate was 0.4 ml/min. The initial condition was 70% solvent A and 30% solvent B. After 1 minute elution by initial condition, a linear gradient was applied with solvent B increasing from 30% to 100% for 3 minutes. Solvent B at 100% was then maintained for 6 minutes to wash out retained substances. Subsequently, the mobile phase was restored to initial condition at 11th minutes for re-equilibration. The total analysis time was 20 minutes per injection.

4.2.5   VALIDATION

The current UPLC-MS/MS methods have been validated in terms of accuracy, precision, stability, specificity and selectivity. Pooled blank plasma from Balb/c mice was used to determine the specificity and selectivity. Stability of the samples in the -20°C storage condition and the internal standard storage at -20°C were determined. The accuracy and precision of the current method was illustrated by intra-day and inter-day analysis of quality control samples. Aliquots of plasma were spiked with **FM04** at 568.2, 71.02 or

8.88 ng/ml spanning across the calibration curve at high, mid and low concentration range were used as quality control samples. The QC samples were prepared similarly as the standard curve solutions. Quality control samples were processed and analyzed on 5 different days and 5 consecutive injections on the same day. They were used to determine the inter-day and intra-day variations, respectively.

4.2.6 APPLICATION OF DETECTION METHOD ON PHARMACOKINETICS STUDY OF **FM04**

Pharmacokinetics study of **FM04** was done on Balb/c mice. **FM04** was prepared in 5% ethanol and 95% saline at a concentration of 10 mg/ml for all animal studies. Animals were dosed with **FM04** either by tail vein injection (IV), intra-peritoneal injection (IP) or passive oral feeding (PO). Blood samples (approximately 400uL) were taken via cardiac puncture at 10, 30, 60, 120, 240 and 420 minutes post administration. Two extra time points at 5 minutes and 600 minutes were collected for intra-peritoneal injection. Blood samples were centrifuged at 16,100 x g for 10 minutes to obtain plasma. One hundred μL aliquots of blood samples were spiked with 5 μL of internal standard (**D7-FM04,** 10 μg/ml). Samples were stored at -20°C until further analysis.

4.2.7   PHARMACOKINETICS ANALYSIS

Plasma concentration-time profiles were analyzed by non-compartmental analysis. The area under the plasma concentration-time curve by trapezoid rules (AUC) (from 0 to infinity), the elimination half life ($t_{1/2\ \beta}$), absorption or distribution half life ($t_{1/2\ \alpha}$), apparent volume of distribution (V_d), systemic clearance (CL), mean residence time (MRT), maximum observed concentration (C_{max}) and time to maximum concentration (T_{max}) were calculated by PK Solutions 2.0 (Summit Research Service, Ashland, U.S.A). Bioavailability (F) was calculated by the dose normalized AUC ratio of IP (or oral) and IV administration.

4.3   RESULTS AND DISCUSSION

Here, **D7-FM04**, the deuterium form of **FM04** containing 7 deuterium atoms has been synthesized and used as internal standard for detection of **FM04**. The MS/MS condition was optimized and the daughter ion, 239m/z was stable for both **D7-FM04** and **FM04** under the same collision energy (Figure 4-1). Quantitation of **FM04** with **D7-FM04** as internal standard was done by multiple-reaction monitoring (MRM) of 416m/z >239m/z and 423m/z >239m/z. When **FM04** and **D7 FM04** were spiked into plasma and analyzed by UPLC-MS/MS, no endogenous interference was detected with the

current detection method and no carry over was observed (Figure 4-2). Standard curve indicated a linear relationship in the range of 2.27 µg/ml to 8.88 ng/mL (Figure 4-3). The lowest quantification done with the current method is 8.9 ng/ml. **D7-FM04** and **FM04** was eluted at 5.7minutes and the complete elution profile required 20minutes. Stability and accuracy of the current detection method was validated by analyzing known concentration of QC samples on 5 consecutive days as well as 5 repeated injections on the same day. The inter-day and intra-day variations were inspected by RSD (relative standard deviation) and RE (relative error) at 3 different concentrations. In general, all intra-day and inter-day variations (RSD and RE) were within 15% to the spiked concentration (Table 7), except for the lowest QC sample concentration, with an intra-day RSD of 17.1%, intra-day RE of 15.8% and inter-day RSD of 19.7%. Storage of deuterium labeled **FM04** in aqueous condition (plasma sample) may foster deuterium-hydrogen exchange, thus leading to higher variation of RSD and RE at the lowest QC sample concentration range. A rational approach to prevent deuterium–hydrogen exchange is to limit the prevent storage in aqueous condition. This can be achieved by conducting ether liquid-liquid extraction and drying the samples in mild heat (i.e. 70°C) prior to storage. Sample storage in dry extracts should minimize variations in RSD and RE at low concentration range.

(A)
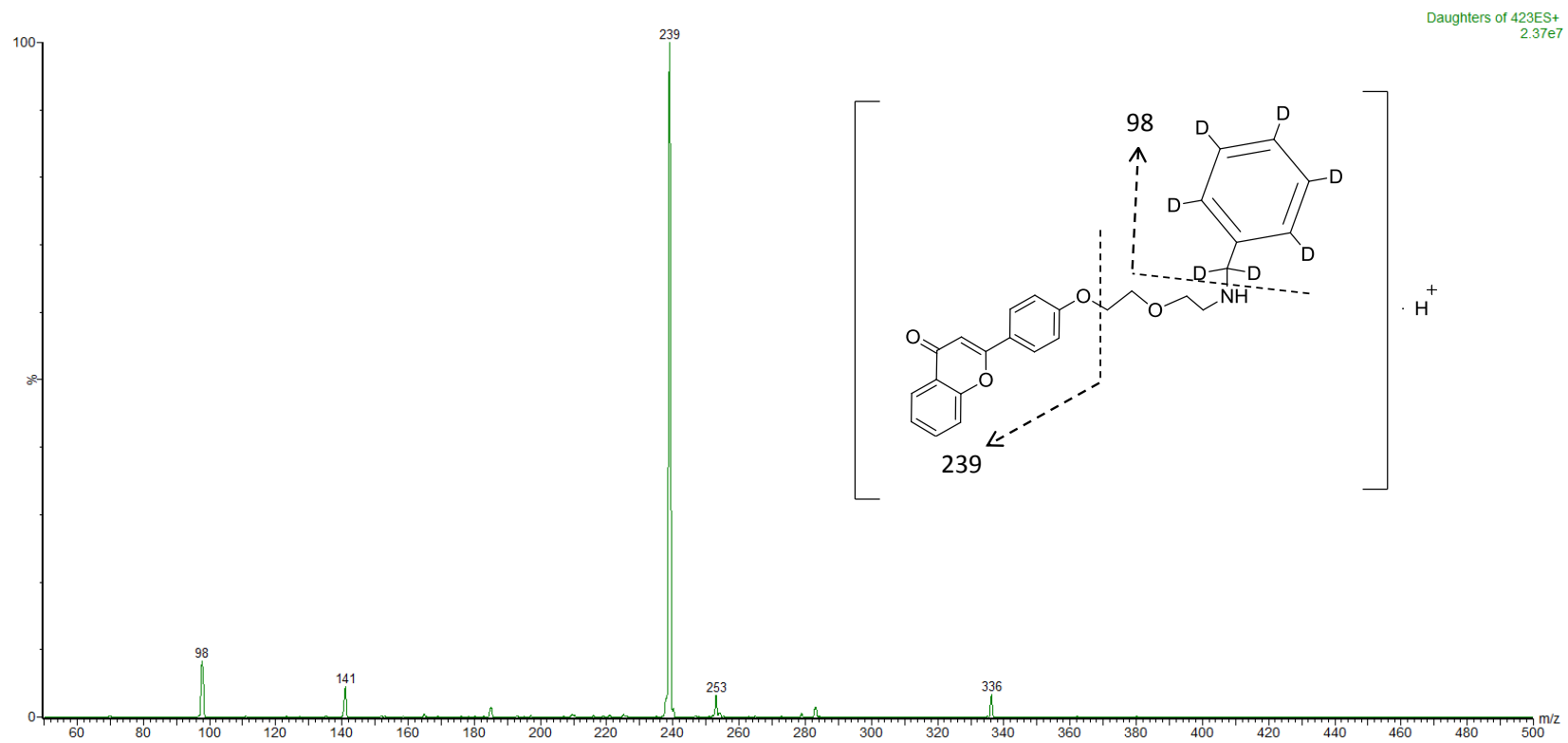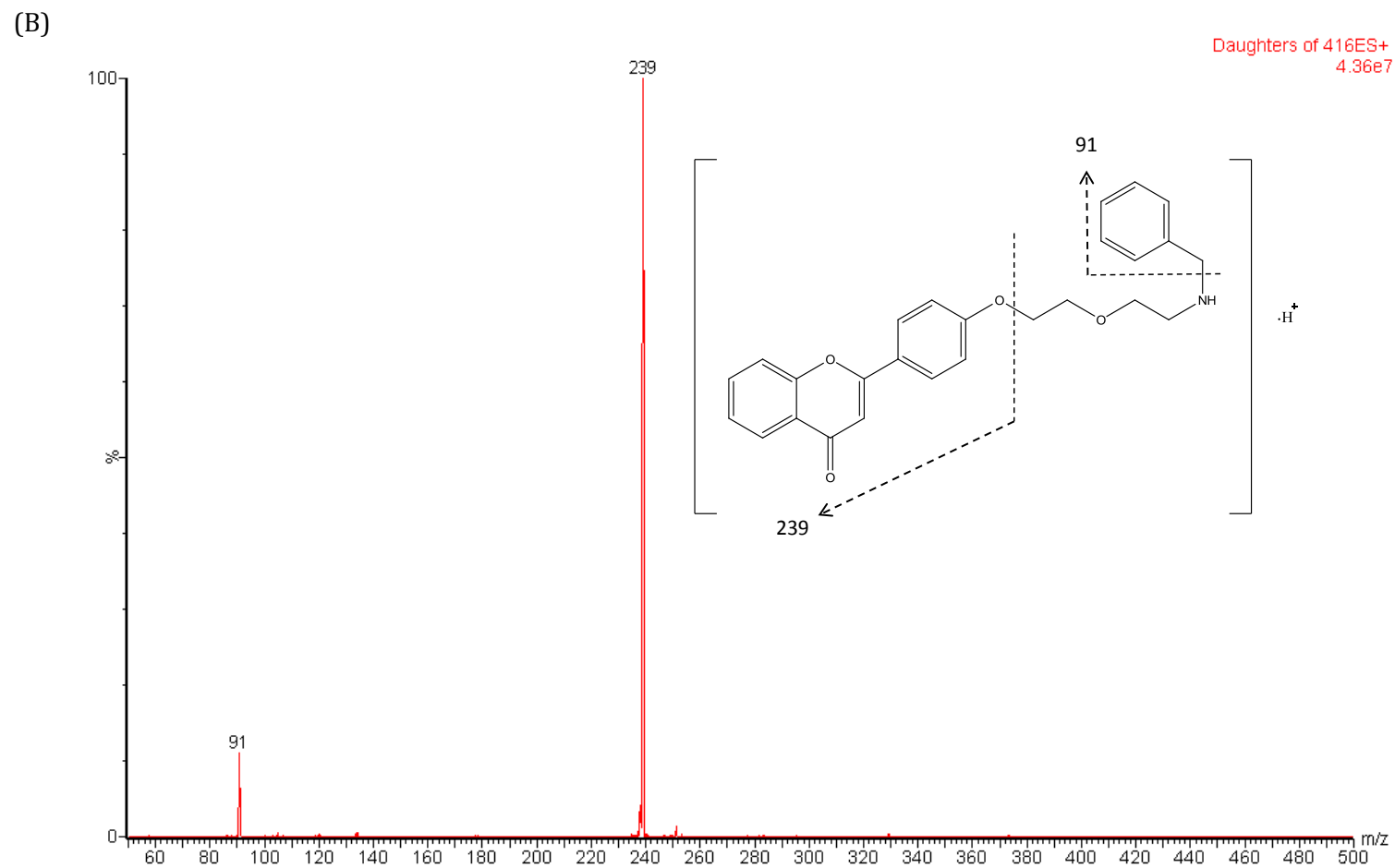
Figure 4-1 Product ion spectra of **D7-FM04** and **FM04**

Standard solutions of **D7-FM04** and **FM04** were subjected to MS/MS analysis. Mass spectrum of **D7-FM04** (423m/z) is shown in (A) Mass spectrum of **FM04** (416m/z) is shown in (B). Same collision energy was employed for both analyses.

(A)
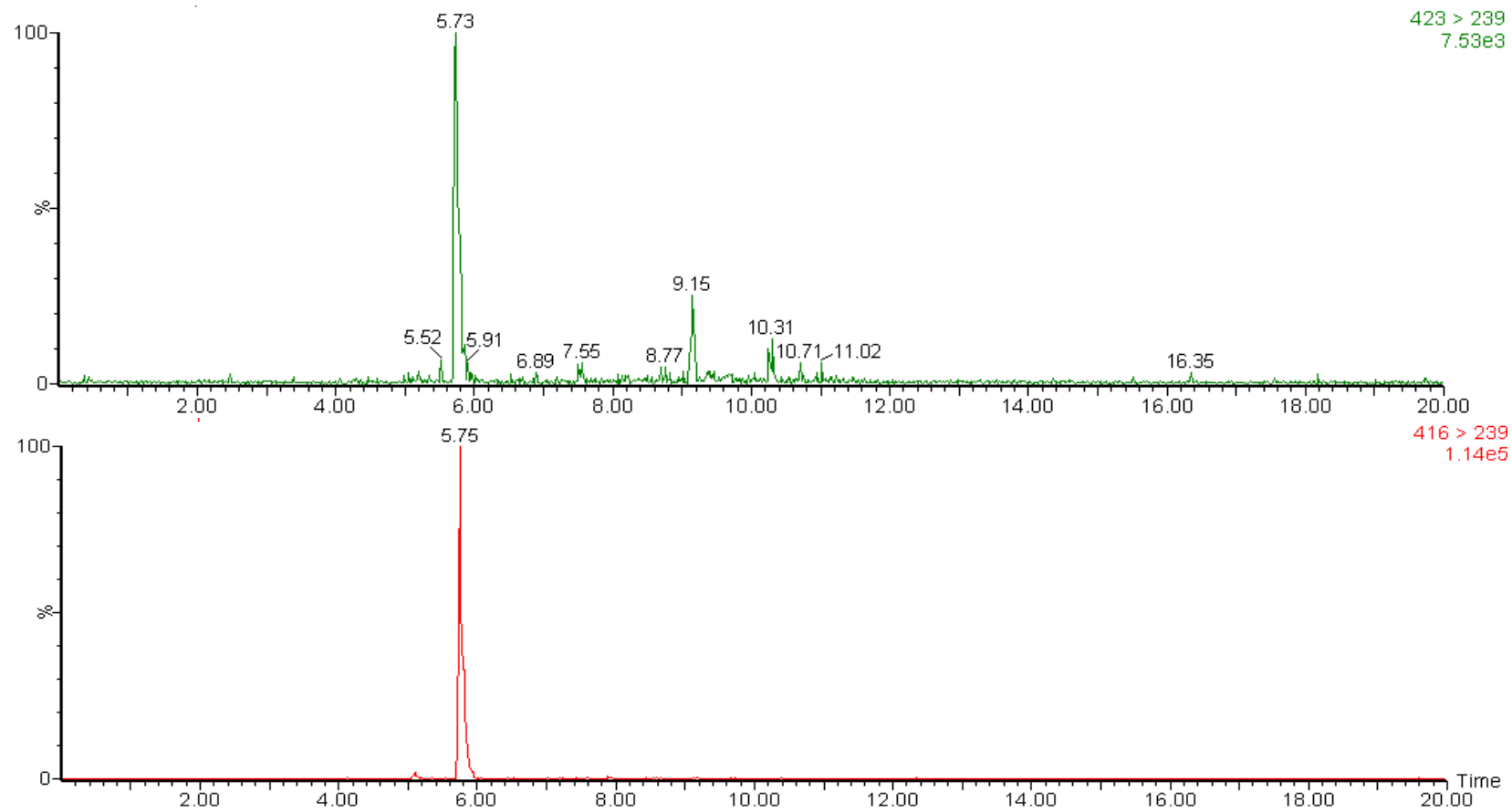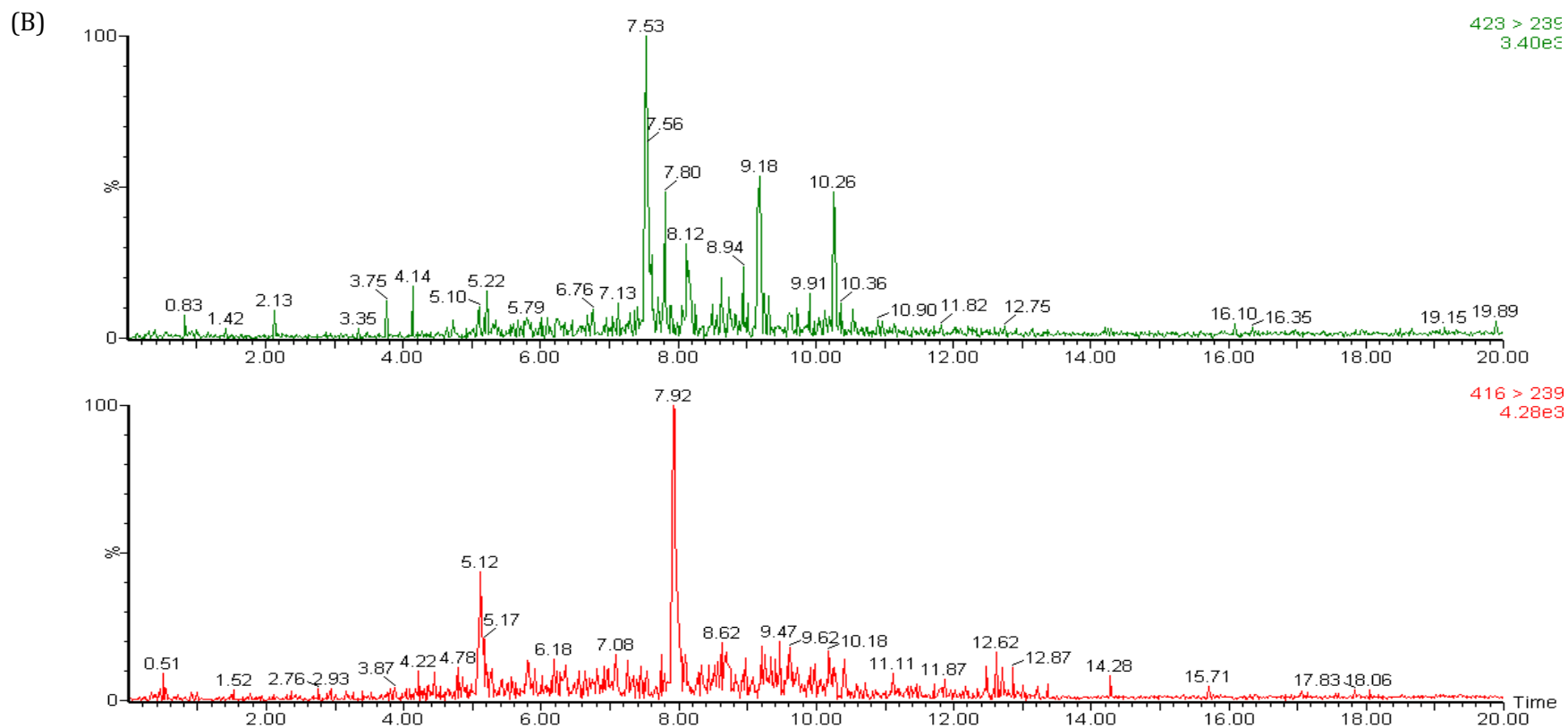
Figure 4-2 Chromatogram of plasma spiked with **D7-FM04** and **FM04** analyzed on UPLC-MS/MS

UPLC-MS/MS was performed on plasma spiked with internal standard **D7-FM04** and **FM04** by monitoring MRM 423>239 and 416>239, respectively.
(A) Chromatogram of blank rat plasma spiked with **FM04** and **D7-FM04**. (B) Chromatogram of blank rat plasma.
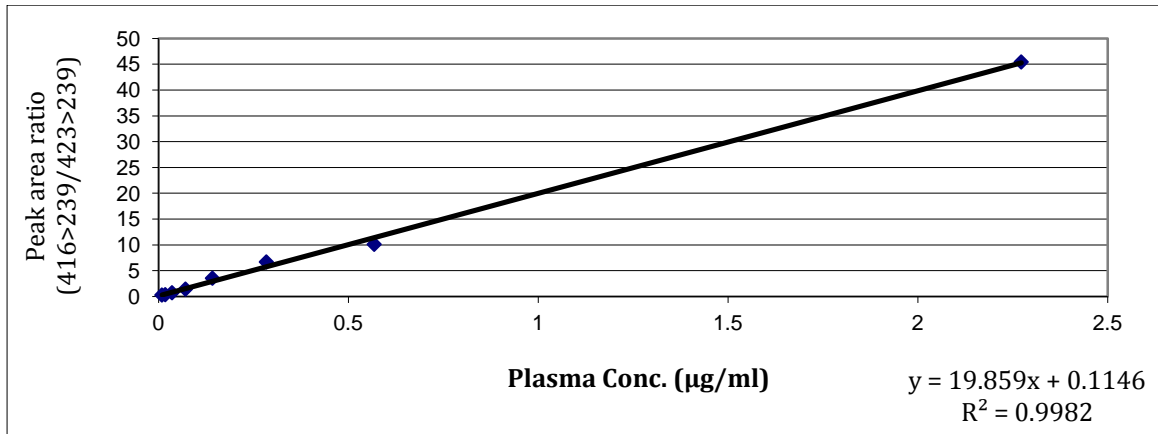
Figure 4-3 Standard curve of **FM04** on UPLC-MS/MS

Plasma concentration of **FM04** is quantified by monitoring the peak area ratio of **FM04** (416>239) against **D7-FM04** (423>239) in spiked plasma.

Table 7 Intra-day and inter-day precision and accuracy studies for detection of **FM04** by UPLC-MS/MS.

Spiked conc. (ng/mL) [a]	Intra-day					Inter-day			
	Detected conc. (ng/mL) [b]	SD [c]	RSD [c/b]	RE [(b-a)/a]		Detected conc. (ng/mL) [d]	SD [e]	RSD [e/d]	RE [(d-a)/a]
568.18	606.97	64.21	10.6%	6.8%		651.60	39.82	6.1%	14.7%
71.02	73.63	10.74	14.6%	3.7%		80.96	6.80	8.4%	14.0%
8.88	10.28	1.76	17.1%	15.8%		8.39	1.65	19.7%	-5.5%

The detection method was verified by quantifying QC samples on intra-day and inter-day basis. Intra-day (n=5) was done by 5 consecutive analysis of the same concentration solution. Inter-day (n=5) was done by analyzing spiked solution for 5 consecutive days.
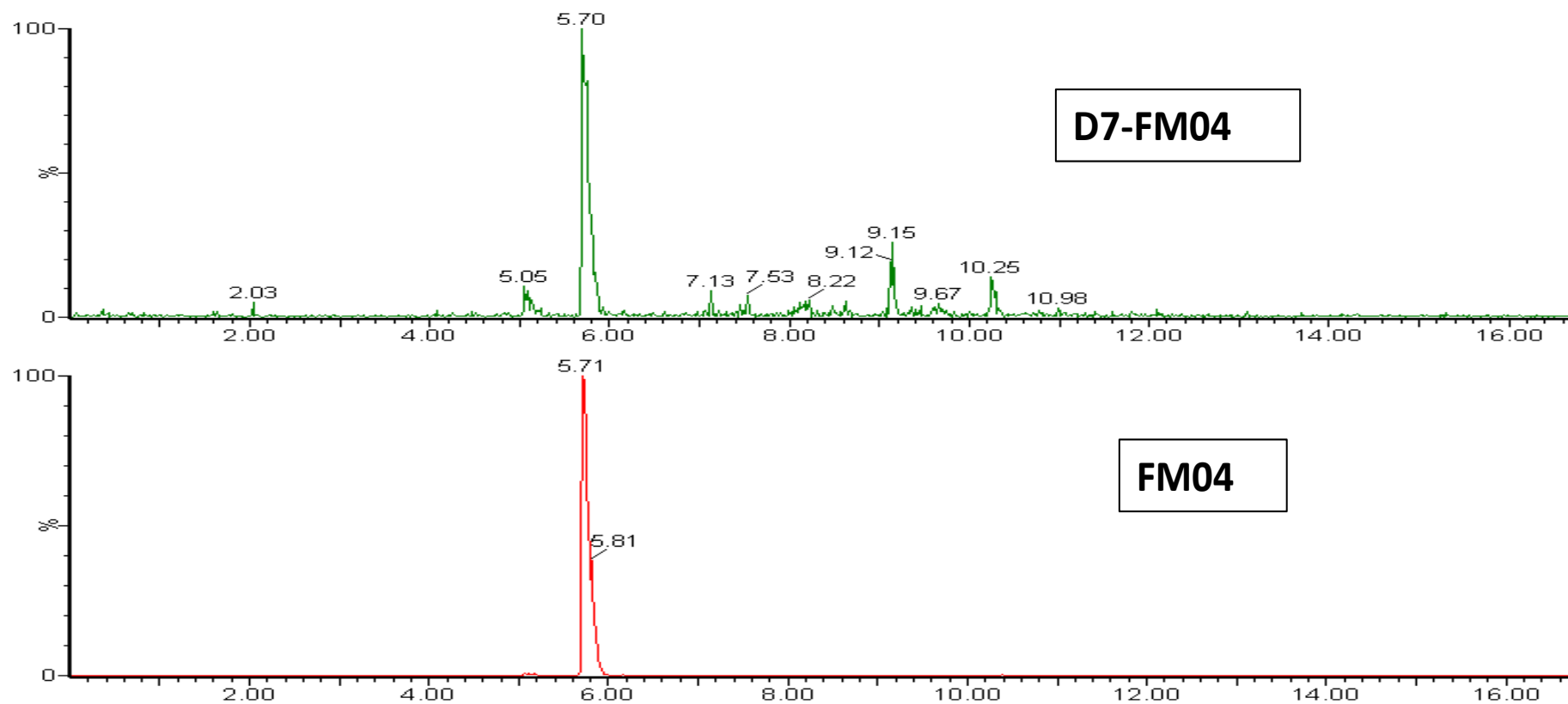
Figure 4-4 UPLC-MS/MS chromatogram of **D7-FM04** and **FM04** from *in vivo* sample.

Balb/c mice were dosed with 10 mg/kg **FM04**. Blood was collected at 15 minutes post-administration of **FM04.** After spiking with **D7-FM04** plasma concentration of **FM04** was quantified with peak area ratio of **FM04** against **D7-FM04.**

Pharmacokinetics study of **FM04** in Balb/c mice was studied using the validated UPLC-MS/MS method. Typical UPLC-MS/MS chromatogram of **FM04** is shown in (Figure 4-4). We have studied the PK profile of three administration routes (PO, 100 mg/kg; IP, 28 mg/kg and IV, 10 mg/kg). This study allowed us to determine which administration route can be used for future studies and whether **FM04** was orally bio-available.

Intravenous administration of **FM04** at 10 mg/kg demonstrated first order kinetics suggesting a two compartment model (Figure 4-5). The initial half life of **FM04** was 12 minutes and the terminal half life was 48 minutes. PK parameters of **FM04** via IV administration are summarized in Table 8.
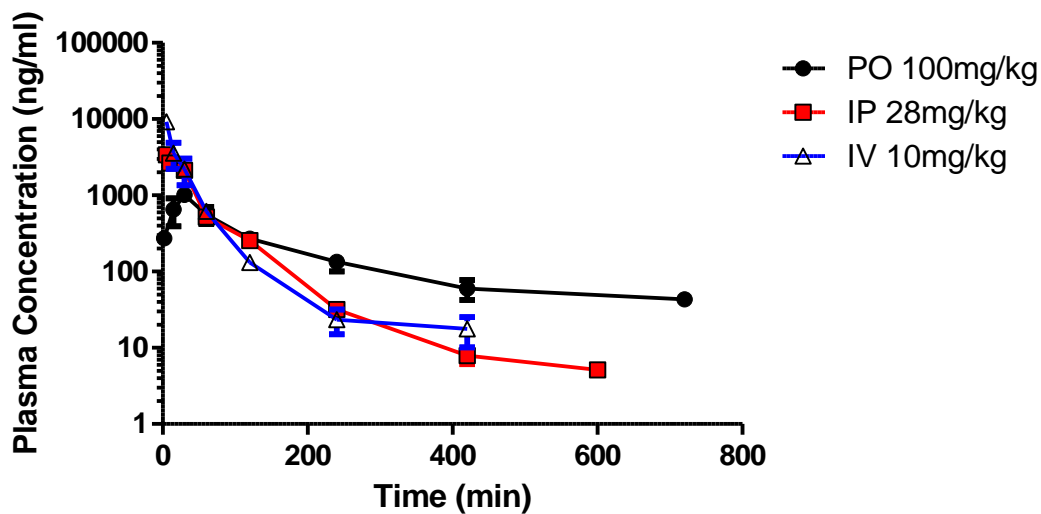
Figure 4-5 Plasma concentration-time profiles of **FM04** administered to Balb/c mice

Pharmacokinetics study of **FM04** was conducted in Balb/c mice. **FM04** solution was prepared as stated previously and was administered through PO (100 mg/kg), IV (10 mg/kg), and IP (28 mg/kg). Terminal blood sample was collected via cardiac puncture. Plasma concentration of **FM04** was quantified with peak area ratio of **FM04** against **D7-FM04.** Four to seven animals were used for each time point. Each time point represents mean ± SEM.

Table 8 Pharmacokinetics parameters of **FM04** in Balb/c mice

FM04			
Administration Route	IV	IP	PO
Dose (mg/kg)	10	28	100
AUC $_{(0 - infinity)}$ (ng-min/ml)	230460	157083	121237
AUC/DOSE	23046	5610	1212
AUC $_{(0-t)}$ (ng-min/ml)	228832	156072	109142
Vd (ml/kg)	3021	N/A	N/A
CL (ml/min/kg)	43	N/A	N/A
MRT (min)	28	57	164
T $_{1/2\,\alpha}$ (min)	12	29	10
T $_{1/2\,\beta}$ (min)	48	137	139
C$_{max}$ (ng/ml)	-	3391	1017
T$_{max}$ (min)	-	5	30
Bioavailability (%)	-	24.34%	5.26%

Plasma-concentration profile was obtained from 3 routes of administration (IV, IP and PO) (Figure 4-5). Non-compartmental pharmacokinetics analysis of **FM04** in Balb/c mice was performed by PK solutions 2.0 (Summit Research Service, Ashland, U.S.A).

Intraperitoneal administration of **FM04** demonstrated a rapid absorption, with T_{max} at 5 minutes. No absorption phase was observed. At the initial time point of IP administration, both T_{max} and C_{max} were noted at 5 minutes and 3391ng/ml, respectively. The terminal half-life for elimination was 137 minutes, similar to terminal half-life following oral administration. The bioavailability following IP administration was 24.34%. The higher bioavailability following IP administration compared to oral administration may reflect a better absorption kinetics and less susceptible to metabolism in the peritoneal cavity.

Passive oral feeding of **FM04** at 100 mg/kg demonstrated a rapid absorption phase (Figure 4-5). The initial half life for distribution and absorption was 10 minutes, with T_{max} at 30 minutes post administration and C_{max} of 1017 ng/ml. The oral bioavailability was 5.26% and was speculated to be the consequence of CYP450 metabolism in GI tract. The MRT and terminal half-life following oral administration was 164 minutes and 134 minutes, respectively. Both MRT and terminal half-life following passive oral administration were apparently longer than values obtained following IV administration (Table 8).

Comparing the 3 routes of administration, it was found that different routes resulted in different systemic exposure of **FM04**. Oral administration has the

lowest systemic exposure among the studied routes with normalized AUC/DOSE of 1212. Such low value of AUC might result from active metabolism and/or physiological GI tract barrier. The systemic exposure was higher following IP administration with AUC/dose of 5610. The systemic exposure was highest following IV administration with AUC/dose of 23046.

The current study characterized initial PK parameters of **FM04** in rodent *in vivo*. PK non-linearity of **FM04** cannot be excluded and may lead to refinement on IP and oral bioavailability parameters; however, the chance of **FM04** illustrating high oral bioavailability is low. Furthermore, investigation is needed to determine whether metabolism and/or physiological barriers are responsible for the observable differences in dose-normalized AUC for IP or oral administration of **FM04**.

4.4 SUMMARY

In this study, a quantification method for **FM04** on UPLC-MSMS system has been optimized and validated with a pharmacokinetics application. Deuterium label **D7-FM04** was used as the internal standard. The accuracy, specificity and reproducibility have been validated on an inter-day and intra-day basis. Among the tested QC samples spanning high, middle and low concentration ranges of **FM04** gave satisfactory precision and accuracy from intra-day and inter-day analysis. **FM04** has a low bioavailability of 5.26%. In general the absorption and distribution of **FM04** in the body was rapid as suggested from plasma-concentration profile following IP and oral administration. With its promising *in vitro* P-gp modulating activity, satisfactory aqueous solubility and low molecular weight, **FM04** could be a favorable candidate for oral administration.

5   FLAVONOID DIMER **18** AND FLAVONOID MONOMER, **FM04** IN ENHANCING ORAL BIOAVAILABILITY OF PTX

5.1   INTRODUCTION

PTX is an effective anticancer drug for various cancers such as breast (ten Tije et al. 2004), non-small cell lung (Chen et al. 2004), ovarian (Vasey et al. 2004), gastric (Kollmannsberger et al. 2000), head and neck (Schena et al. 2005) and prostate (Vaughn et al. 2004) via intravenous infusion administration. PTX has demonstrated the effectiveness in inhibiting cancers in preclinical (Kwak et al. 2010) and clinical studies. One of the problems of PTX is its poor aqueous solubility and it therefore requires CremophorEL to act as a carrier vehicle. Intravenous infusion of CremophorEL, however, might lead to hypersensitivities and would require premedication including dexamethasone (immunosuppressant) as well as piriton and cimetidine to block histamine receptors prior to PTX IV infusion (Preston 1996; Gelderblom et al. 2001; Singla et al. 2002). This increases the chance of interfering with PTX metabolism (Singla et al. 2002). Oral administration of PTX is more convenient and could potentially avoid the CremophorEL-related hypersensitivity reactions (Sparreboom et al. 1997; ten Tije et al. 2003; de Jonge et al. 2005). Oral bioavailability of PTX,

however, has been limited by active efflux of PTX by P-gp and metabolism of PTX in the gastrointestinal (GI) tract.

Expression of P-gp was found on luminal surface of epithelial cells of kidney proximal tubules, biliary hepatocytes as well as small and large intestine in the GI tract (Gottesman et al. 1996). The location of the P-gp suggests a protective role against endogenous and exogenous toxin for the body. When PTX is administered orally, P-gp in the enterocytes serves as a protective barrier and actively removes PTX back to GI tract (Sparreboom et al. 1997). The role of P-gp in limiting oral bioavailability of drugs has been confirmed by gene knockout studies in mice where mice lacking P-gp (Mdr1a/1b) and/or Cyp3a showed increased oral bioavailability of drugs including PTX (Sparreboom et al. 1997; van Herwaarden et al. 2007).

Co-administration of P-gp modulator has been tried to enhance oral bioavailability of PTX. Oral bioavailability of PTX (10 mg/kg) can be increased by 13.4-fold using 50 mg/kg cyclosporine A (CsA) (van Asperen et al. 1998) or increased by 10-fold using SDZ PSC833 (valspodar) (van Asperen et al. 1997). Concurrent oral administration of PTX (10mg/kg) with 25mg/kg GF120918 also led to an increase in oral bioavailability of PTX by 4.7-fold (Bardelmeijer et al.

2000). Recently, HM30181 (another potent P-gp inhibitor) can increase oral bioavailability of PTX from 3.4% to 41.3% in rats (Kwak et al. 2010). All these evidences suggested that modulation of P-gp in the GI tract can be an effective way to enhance oral bioavailability of PTX.

In the current study, we investigated whether flavonoid dimer **18** or its metabolite **FM04** was capable of improving the oral bioavailability of PTX *in vivo*. The effect of concurrent oral administration of flavonoid compounds with PTX was also investigated in a breast carcinoma LCC6 xenograft model on athymic nude mice (Balb/c nu/nu) *in vivo*.

5.2   MATERIALS AND METHODS

PTX was purchased from Wuhan Hezhong Biochemical Manufacture Co. Ltd. Isotopic PTX, [$^{13}C_6$] PTX, was purchased from ALSACHIM (France). Purity of [$^{13}C_6$] PTX was > 98%. Heparin Sodium Salt and diethyl ether were purchased from Sigma-Aldrich. All other reagents or solvents were either analytical or high-performance liquid chromatography (HPLC) grade and were purchased from Tedia. Acquity UPLC BEH C8 (2.1 x 50 mm, 1.7μM) from Waters was used for separation. All flavonoid compounds, (i.e. **18** and **FM04**) were synthesized in our lab. Purity of all compounds used in this project is >98%. Stock solutions of **18** and **FM04** were weighed and prepared in methanol and Milli-Q water (50:50, v/v) to a stock concentration of 10 μg/ml. Serial dilution of **FM04** stock solution in 50% methanol was done to obtain standard curve and quality control samples.

5.2.1   ANALYTICAL   METHOD   BY   UPLC-TRIPLE QUADRUPOLE TANDEM MASS SPECTROMETRY

The UPLC-MS/MS system consists of an Acquity Waters UPLC interfaced with triple quadrupole mass spectrometer (Micromass model Quattro Ultima) equipped with an electrospray ionization source in positive mode. The

desolvation temperature, capillary voltage, cone gas and desolvation gas were 350°C, 3 Kv, 150 L/Hr and 600 L/Hr, respectively. Multiple reaction monitoring (MRM) was set to monitor the transitions as indicated below.

Table 9 LC-MSMS MRM quantification for enhancing PTX oral bioavailability

Compound	MRM	Collision Energy
18	724 > 239	30
FM04	416 >239	30
PTX	876 >308	40
[$^{13}C_6$] PTX	882 >314	40

Chromatography separation was done with an Acquity UPLC BEH C8 column (2.1 x 50 mm, 1.7 µM). The mobile phase consisted of methanol + 0.1% formic acid (solvent B) and Milli-Q water + 0.1% formic acid (solvent A). The flow rate was 0.4 ml/min. The initial condition was 90% solvent A and 10% solvent B. After 1 minute elution by initial condition, a linear gradient was performed with solvent B increasing from 10% to 100% for 10 minutes. Afterwards, mobile phase was restored to initial condition for re-equilibration. The total analysis time was 20 minutes per injection. PTX standard curve was detectable from 1 µg/ml to 0.00355 µg/ml with R^2 = 0.9944.

5.2.2 ANIMAL STUDY

Balb/c mice (body weight 18-20 g) and athymic nude mice (Balb/c nu/nu, 15-23g) were obtained from Laboratory Animal Unit, The University of Hong Kong and Animal and Plant Care Facilities. Animals were kept in a temperature and humidity controlled environment with 12 hour light-dark cycle with standard diet and water. Animal experiment protocol was approved by the Animal Subjects Ethics Sub-Committee of The Hong Kong Polytechnic University. Animal were fasted overnight and had free access to water throughout the experiment. All drug solution was prepared on the day of use and used for animal study within half an hour.

5.2.3 DRUG PREPARATION

PTX drug solution for all experiments in this study was prepared in standard formulation (5% CremophorEL, 5% ethanol, 90% saline). PTX was first dissolved in ethanol and heated to clear solution in 80^oC heat. CremophorEL was then added and vortex mixed for homologous solution PTX stock solution at 40 mg/ml.

The solution was diluted with saline to achieve final composition for animal study.

Drug solution for concurrent administration of PTX with **FM04** (or **FM04** solvent as solvent control) was prepared by mixing PTX stock solution with the corresponding drug solution. The final formulation for the drug solution was 7% CremophorEL, 10% ethanol and 83% saline. **FM04** drug solution was prepared in 2% CremophorEL, 5% ethanol and 93% saline at 10 mg/ml. Ethanol and saline was added to **FM04** and heated under 80°C until clear. CremophorEL was then added to stabilize the solution. Prior to administration for animal study, **FM04** drug solution was mixed with PTX.

Drug solution for concurrent administration of PTX with **18** (or **18** solvent as solvent control) was prepared by mixing PTX stock solution with the corresponding drug solution. The final formulation for the drug solution was 13% CremophorEL, 13% ethanol and 73% saline. Drug solution of **18** was prepared in 33% CremophorEL, 33% ethanol and 33% saline at 24.33 mg/ml. Ethanol and CremophorEL was added to **18** and heated under 80°C until clear. Saline was then added to the solution for final dilution. Prior to administration for animal study **18** drug solution was mixed with PTX.

5.2.4   PHARMACOKINETICS STUDY

Pharmacokinetics study was conducted for oral administration of PTX with or without **18** or **FM04**. Drug was administered to Balb/c mice (n=4-5) via oral administration (Oral) or intravenous administration (IV). Blood samples were collected in heparinized tubes by cardiac puncture after deep anesthesia by ethyl ether at 0.17, 0.5, 1, 2, 4, 7, 10, 12 and 16 hours post-administration. Blood samples were centrifuged at 16,100 g for 10 minutes immediately after collection to obtain blood plasma. Blood plasma was stored at -20°C until analysis.

5.2.5   EFFICACY STUDY ON LCC6 XENOGRAFT MODEL

The experimental set up on the xenograft model has been established by Miss Yan Clare. Female Balb/c nu nu mice were intraperitoneally injected with 1-5 x 10^7 cells of LCC6 re-suspended in 200 μL of PBS. Cells were grown for at least two and no more than ten peritoneal passages before inoculated subcutaneously (s.c.) onto the rear flank (either left or right) of female Balb/c nu nu mice. Subsequently, solid tumor was harvested to graft 1 mm^3 cubes of LCC6 onto rear flank of female Balb/c nu nu mouse for efficacy study. Mice grafted with tumor cubes were allowed to grow until

the tumor could be measured accurately. Mice were randomized and treatment was initiated accordingly. Nine treatment groups were conducted, (a) **FM04** 45 mg/kg with PTX 20 mg/kg (oral, 2 courses of q.d. x 4) , (b) **FM04** 45 mg/kg with PTX 40 mg/kg (oral, 2 courses of q.d. x 4), (c) **FM04** 45 mg/kg with PTX 80 mg/kg (oral, 2 courses of q.d. x 4), (d) **18** 30 mg/kg with PTX 40 mg/kg (oral, 2 courses of q.d. x 4), (e) **18** 30 mg/kg with PTX 80 mg/kg (oral, 2 courses of q.d. x 4), (f) PTX 12 mg/kg (IV, 2 courses of q.d. x 4), (g) PTX 20 mg/kg (oral, 2 courses of q.d. x 4), (h) PTX 40 mg/kg (oral, 2 courses of q.d. x 4), (i) PTX 80 mg/kg (oral, 2 courses of q.d. x 4) and (j) no treatment group. The above treatments were made every 2 days. All tumors were measured by digital caliper and tumor volumes were calculated by (L x W x H) x (π /6)(Liang et al. 2007). Specific growth rate (SGR) was calculated as follow, SGR= (ln(V_2/V_1)/ (t_2-t_1)). Doubling time (DT) was calculated as follows, DT = ln2/SGR (Mehrara et al. 2007). Tumor volumes were normalized to that on day one. Tumor volume was monitored for 30 days post initial treatment. Statistical significance was tested using unpaired t-test.

5.2.6   PHARMACOKINETICS ANALYSIS

Plasma concentration-time profiles were analyzed by non-compartmental

analysis using PK solutions 2.0 (Summit Research Service, Ashland, U.S.A). The area under curve (AUC) from time zero to last quantified time point post administration AUC $_{(0\text{-last})}$ was calculated using trapezoidal method. AUC from time zero to infinity (AUC$_{(0\text{-inf})}$) was calculated by AUC $_{(0\text{-last})}$ + (last concentration/elimination rate constant). Elimination rate constant was the slope of the concentration versus time curve during terminal phase determined by linear regression. Elimination rate constant also served to determine the elimination half life ($t_{1/2}$). Elimination half life ($t_{1/2\ \beta}$), absorption or distribution half life ($t_{1/2\ \alpha}$), apparent volume of distribution (V_d), systemic clearance (CL), mean residence time (MRT), maximum observed concentration (C_{max}) and time to maximum concentration (T_{max}) were calculated by PK Solutions 2.0 (Summit Research Service, Ashland, U.S.A). Bioavailability (F) was calculated by the dose normalized AUC ratios of oral and IV administration with identical solvent composition and dosage. Relative fold change in AUC $_{(infinity)}$ was used to illustrate the effect of **FM04** or **18** on oral bioavailability of PTX.

5.3   RESULTS AND DISCUSSION

Our previous study indicated that PTX (IV, 12 mg/kg) is capable of suppressing

tumor growth of a breast carcinoma LCC6 xenograft model on athymic nude mice

(Balb/c nu/nu) *in vivo*. We are interested in whether modulation of P-gp by **18** or

FM04 in the GI tract can enhance dose exposure of oral PTX to IV PTX level. Oral

bioavailability is used as an indicator to demonstrate the change of improved

oral absorption. We studied PK profile of PTX with or without co-administration

of **FM04**. Solvent effect and non-linear PK of PTX was added into consideration,

only identical solvent composition and dosage were compared to illustrate oral

bioavailability enhancement. Plasma level of PTX (oral, 12 mg/kg) increased

significantly in the presence of **FM04** (oral, 45 mg/kg) when compared to PTX

(oral, 12 mg/kg) in standard solvent composition of 5% CremophorEL, 5%

ethanol and 90% Saline (Figure 5-1). Further investigation in excluding the

solvent effect and non-linear PK of PTX illustrated the effect of **FM04** in

enhancing oral bioavailability of PTX. Oral administration of PTX (20 mg/kg)

with **FM04** (45 mg/kg) increased the plasma concentration of PTX leading to a

change in plasma concentration profile (Figure 5-2). The dose exposure of PTX

expressed in $AUC_{(infinity)}$ was increased by 7 fold when **FM04** (45 mg/kg) was

concurrently administered orally (Figure 5-3). C_{max} was also increased from 108

ng/ml to 751 ng/ml and from 547 ng/ml to 2457 ng/ml when PTX was

administered orally at 12 mg/kg and 20 mg/kg, respectively (Figure 5-4). All

detailed PK parameters are summarized in Table 10.
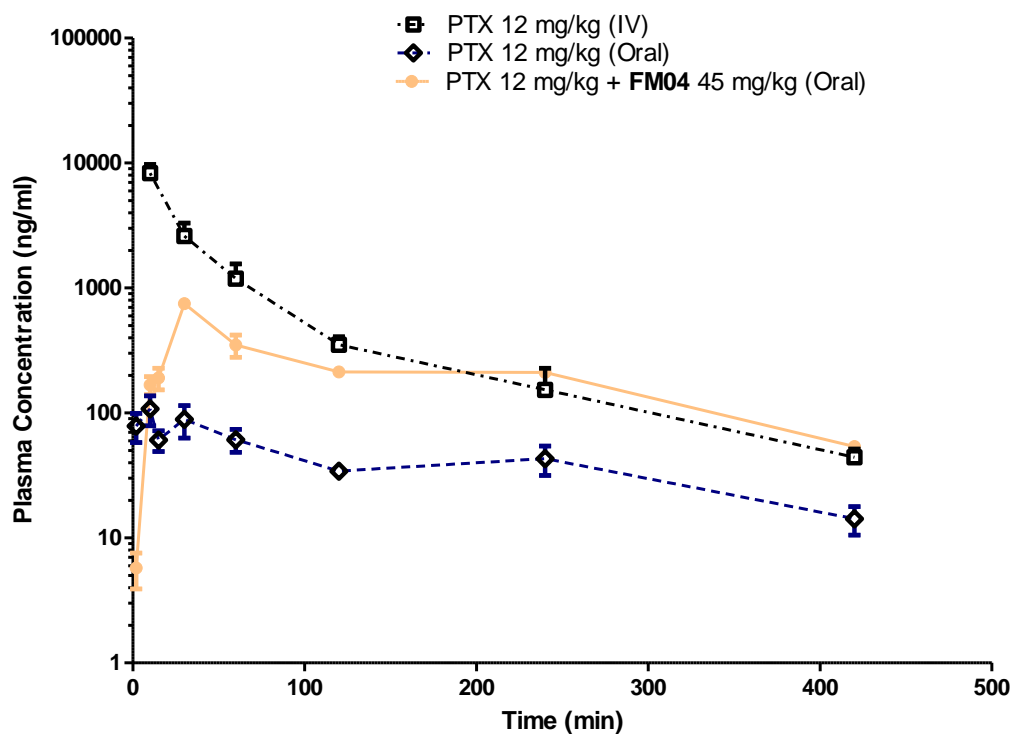
Figure 5-1 Plasma concentration profile of PTX with or without **FM04** (45mg/kg)

PTX was administered to Balb/c mice at indicated dosage and route of administration.
At the indicated time points, mice were sacrificed and plasma extracted. Plasma level of
PTX was determined by UPLC-MS/MS. Each data point represents mean $\pm$ SEM (n=4-5).
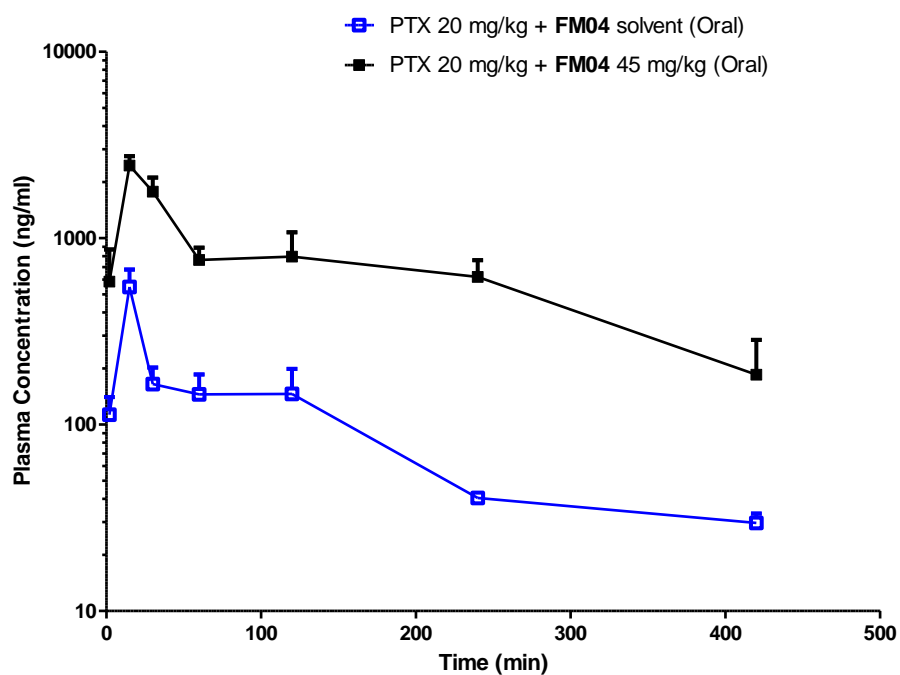
Figure 5-2 Plasma concentration profile of 20mg/kg PTX with or without 45mg/kg **FM04** via oral administration

PTX was administered to Balb/c mice via oral administration. At the indicated time points, mice were sacrificed and plasma extracted. Plasma level of PTX was determined by LCMSMS. Each data point represents mean ± SEM (n=4).
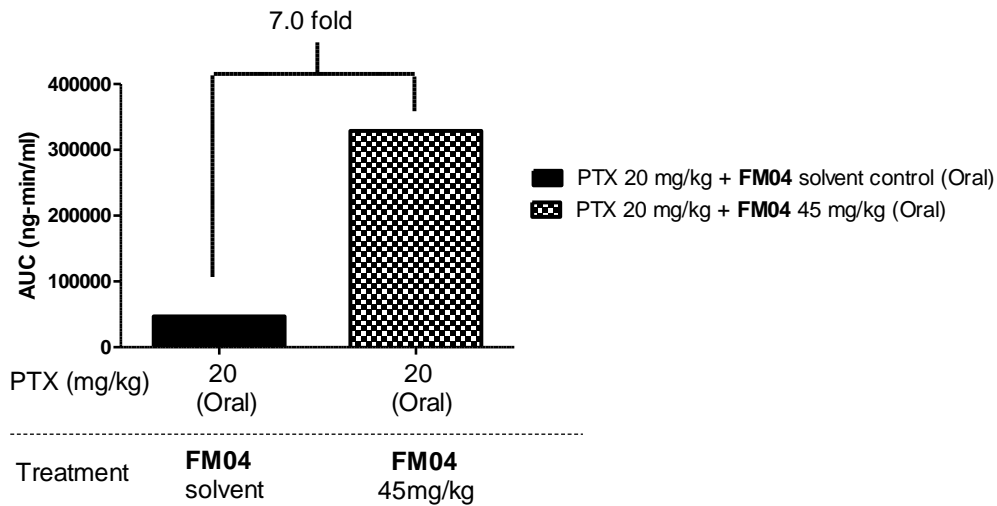
Figure 5-3 Effect of **FM04** on oral bioavailability of PTX

$AUC_{(infinity)}$ of PTX is used to quantify the effect of **FM04** on oral bioavailability of PTX on Balb/c mice. PTX (20 mg/kg) is administered through oral administration with or without **FM04** (45 mg/kg). Solvent composition of the treatments is identical at 7% CremophorEL, 10% ethanol and 83% saline. PK parameters are summarized in Table 10.
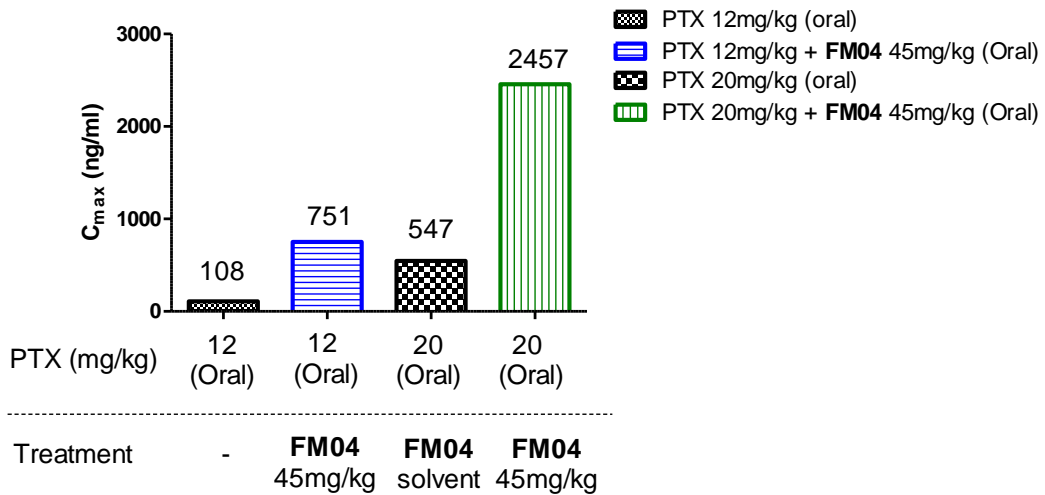
Figure 5-4 Effect of **FM04** on C_{max} of PTX

C_{max} values of PTX with or without **FM04** are plotted using pharmacokinetics data from Table 10.

102

Table 10 PTX pharmacokinetics in mice with or without concurrent oral administration of **FM04** (45 mg/kg)

Parameter					
Dose of PTX (mg/kg)	12	12	20	12	20
Treatment	-	-	SC[1]	**FM04** 45mg/kg	**FM04** 45mg/kg
Route of administration	IV	oral	oral	oral	oral
AUC($_{0\text{-inf}}$) (ng-min/ml)	364606	22215	46787	101265	328958
AUC/DOSE	30384	1851	2339	8439	16448
AUC($_{0\text{-last}}$) (ng-min/ml)	358214	18270	41543	91473	294536
Half-life β (min)	100	185	114	123	129
Half-life α (min)	15	253	3	19	3
MRT (min)	58	246	170	191	190
C$_{max}$ (ng/ml)	-	108	547	751	2457
T$_{max}$ (min)	-	10	15	30	15
Bioavailability	-	6.09%[2]	-	-	-
Relative fold of AUC$_{(infinity, oral)}$	-	-	-	-	7.03[3]

[1] SC: solvent control of **FM04**; Final composition of PTX solution is made of 7% CremophorEL, 10% ethanol and 83% saline.

[2] Calculated by (dose normalized AUC $_{(infinity)}$ of oral PTX)/ (dose normalized AUC $_{(infinity)}$ of IV PTX)

[3] Calculated by (AUC $_{(infinity, oral)}$ of PTX 20 mg/kg + **FM04** 45 mg/kg)/ (AUC $_{(infinity, oral)}$ of PTX 20 mg/kg + **FM04** solvent control)

We were also interested in determining whether **18** can increase oral bioavailability of PTX. We found that $AUC_{(infinity)}$ of PTX (oral 20 mg/kg) increased significantly in the presence of **18** (oral, 30 mg/kg) (Figure 5-5). In the presence of **18** (oral, 30 mg/kg) $AUC_{(infinity)}$ of PTX increased by 4.14 fold (Figure 5-7). The effect of **18** (oral, 30 mg/kg) on oral administered PTX was also investigated by various dosage, **18** (oral, 30 mg/kg) was concurrently administered with PTX (oral) at 5, 20 and 40 mg/kg (Figure 5-6). C_{max} of PTX was increased dose dependently. In the presence of **18** (30 mg/kg, oral) C_{max} of PTX (20 mg/kg, oral) increased from 350 ng/ml to 1242 ng/ml further confirming the effect of **18** (30 mg/kg, oral) in enhancing oral absorption and increasing plasma concentration of PTX (Figure 5-8). All detailed PK parameters are summarized in Table 11.
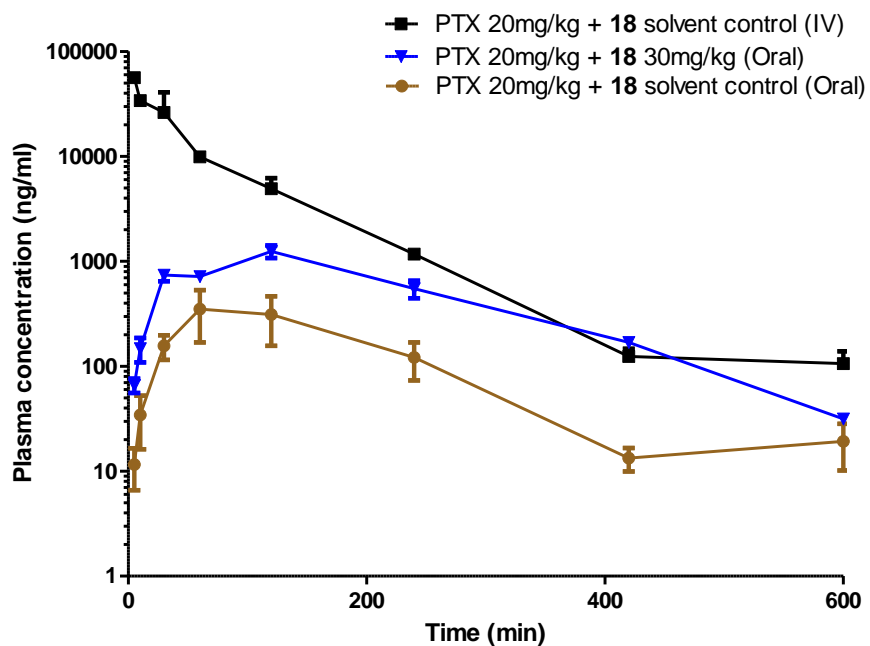
Figure 5-5 Plasma concentration profile of 20 mg/kg PTX with or without **18** (30 mg/kg)

PTX was administered to Balb/c mice at 20 mg/kg with **18** solvent control through intravenous administration. **18** (oral, 30 mg/kg) or **18** solvent control was concurrently administered with PTX (oral, 20 mg/kg). Each data point represents mean ± SEM (n=4-6).
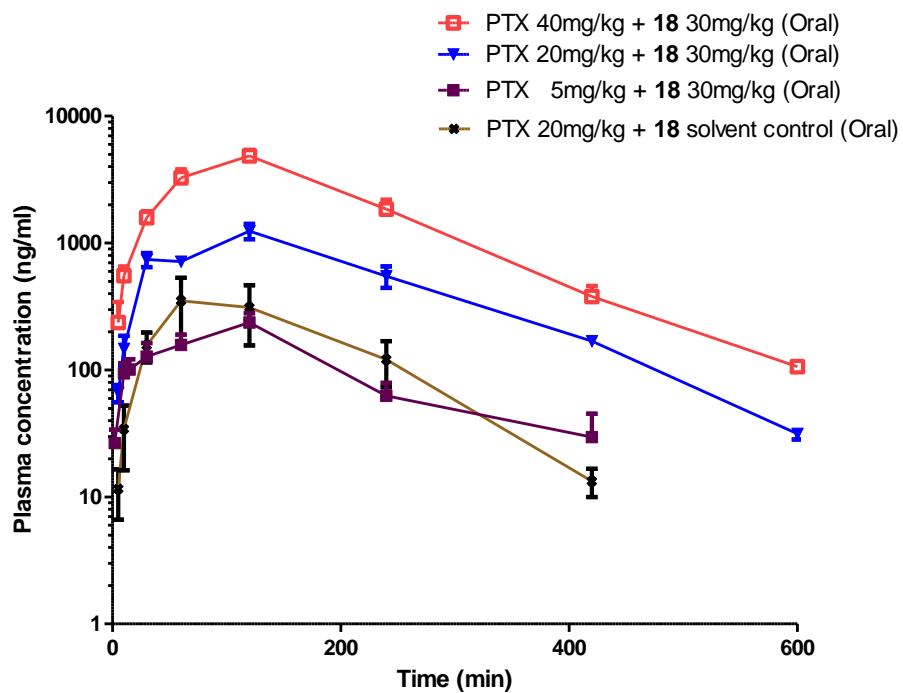
Figure 5-6 Plasma concentration profile of various doses of oral PTX with **18** (30 mg/kg)

Various doses of PTX (5, 20, and 40 mg/kg) was orally administered to Balb/c mice with either **18** (oral, 30 mg/kg) or **18** solvent control. Each data point represents mean ± SEM (n=4-6).
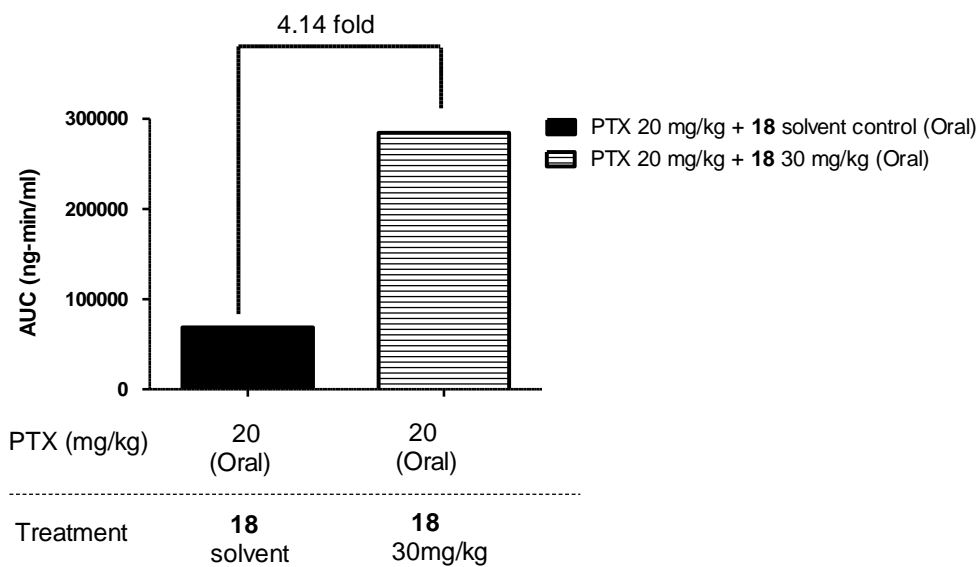
Figure 5-7 Effect of **18** on oral bioavailability of PTX

Effect of 30 mg/kg **18** on PTX oral bioavailability was obtained by comparing the AUC $_{(infinity, oral)}$ of PTX with or without **18** (30 mg/kg). Solvent control is incorporated in the comparison to exclude the effect from altered solvent composition. Solvent composition of the treatments are identical at 13% CremophorEL, 13% ethanol and 74% Saline. PK parameters are summarized in Table 11.
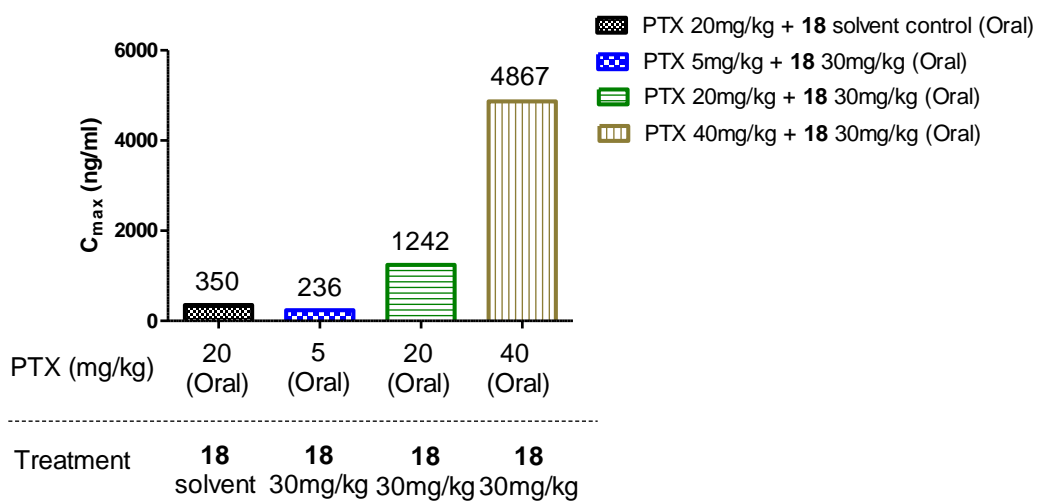
Figure 5-8 Effect of **18** on C_{max} of PTX

C_{max} values of PTX with **18** or **18** solvent control are plotted using pharmacokinetics data from Table 11.

Table 11 PTX pharmacokinetics in mice with or without concurrent oral administration of **18** (30mg/kg)

Parameters					
Dose of PTX (mg/kg)	20	20	5	20	40
Treatment	SC[1]	SC[1]	**18** 30mg/kg	**18** 30mg/kg	**18** 30mg/kg
Route of administration	IV	Oral	Oral	Oral	Oral
AUC$_{(0\text{-inf})}$ (ng-min/ml)	2583007	68764	49481	284386	1001216
AUC/DOSE	129150	3438	9896	14219	25030
AUC$_{(0\text{- last})}$ (ng-min/ml)	2572826	67515	45068	280221	988003
Half-life β (min)	57	65	103	92	86
Half-life α(min)	19	30	36	36	49
MRT (min)	61	144	181	187	173
C$_{max}$ (ng/ml)	-	350	236	1242	4867
T$_{max}$ (min)	-	60	120	120	120
Bioavailability	-	2.66% [2]	-	-	-
Relative fold of AUC$_{(infinity, oral)}$	-	-	-	4.14 [3]	-

[1] SC: solvent control of **18**; Final composition of PTX solution is composed of 13% CremophorEL, 13% ethanol and 74% saline.

[2] Calculated by (dose normalized AUC $_{(infinity)}$ of oral PTX + **18**)/ (dose normalized AUC $_{(infinity)}$ of IV PTX 20mg/kg + **18** solvent control)

[3] Calculated by (AUC $_{(infinity, oral)}$ of PTX 20 mg/kg + **18** 30 mg/kg)/ (AUC $_{(infinity, oral)}$ of PTX 20 mg/kg + **18** solvent control)

The above data suggested that both **FM04** and **18** can increase oral bioavailability of PTX significantly. We therefore tested if such increase in oral bioavailability of PTX can result in effective chemotherapeutic effect of PTX on a LCC6 breast carcinoma xenograft model. Intravenous PTX (12 mg/kg) was highly effective in suppressing xenograft growth whereas PTX (oral, 80 mg/kg) has no effect at all (Figure 5-9). In contrast, co-administration of PTX (oral, 80 mg/kg) with either oral **FM04** (45 mg/kg) or **18** (30 mg/kg) resulted in almost the same level of suppression of xenograft growth as PTX administered intravenously (12 mg/kg) (Figure 5-9).
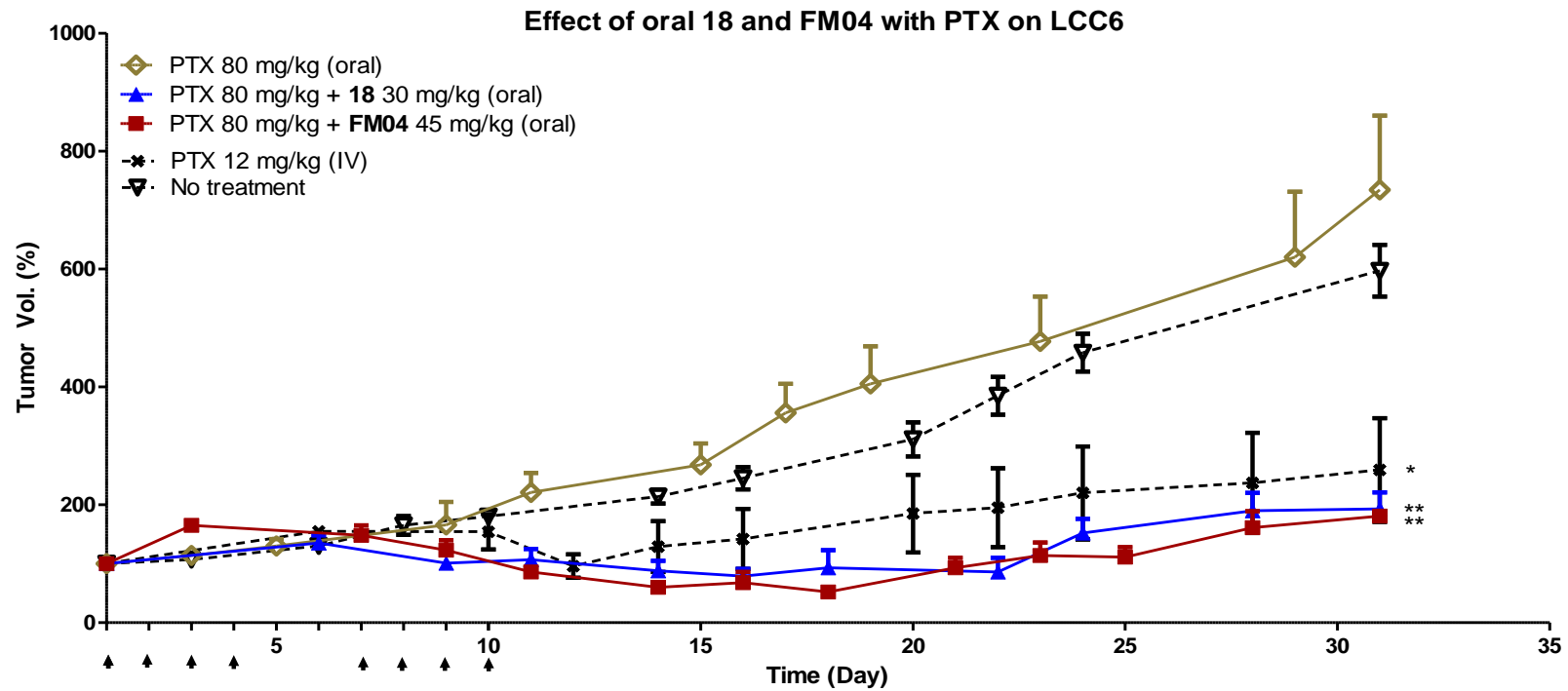
Figure 5-9 Effect of **18** and **FM04** with concurrent oral administration of PTX on LCC6 xenograft efficacy study

Balb/c nude mice bearing LCC6 breast cancer xenograft were treated with PTX (IV, 12 mg/kg) or PTX (oral, 80 mg/kg) as control. Other groups of animal were treated with concurrently oral administration of **FM04** (45 mg/kg) or **18** (30 mg/kg) with PTX (80 mg/kg). Arrows indicated days of treatment. PTX 12 mg/kg (N=6), PTX 80 mg/kg (N=8), **18** 30 mg/kg + PTX 80 mg/kg (N=8), **FM04** + PTX 80 mg/kg (N=4) and no treatment control (N=8). *, $P<0.05$ and **, $P<0.01$, t-test; significantly different from no treatment group.

We determined the minimum dose of oral PTX that can be used together with oral **18** in achieving chemotherapeutic response as PTX (IV, 12 mg/kg). Oral administration of PTX alone (20, 40 or 80 mg/kg) did not have any significant effect on LCC6 xenograft compared with no treatment control. Co-administration of **18** (oral, 30 mg/kg) with PTX (oral, 40 mg/kg) did not show significant effect either. Only when co-administration of **18** (oral, 30 mg/kg) with PTX (oral, 80 mg/kg) did we see significant tumor suppression effect (Figure 5-10). Such effect was comparable with that of IV administration of PTX (IV, 12 mg/kg) (Figure 5-10).
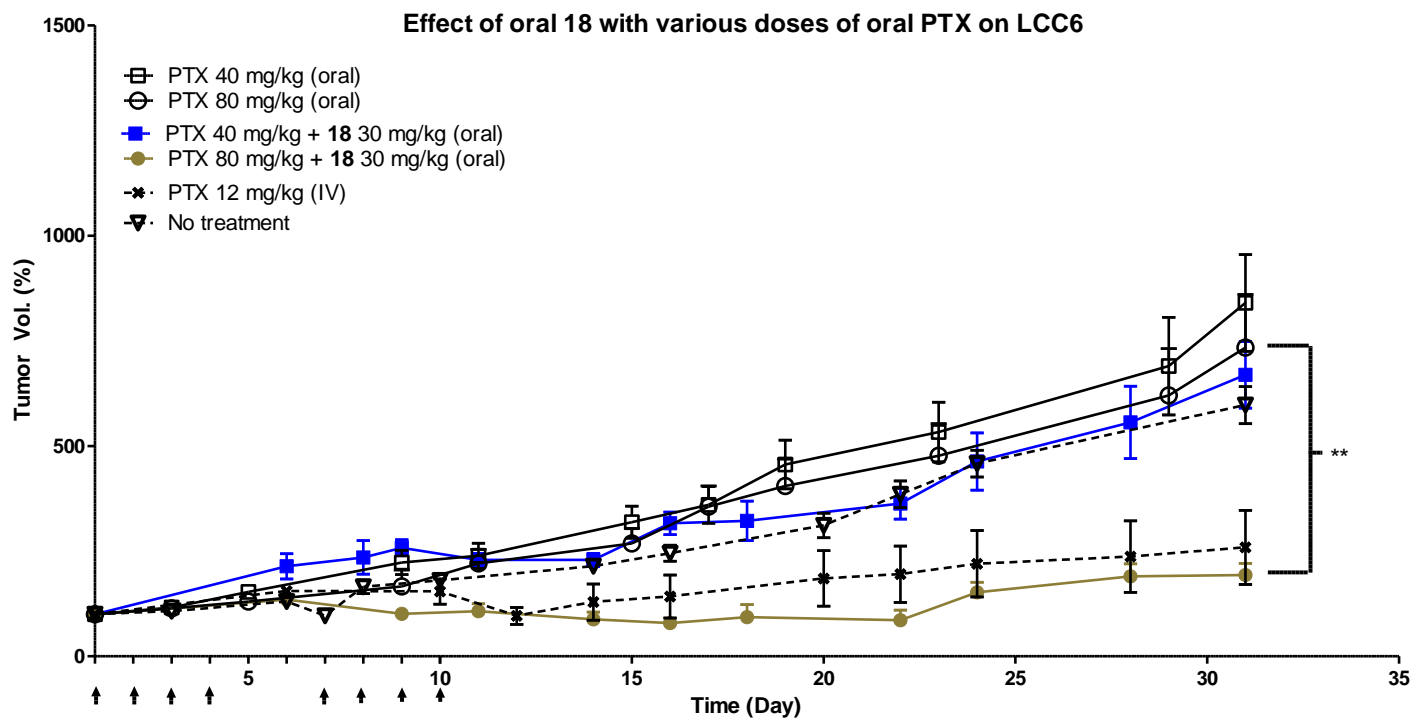
Figure 5-10 Effect of **18** with various doses of orally administered PTX on LCC6 xenograft efficacy study

Balb/c nude mice bearing LCC6 breast cancer xenograft were treated with orally administered PTX (40 mg/kg and 80 mg/kg). PTX (IV, 12 mg/kg) and no treatment groups serve as controls. Oral administration of PTX (40 mg/kg or 80 mg/kg) with **18** (oral, 30 mg/kg) serves as treatment groups. Arrows indicated days of treatment. PTX 40 mg/kg (N=8), PTX 80 mg/kg (N=8), PTX 40 mg/kg + **18** 30 mg/kg (N=8) and PTX 80 mg/kg + **18** 30 mg/kg (N=8). **,$P<0.01$, t-test; significantly different from oral PTX (80 mg/kg).

113

When we performed similar experiment on **FM04**, we found that co-administration of **FM04** (oral, 45 mg/kg) with PTX (oral, 40 mg/kg) demonstrated a small tumor suppression effect (Figure 5-11). When **FM04** (oral, 45 mg/kg) was combined with the highest concentration of PTX (oral, 80 mg/kg), we observed the maximal suppression effect, similar to that observed in IV administration of PTX (IV, 12 mg/kg) (Figure 5-11).

Effect of oral FM04 with various dose of PTX on LCC6

Legend:
- PTX 20 mg/kg (oral)
- PTX 40 mg/kg (oral)
- PTX 80 mg/kg (oral)
- PTX 20 mg/kg + **FM04** 45 mg/kg (oral)
- PTX 40 mg/kg + **FM04** 45 mg/kg (oral)
- PTX 80 mg/kg + **FM04** 45 mg/kg (oral)
- PTX 12 mg/kg (IV)
- No treatment

Y-axis: Tumor Vol. (%); X-axis: Time (Day)
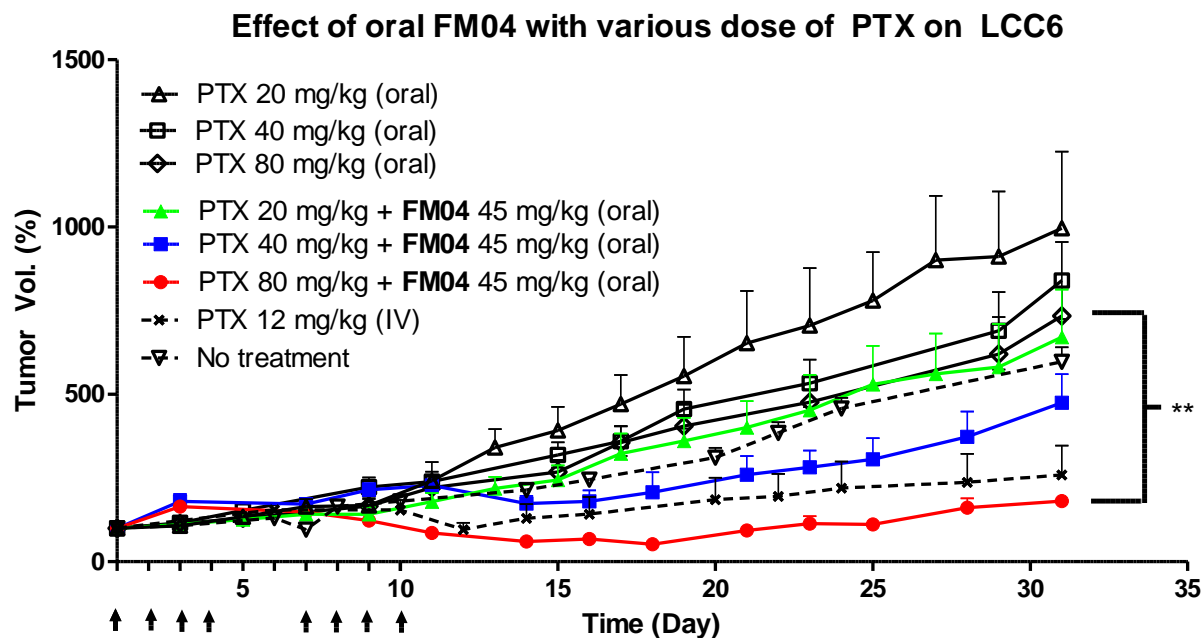
Figure 5-11 Effect of **FM04** with various doses of orally administered PTX on LCC6 xenograft efficacy study

Balb/c nude mice bearing LCC6 breast cancer xenograft were treated with orally administered PTX (20 mg/kg, 40 mg/kg and 80 mg/kg). PTX (IV, 12 mg/kg) and no treatment groups serve as controls. Oral administration of PTX (20 mg/kg, 40 mg/kg or 80 mg/kg) with **FM04** (oral, 45 mg/kg) serves as treatment groups. Arrows indicated days of treatment. PTX 20 mg/kg (N=7,) PTX 40 mg/kg (N=8), PTX 80 mg/kg (N=8), PTX 20 mg/kg + **FM04** 45 mg/kg (N=7), PTX 40 mg/kg + **FM04** 45 mg/kg (N=8) and PTX 80 mg/kg + **FM04** 45 mg/kg (N=4). **,$P<0.01$, t-test; significantly different from oral PTX (80 mg/kg).

When tumor doubling time from the above experiment was determined, we found that PTX (IV, 12 mg/kg) can increase the tumor doubling time from 12 ± 0.6 days in no treatment group to 21.9 days (Figure 5-12). For the two treatment groups that showed significant tumor suppression effect in the above *in vivo* efficacy experiments: co-administration of **18** (oral, 30 mg/kg) with PTX (oral, 80 mg/kg) or co-administration of **FM04** (oral, 45 mg/kg) with PTX (oral, 80 mg/kg), both can increase tumor doubling time to 35.3 ±6.4 days and 35.3 ± 1.8 days, respectively (Figure 5-12). All other combinations did not show any significant differences compared to no treatment control.
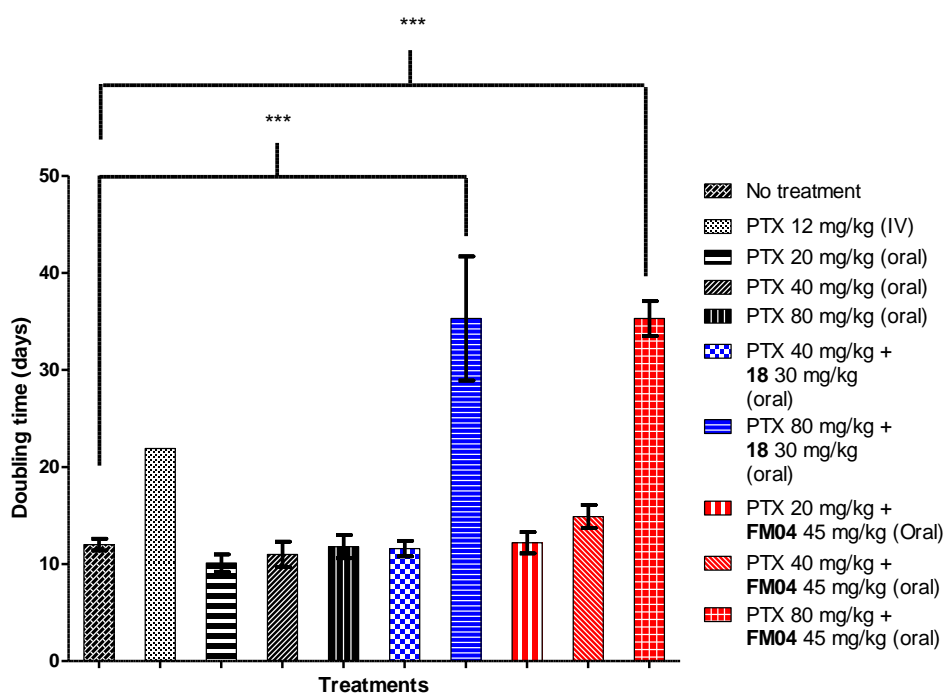
Figure 5-12 Doubling time of LCC6 under various treatments of PTX

Doubling time for various treatments of PTX with or without **18** or **FM04** was calculated as mentioned previously. ***, *P*<0.001, t-test; significantly different from no treatment group.

Despite the fact that both treatment groups of **18** (oral, 30 mg/kg) with PTX (oral 80 mg/kg) and **FM04** (oral, 45 mg/kg) with PTX (oral, 80 mg/kg) showed statistically significant difference in tumor doubling time compared with no treatment group (Figure 5-12), toxicity was noted in both groups (Figure 5-13). In case of **18**, percentage survival was decreased to 38% on day 9 and remained at that level till the end of experiment on day 31. In case of **FM04**, percentage

survival was decreased to 75% on day 6 and remained at that level till the end.

This suggests that **FM04** was less toxic than **18** when co-administered orally

with oral PTX.
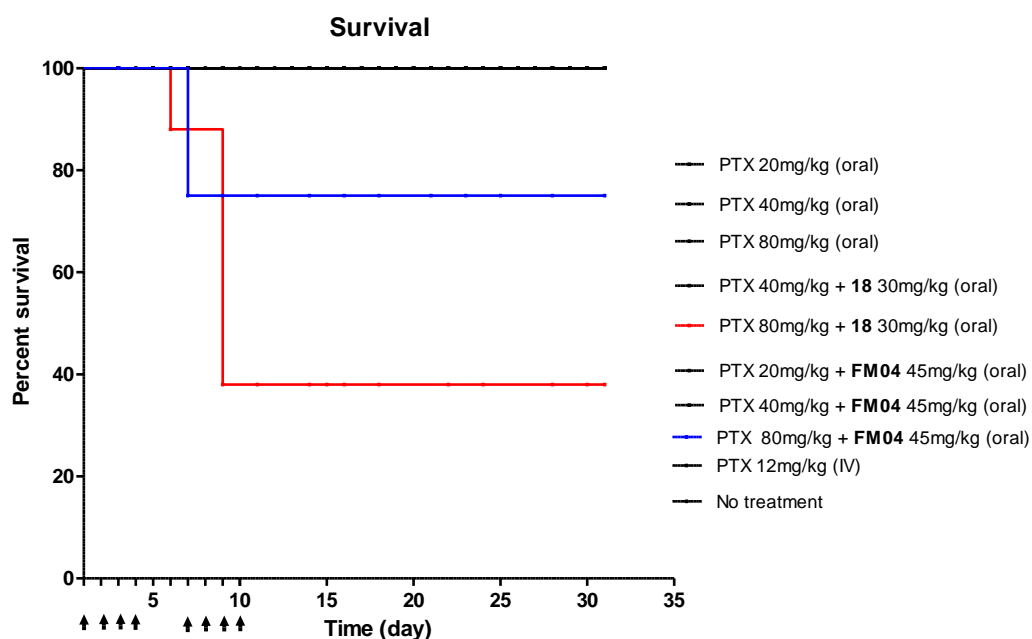
Figure 5-13 Survival curve of LCC6 xenograft efficacy treated with PTX +/- **18** or **FM04**

Balb/c nude mice bearing LCC6 breast cancer xenograft were treated with various doses of PTX either with or without concurrent oral administration of **FM04** (45 mg/kg) or **18** (30 mg/kg). The percentage of survival is plotted against the course of experiment.

5.4   CONCLUSION

Pharmacokinetics study demonstrated that oral bioavailability of PTX could be enhanced by concurrent administration of oral **FM04** (45 mg/kg) (Figure 5-1, Figure 5-2) or **18** (30 mg/kg) (Figure 5-5) on Balb/c mice. When co-administered with **18** (30 mg/kg, oral) or **FM04** (45 mg/kg, oral), oral bioavailability of PTX could be enhanced by 4.13 folds (Figure 5-7) or 7 folds (Figure 5-3), respectively. Oral bioavailability and C_{max} values were PTX dose dependent when concurrently administered with **18** (oral, 30 mg/kg) (Figure 5-6, Figure 5-7, Figure 5-8). Detailed PK parameters on **FM04** and **18** are listed on Table 10 and Table 11, respectively.

In vivo LCC6 xenograft efficacy studies demonstrated that oral administration of PTX (80 mg/kg) with **18** (30 mg/kg) or **FM04** (45 mg/kg) both demonstrated statistical significant tumor suppression effects (Figure 5-9). When PTX (oral, 40 mg/kg) was co-administered with **FM04** (oral, 45 mg/kg), a moderate tumor suppression effect was noted (Figure 5-11); however, this was not observed when PTX (oral, 40 mg/kg) was co-administered with **18** (oral, 30 mg/kg) (Figure 5-10). When PTX was administered orally at 20, 40 or 80 mg/kg, no tumor suppression effect was found (Figure 5-10). Assessing the tumor doubling time, only PTX (oral, 80 mg/kg) with **18** (oral, 30 mg/kg) and PTX (oral, 80

mg/kg) with **FM04** (oral, 45 mg/kg) increased tumor doubling time from 12 ± 0.6 days to 35.3 ±6.4 days and 35.3 ± 1.8 days, respectively (Figure 5-12).

In terms of toxicity, the survival curve of LCC6 xenograft efficacy study revealed that concurrent oral administration of **FM04** with PTX (survival rate is 75%) was less toxic than **18** with PTX (survival rate is 38%) in 30 days on 2 courses of treatment (Figure 5-13).

To conclude, the current study suggests that **FM04** and **18** are capable of enhancing PTX oral bioavailability. The current data suggests that **FM04** is a better candidate than **18** with lower toxicity and better dose-dependent effect when concurrently administered with PTX orally.

6   CONCLUSION AND PERSPECTIVES

6.1   OVERVIEW

Overexpression of P-glycoprotein (P-gp) confers drug resistance by reducing intracellular drug concentration is evident in *ex vivo, in vitro* and *in vivo* studies (Gottesman et al. 1996; Gottesman et al. 2002; Gottesman and Ling 2006; Szakacs et al. 2006). However, the hope to reverse cancer drug resistance by inhibiting P-gp has yet to reach clinical success. Promising P-gp modulators such as valspodar (PSC-833) did not demonstrate beneficial effects on patients in clinical studies (Kolitz et al. 2010).

We investigated the use of synthetic flavonoid homodimer in modulating P-gp. The objective of the current project is to study the drug metabolism and pharmacokinetics profile of a newly developed P-gp modulator flavonoid dimer **18**. Surprisingly we discovered **FM04**, an active metabolite of **18** during the metabolism investigation. We then investigated the effect of **18** or **FM04** on enhancing oral bioavailability of PTX for therapeutic use.

6.2 FLAVONOID DIMERS ON MODULATING P-GLYCOPROTEIN

P-gp is a transmembrane protein with pseudodimeric nature. To the best of our knowledge, no one has reported the use of flavonoid homodimers in modulating P-gp. Our previous structure activity relationship (SAR) study has investigated the effect of flavonoid homodimers and hetero-dimers on modulating P-gp. In general, we found that flavonoid heterodimers demonstrated lower modulating activity than flavonoid homodimers (Chan et al. 2009). This suggested that flavonoid homodimer worked on two similar binding sites of P-gp.

Further lead optimization led to the discovery of a highly potent and specific flavonoid dimer **18**. **18** has an amine group in the linker region in order to achieve better solubility. **18** in hydrochloride salts has tremendous improvement in solubility and allowed *in vivo* study to proceed.

6.3 DUAL MECHANISM OF ACTION OF **18**

Drug metabolism and pharmacokinetics study was conducted on **18** as part of the drug development process. Pharmacokinetics study of **18** provided information for dose regimen design on reversing P-gp mediated drug resistance in a LCC6 MDR breast carcinoma xenograft model *in vivo*. Based on the current

122

pharmacokinetics data and preliminary PK data, **18** was administered via IP route at 45mg/kg in the abovementioned animal model. **18** was found to be active in sensitizing LCC6 MDR xenograft to PTX.

In the metabolism study of **18**, three novel metabolites of **18** were found and one of them (**FM04**) possessed a more potent P-gp modulating activity than parent compound **18**. This result suggests that **18** may modulate P-gp by dual mechanisms. **18** itself is a P-gp modulator and at the same time capable of forming **FM04**, a more potent P-gp modulator, during metabolism. This unexpected result will predict that **18** can be a very good P-gp modulating agent as it can sustain a relatively strong P-gp modulation *in vivo*.

6.4 ENHANCING PTX ORAL BIOAVAILABILITY BY MODULATING P-GP IN THE GI TRACT

FM04 is a metabolite of **18** with more potent P-gp modulating activity and better aqueous solubility. We explored the possibility of using **FM04** as a P-gp modulating agent.

Pharmacokinetics study of **FM04** has demonstrated that **FM04** has a low oral bioavailability. This result implies that **FM04**, if administered orally, will exert a

P-gp modulating effect locally in the GI tract and has a minimal disturbance to other organs. PTX is an intravenously administered drug and a substrate of P-gp. Low oral bioavailability of PTX is limited by P-gp efflux. Pharmacokinetics study on PTX demonstrated that oral bioavailability of PTX could be enhanced by co-administration of **18** or **FM04**.

The therapeutic effect of oral PTX co-administered with **FM04** or **18** was investigated using a LCC6 breast carcinoma xenograft model. Both treatment groups of PTX with either **FM04** or **18** were capable of suppressing tumor growth of LCC6 xenograft. In terms of toxicity, co-oral administration of **FM04** with PTX resulted in a lower toxicity than co-oral administration of PTX with **18**.

The above experiment proved that oral bioavailability of PTX can be increased to therapeutic level by co-administering **18** or **FM04**. The data suggests a therapeutic window of using PTX from 80 mg/kg to 40 mg/kg for oral administration with **18** or **FM04**. Further refinement should lead us to a therapeutic useful dose regimen for oral administration of PTX with low toxicity. Oral administration of PTX is advantageous to patients for its convenience of use and lower economical burden by replacing intravenous administration.

7 APPENDIX

Table 12. List of flavonoid dimers and derivatives used in this project

Compound	Chemical structure	Reference
18		(Chan et al. 2012)
14a		(Chan et al. 2012)
D7NBn		Newly synthesized
FM327		Newly synthesized
FM04		Newly synthesized
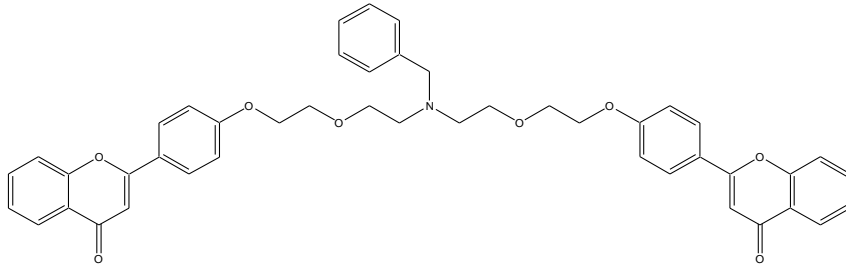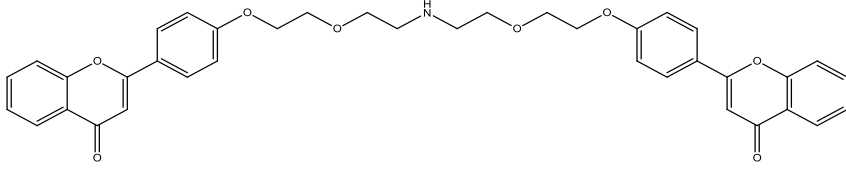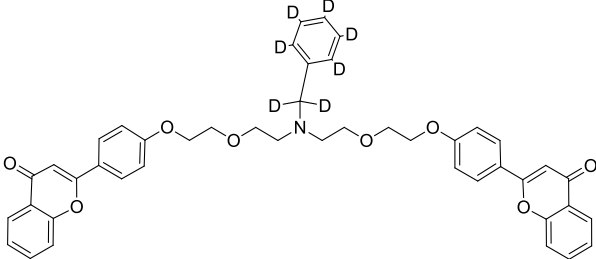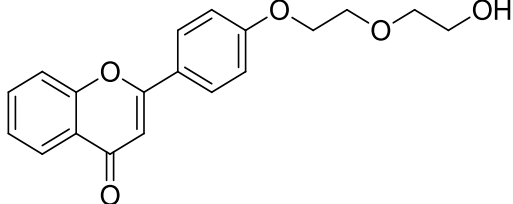
| D7 FM04 | | Newly synthesized |

8   REFERENCE

Advani, R., G. A. Fisher, et al. (2001). "A phase I trial of doxorubicin, paclitaxel, and valspodar (PSC 833), a modulator of multidrug resistance." Clin Cancer Res **7**(5): 1221-9.

Aller, S. G., J. Yu, et al. (2009). "Structure of P-glycoprotein reveals a molecular basis for poly-specific drug binding." Science **323**(5922): 1718-22.

Ambudkar, S. V., C. Kimchi-Sarfaty, et al. (2003). "P-glycoprotein: from genomics to mechanism." Oncogene **22**(47): 7468-85.

Asha, S. and M. Vidyavathi (2010). "Role of human liver microsomes in in vitro metabolism of drugs-a review." Appl Biochem Biotechnol **160**(6): 1699-722.

Atadja, P., T. Watanabe, et al. (1998). "PSC-833, a frontier in modulation of P-glycoprotein mediated multidrug resistance." Cancer Metastasis Rev **17**(2): 163-8.

Baranczewski, P., A. Stanczak, et al. (2006). "Introduction to early in vitro identification of metabolites of new chemical entities in drug discovery and development." Pharmacol Rep **58**(3): 341-52.

Bardelmeijer, H. A., J. H. Beijnen, et al. (2000). "Increased oral bioavailability of paclitaxel by GF120918 in mice through selective modulation of P-glycoprotein." Clin Cancer Res **6**(11): 4416-21.

Bardelmeijer, H. A., T. Buckle, et al. (2003). "Cannulation of the jugular vein in mice: a method for serial withdrawal of blood samples." Lab Anim **37**(3): 181-7.

Bates, S., M. Kang, et al. (2001). "A Phase I study of infusional vinblastine in combination with the P-glycoprotein antagonist PSC 833 (valspodar)." Cancer **92**(6): 1577-90.

Baumert, C. and A. Hilgeroth (2009). "Recent Advances in the Development of P-gp Inhibitors." Anti-Cancer Agents in Medicinal Chemistry **9**: 415-436.

Boesch, D., C. Gaveriaux, et al. (1991). "In vivo circumvention of P-glycoprotein-mediated multidrug resistance of tumor cells with SDZ PSC 833." Cancer Res **51**(16): 4226-33.

Borges, N. C., V. M. Rezende, et al. (2011). "Chlorpromazine quantification in human plasma by UPLC-electrospray ionization tandem mass spectrometry. Application to a comparative pharmacokinetic study." J Chromatogr B Analyt Technol Biomed Life Sci **879**(31): 3728-34.

Brandon, E. F., C. D. Raap, et al. (2003). "An update on in vitro test methods in human hepatic drug biotransformation research: pros and cons." Toxicol Appl Pharmacol **189**(3): 233-46.

Breedveld, P., J. H. Beijnen, et al. (2006). "Use of P-glycoprotein and BCRP inhibitors to improve oral bioavailability and CNS penetration of anticancer drugs." Trends Pharmacol Sci **27**(1): 17-24.

Cairo, M. S., S. Siegel, et al. (1989). "Clinical trial of continuous infusion verapamil, bolus vinblastine, and continuous infusion VP-16 in drug-resistant pediatric tumors." Cancer Res **49**(4): 1063-6.

Chan, K.-F., Y. Zhao, et al. (2009). "Flavonoid Dimers as Bivalent Modulators for P-Glycoprotein-Based Multidrug Resistance: Structure–Activity Relationships." ChemMedChem: 1-22.

Chan, K. F., I. L. Wong, et al. (2012). "Amine linked flavonoid dimers as modulators for p-glycoprotein-based multidrug resistance: structure-activity relationship and mechanism of modulation." J Med Chem **55**(5): 1999-2014.

Chan, K. F., I. L. K. Wong, et al. (2010). "Flavonoid dimer as modulator of drug resistance in cancer." Progress in Nutrition **12**: 1-7.

Chan, K. F., Y. Zhao, et al. (2006). "Flavonoid dimers as bivalent modulators for P-glycoprotein-based multidrug resistance: synthetic apigenin homodimers linked with defined-length poly(ethylene glycol) spacers increase drug retention and enhance chemosensitivity in resistant cancer cells." J Med Chem **49**(23): 6742-59.

Chan, K. F., Y. Zhao, et al. (2009). "Flavonoid dimers as bivalent modulators for p-glycoprotein-based multidrug resistance: structure-activity relationships." ChemMedChem **4**(4): 594-614.

Chauret, N., A. Gauthier, et al. (1998). "Effect of common organic solvents on in vitro cytochrome P450-mediated metabolic activities in human liver microsomes." Drug Metab Dispos **26**(1): 1-4.

Chen, Y. M., R. P. Perng, et al. (2004). "A randomised phase II study of weekly paclitaxel or vinorelbine in combination with cisplatin against inoperable non-small-cell lung cancer previously untreated." <u>Br J Cancer</u> **90**(2): 359-65.

Chi, K. N., S. K. Chia, et al. (2005). "A phase I pharmacokinetic study of the P-glycoprotein inhibitor, ONT-093, in combination with paclitaxel in patients with advanced cancer." <u>Investigational new drugs</u> **23**: 311-315.

Dalton, W. S. (1993). "Drug resistance modulation in the laboratory and the clinic." <u>Semin Oncol</u> **20**(1): 64-9.

Dawson, R. J. and K. P. Locher (2006). "Structure of a bacterial multidrug ABC transporter." <u>Nature</u> **443**(7108): 180-5.

Dawson, R. J. P. and K. P. Locher (2006). "Structure of a bacterial multidrug ABC transporter." <u>Nature</u> **443**(14): 180-185.

de Jonge, M. E., A. D. Huitema, et al. (2005). "Population pharmacokinetics of orally administered paclitaxel formulated in Cremophor EL." <u>Br J Clin Pharmacol</u> **59**(3): 325-34.

E.Dates, S. and T. Fojo (2004). ABC Transporters Involvement in Multidrug Resistance and Drug Disposition. <u>Handbook of Anticancer Pharmacokinetics and Pharmacodynamics</u>. W. D.Figg and H. L.McLeod. Totowa, New Jersey, Humana Press**: 273-277**.

Friedenberg, W. R., M. Rue, et al. (2006). "Phase III study of PSC-833 (valspodar) in combination with vincristine, doxorubicin, and dexamethasone (valspodar/VAD) versus VAD alone in patients with recurring or refractory multiple myeloma (E1A95): a trial of the Eastern Cooperative Oncology Group." <u>Cancer</u> **106**(4): 830-8.

Gelderblom, H., J. Verweij, et al. (2001). "Cremophor EL: the drawbacks and advantages of vehicle selection for drug formulation." <u>Eur J Cancer</u> **37**(13): 1590-8.

Gergely Szakacs, Jill K. Paterson, et al. (2006). "Targeting multidrug resistance in cancer." <u>Nature Reviews: Drug discovery</u> **5**: 219-234.

Ghosal, A., R. Ramanathan, et al. (2005). Cytochrome P450 (CYP) and UDP-Glucuronosyltransferase (UGT) enzymes: role in drug metabolism,

polymorphism, and identification of their involvement in drug metabolism. Identification and Quantification of Drugs, Metabolites and Metabolizing Enzymes by LC-MS S. K.Chowdhury. Kenilworth, New Jersey, Elsevier B.V 295-336.

Gillespie, W. R. (1991). "Noncompartmental versus compartmental modelling in clinical pharmacokinetics." Clin Pharmacokinet **20**(4): 253-62.

Gottesman, M. M., T. Fojo, et al. (2002). "Multidrug resistance in cancer: role of ATP-dependent transporters." Nat Rev Cancer **2**(1): 48-58.

Gottesman, M. M. and V. Ling (2005). "The molecular basis of multidrug resistance in cancer: The early years of P-glycoprotein research." FEBS letters **580**: 998-1009.

Gottesman, M. M. and V. Ling (2006). "The molecular basis of multidrug resistance in cancer: the early years of P-glycoprotein research." FEBS Lett **580**(4): 998-1009.

Gottesman, M. M., I. Pastan, et al. (1996). "P-glycoprotein and multidrug resistance." Current Opinion in Genetics & Development **6**(5): 610-617.

Gottesman, M. M., I. Pastan, et al. (1996). "P-glycoprotein and multidrug resistance." Curr Opin Genet Dev **6**(5): 610-7.

Grossi, A. and M. Biscardi (2004). "Reversal of MDR by verapamil analogues." Hematology **9**(1): 47-56.

Gumustas, M., S. Kurbanoglu, et al. (2013). "UPLC versus HPLC on Drug Analysis: Advantageous, Applications and Their Validation Parameters." Chromatographia **76**: 1365-1427.

Holland, I. B., S. P. C. Cole, et al. (2003). ABC Protein. San Diego, California, Academic Press.

Jin, M. S., M. L. Oldham, et al. (2012). "Crystal structure of the multidrug transporter P-glycoprotein from Caenorhabditis elegans." Nature **490**(7421): 566-9.

Keller, T. H., A. Pichota, et al. (2006). "A practical view of 'druggability'." Curr Opin Chem Biol **10**(4): 357-61.

Kelly, R. J., D. Draper, et al. (2011). "A Pharmacodynamic Study of Docetaxel in Combination with the P-glycoprotein Antagonist Tariquidar (XR9576) in Patients with Lung, Ovarian, and Cervical Cancer." Clin Cancer Res.

Kodan, A., T. Yamaguchi, et al. (2014). "Structural basis for gating mechanisms of a eukaryotic P-glycoprotein homolog." Proc Natl Acad Sci U S A **111**(11): 4049-54.

Kolitz, J. E., S. L. George, et al. (2010). "P-glycoprotein inhibition using valspodar (PSC-833) does not improve outcomes for patients younger than age 60 years with newly diagnosed acute myeloid leukemia: Cancer and Leukemia Group B study 19808." Blood **116**(9): 1413-21.

Kollmannsberger, C., D. Quietzsch, et al. (2000). "A phase II study of paclitaxel, weekly, 24-hour continous infusion 5-fluorouracil, folinic acid and cisplatin in patients with advanced gastric cancer." Br J Cancer **83**(4): 458-62.

Kwak, J. O., S. H. Lee, et al. (2010). "Selective inhibition of MDR1 (ABCB1) by HM30181 increases oral bioavailability and therapeutic efficacy of paclitaxel." Eur J Pharmacol **627**(1-3): 92-8.

Liang, Y., C. Besch-Williford, et al. (2007). "Progestin-dependent progression of human breast tumor xenografts: a novel model for evaluating antitumor therapeutics." Cancer Res **67**(20): 9929-36.

Loo, T. W., M. C. Bartlett, et al. (2006). "Transmembrane segment 7 of human P-glycoprotein forms part of the drug-binding pocket." Biochem J **399**(2): 351-9.

Loo, T. W. and D. M. Clarke (1997). "Identification of residues in the drug-binding site of human P-glycoprotein using a thiol-reactive substrate." J Biol Chem **272**(51): 31945-8.

Loo, T. W. and D. M. Clarke (2005). "Recent progress in understanding the mechanism of P-glycoprotein-mediated drug efflux." J Membr Biol **206**(3): 173-85.

Mansouri, A., K. J. Henle, et al. (1994). "Tumor drug-resistance: a challenge to therapists and biologists." Am J Med Sci **307**(6): 438-44.

Mehrara, E., E. Forssell-Aronsson, et al. (2007). "Specific growth rate versus doubling time for quantitative characterization of tumor growth rate." Cancer Res **67**(8): 3970-5.

Olivier Dangels and C. Dufour (2006). Flavonoid-Protein Interactions. Flavonoids Chemistry, Biochemistry and applications. Ø yvind M.Andersen and K. R.markham. Boca Raton, Taylor & Francis**: 444-460**.

Pabbisetty, D., A. Illendula, et al. (2012). "Determination of antimalarial compound, ARB-89 (7beta-hydroxy-artemisinin carbamate) in rat serum by UPLC/MS/MS and its application in pharmacokinetics." J Chromatogr B Analyt Technol Biomed Life Sci **889-890**: 123-9.

Panaro, N. J., N. C. Popescu, et al. (1999). "Flavone acetic acid induces a G2/M cell cycle arrest in mammary carcinoma cells." Br J Cancer **80**(12): 1905-11.

Preston, N. J. (1996). "Paclitaxel (Taxol)--a guide to administration." Eur J Cancer Care (Engl) **5**(3): 147-52.

Ramanathan, R., S. K.Chowdhury, et al. (2005). Oxidative metabolites of drugs and xenobiotics: LC-MS methods to identify and characterize in biological matrices. Identification and Quantification of Drugs, Metabolites and Metabolizing Enzymes by LC-MS S. K.Chowdhury. Kenilworth, New Jersey, Elsevier B.V 225-276.

Raviv, Y., H. B. Pollard, et al. (1990). "Photosensitized labeling of a functional multidrug transporter in living drug-resistant tumor cells." J Biol Chem **265**(7): 3975-80.

Robey, R. W., P. R. Massey, et al. (2010). "ABC transporters: unvalidated therapeutic targets in cancer and the CNS." Anticancer Agents Med Chem **10**(8): 625-33.

Saeki, T., T. Tsuruo, et al. (2005). "Drug resistance in chemotherapy for breast cancer." Cancer Chemother Pharmacol **56 Suppl 1**: 84-9.

Schena, M., C. Barone, et al. (2005). "Weekly cisplatin paclitaxel and continuous infusion fluorouracil in patients with recurrent and/or metastatic head and neck squamous cell carcinoma: a phase II study." Cancer Chemother Pharmacol **55**(3): 271-6.

Schroeter, H. and J. P. E. Spencer (2003). Flavonoids: Neuroprotective Agents? Modulation of Oxidative Stress-Induced MAP Kinase Signal Transduction Flavonoids in Health and Disease Second Edition Revised and Expanded. C. A.Rice-Evans and L. Packer. New York, Marcel Dekker Inc**:** 233-272.

Shukla, S., S. Ohnuma, et al. (2011). "Improving cancer chemotherapy with modulators of ABC drug transporters." Curr Drug Targets **12**(5): 621-30.

Singla, A. K., A. Garg, et al. (2002). "Paclitaxel and its formulations." Int J Pharm **235**(1-2): 179-92.

Sparreboom, A., J. van Asperen, et al. (1997). "Limited oral bioavailability and active epithelial excretion of paclitaxel (Taxol) caused by P-glycoprotein in the intestine." Proc Natl Acad Sci U S A **94**(5): 2031-5.

Sparreboom, A., O. van Tellingen, et al. (1996). "Tissue distribution, metabolism and excretion of paclitaxel in mice." Anticancer Drugs **7**(1): 78-86.

Spencer, J. P. E., C. A.Rice-Evans, et al. (2003). Cytoprotective and Cytotoxic Effects of Flavonoids. Flavonoids in Health and Disease Second Edition Revised and Expanded. C. A.Rice-Evans and L. Packer. New York, Marcel Dekker Inc**:** 309-347.

Sun, L., H. Li, et al. (2012). "Ultrasensitive Liquid Chromatography-Tandem Mass Spectrometric Methodologies for Quantification of Five HIV-1 Integrase Inhibitors in Plasma for a Microdose Clinical Trial." Anal Chem **84**(20): 8614-21.

Szakacs, G., J. K. Paterson, et al. (2006). "Targeting multidrug resistance in cancer." Nat Rev Drug Discov **5**(3): 219-34.

ten Tije, A. J., C. H. Smorenburg, et al. (2004). "Weekly paclitaxel as first-line chemotherapy for elderly patients with metastatic breast cancer. A multicentre phase II trial." Eur J Cancer **40**(3): 352-7.

ten Tije, A. J., J. Verweij, et al. (2003). "Pharmacological effects of formulation vehicles : implications for cancer chemotherapy." Clin Pharmacokinet **42**(7): 665-85.

Thomas, H. and H. M. Coley (2003). "Overcoming multidrug resistance in cancer: an update on the clinical strategy of inhibiting p-glycoprotein." <u>Cancer Control</u> **10**(2): 159-65.

van Asperen, J., O. van Tellingen, et al. (1997). "Enhanced oral bioavailability of paclitaxel in mice treated with the P-glycoprotein blocker SDZ PSC 833." <u>Br J Cancer</u> **76**(9): 1181-3.

van Asperen, J., O. van Tellingen, et al. (1998). "Enhanced oral absorption and decreased elimination of paclitaxel in mice cotreated with cyclosporin A." <u>Clin Cancer Res</u> **4**(10): 2293-7.

van Herwaarden, A. E., E. Wagenaar, et al. (2007). "Knockout of cytochrome P450 3A yields new mouse models for understanding xenobiotic metabolism." <u>J Clin Invest</u> **117**(11): 3583-92.

van Tellingen, O., M. T. Huizing, et al. (1999). "Cremophor EL causes (pseudo-) non-linear pharmacokinetics of paclitaxel in patients." <u>Br J Cancer</u> **81**(2): 330-5.

Vasey, P. A., G. C. Jayson, et al. (2004). "Phase III randomized trial of docetaxel-carboplatin versus paclitaxel-carboplatin as first-line chemotherapy for ovarian carcinoma." <u>J Natl Cancer Inst</u> **96**(22): 1682-91.

Vaughn, D. J., A. W. Brown, Jr., et al. (2004). "Multicenter Phase II study of estramustine phosphate plus weekly paclitaxel in patients with androgen-independent prostate carcinoma." <u>Cancer</u> **100**(4): 746-50.

Winniford, M. D. and L. D. Hillis (1985). "Calcium antagonists in patients with cardiovascular disease. Current perspectives." <u>Medicine (Baltimore)</u> **64**(1): 61-73.

Wong, I. L., K. F. Chan, et al. (2007). "Flavonoid dimers as bivalent modulators for pentamidine and sodium stiboglucanate resistance in leishmania." <u>Antimicrob Agents Chemother</u> **51**(3): 930-40.

Wong, I. L., K. F. Chan, et al. (2012). "Flavonoid Dimers as Novel, Potent Antileishmanial Agents." <u>J Med Chem</u> **55**(20): 8891-902.

Wong, I. L., K. F. Chan, et al. (2009). "Modulation of multidrug resistance protein 1 (MRP1/ABCC1)-mediated multidrug resistance by bivalent apigenin homodimers and their derivatives." <u>J Med Chem</u> **52**(17): 5311-22.